Optimal Application of Phase Change Materials and Passive Cooling Systems to Improve Energy and Indoor Environmental Performance of a Highly Glazed Commercial Space in Cold Climates

By

Ali Mohammadzadeh

A thesis submitted to the Faculty of Graduate Studies of

The University of Manitoba

in partial fulfillment of the requirements for the degree of

Master of Science

Department of Civil Engineering

Faculty of Engineering

University of Manitoba

Winnipeg, Manitoba

August 2019

© Copyright 2019, Ali Mohammadzadeh

Abstract

Passive energy systems hold the potential to achieve high heating and cooling energy savings when integrated with building systems. Proper integration of these systems can contribute to the efficiency of heating and cooling energy uses as well as improvement of daylight in nearly any buildings, and in particular in highly-glazed and lightweight buildings, which are becoming popular worldwide. This study aims to investigate the optimal application of Phase Change Materials (PCMs), natural ventilation, and solar shading systems in maximizing energy conservation and comfort level in a highly-glazed study room located in a cold climate. For this purpose, a whole-building energy model of the Stanley Pauley Engineering Building (SPEB) is developed using a building performance simulation (BPS) tool, EnergyPlus. In order to gain confidence in the SPEB model, its outputs are compared against the SPEB model developed in an IES tool. The discrepancies of around 2.1% and 1.7% between the predictions of the total energy consumption and energy use intensity, respectively, suggest excellent agreement between the two models. Afterward, the SPEB model is used to examine, test, and analyze different design strategies for optimal application and use of PCM, shading, and natural ventilation. This is accomplished by using sophisticated Energy Management System (EMS) within the EnergyPlus as well as coupling the SPEB model with the programing language MATLAB. A case study in this research was a graduate study room located on the top floor of the SPEB. The study concluded that the integration of PCM_{28} with the hydronic radiant floor system significantly reduces the annual heating and total energy demand by around 24% and 19%, respectively. Also, the economic analysis showed that the application of PCM-enhanced radiant floor, when incorporated with a thin layer of insulation, could recover the initial investment within 5 to 10 years, which indicates a high economic value and appears to be cost-effective. Furthermore, the findings from the optimal

integration of passive cooling systems show that an integrated approach for automatic control of shading is more efficient compared to the individual strategies and can reduce the cooling and heating energy demand by around 20% and 5.6%, respectively.

Acknowledgments

I want to express my deep and sincere gratitude to my research supervisor, Dr. Miroslava Kavgic, for providing invaluable support and excellent guidance throughout this challenging research. Her dedication and keen interest along with critical problem-solving skills have helped me in all the time of research and writing of this thesis. In addition, I would like to express my great appreciation to my advisory committee members, Dr. Pooneh Maghoul and Dr. Shaahin Filizadeh, for their constructive comments and thoughtful judgment.

Many other individuals and organizations provided valuable guidance in developing and completing this research study. I would like to start by thanking the Compute Canada team at the University of Manitoba, Mr. Grigory Shamov and Dr. Ali Kerrache, for their valuable assistance with providing excellent support and easy access to computational facilities. I would also like to thank Stantec Consulting Company and the Faculty of Engineering of the University of Manitoba for providing access to the architectural drawings and other necessary information required for the development of the Stanley-Pauley engineering building energy model. My sincere thanks also go to my friend, Mr. Ali Al-Janabi for his technical supports during these two years.

Last but not least, great thanks to my parents and my brother, for being helpful and encouraging me throughout the process of completing my studies. Without their encouragement and support, I would not have been where I am today. I would like to dedicate this dissertation to my loving parents, who have always been the source of love, support, and encouragement to me.

Table of Contents

List of tables

List of figures

Copyright acknowledgement

According to the Elsevier publisher of the papers, "authors are allowed to use their articles, in full or in part, for a wide range of scholarly, non-commercial purposes such as inclusion in a thesis or dissertation (provided that this is not to be published commercially)"(Elsevier, 2019).

In this thesis, chapter 3, sections 3.3 to 3.4 and chapter 6, section 6.2 are reprinted with permission from the authors from “Ali Al-janabi, Miroslava Kavgic, Ali Mohammadzadeh and Afaf Azzouz, .2019. Comparison of EnergyPlus and IES to model a complex university building using three scenarios: Free-floating, ideal air load system, and detailed, Journal of Building Engineering, 22, 262 – 280, doi: https://doi.org/10.1016/j.jobe.2018.12.022”. This material is copyrighted, and any further reproduction or distribution requires written permission.

List of symbols

Symbol	Description	Unit
Q	Quantity of stored heat	J
m	Mass of the object	g
C_p	Specific heat capacity of the material	J/g/°C
T	Temperature of the material	°C
Δh_r	Endothermic heat of reaction	J
a_r	Extent of conversion	moles
C_{ps}	Average specific heat of the solid phase	J/g/°C
C_{pl}	Average specific heat of the liquid phase	J/g/°C
f	Melting fraction	-
Δq	Latent heat of fusion	J/kg
α	Thermal diffusivity of the material	m^2/s
Δt	Time step	s
h	Enthalpy	J/kg
K	Thermal conductivity	W/m·K
PCM_{MT}	PCM melting temperature	°C
PCM_T	PCM thickness	cm
I_T	Insulation thickness	cm
I_k	Insulation conductivity	W/m·K
F_T	Floor thickness	cm
F_k	Floor conductivity	W/m·K
F_α	Floor solar absorbance	-
S	Sensitivity index	-
Δ_{ei}	Variation in model variable	-
e_i	Model variable	-
M_o	Model output	-
Q_v	Volumetric flow rate	m^3/s
A	Area	m^2
V	Air velocity	m/s
C_d	Discharge coefficient	-
R	Radiation level	W
I_{cl}	Occupants' clothing insulation	-
M	Occupants' Metabolic rate	-

List of abbreviation and acronym

Acronym	Description
BEMS	Building Energy Management System
BEM	Building Energy Modeling
BEST	Building Energy Simulation Tools
COP	Coefficient of Performance
CondFD	Conduction Finite Difference
CAV	Constant Air Volume
EMS	Energy Management Systems
EUI	Energy Use Intensity
Erl	EnergyPlus Runtime Language
EPW	EnergyPlus Weather
ERV	Energy-Recovery Ventilator
GA	Genetic Algorithm
GHG	Greenhouse Gas
HVAC	Heating, Ventilation, and Air-Conditioning
IESC	Indices of Energy Savings for Cooling energy
IESH	Indices of Energy Savings for Heating energy
IEST	Indices of Energy Savings for Total energy
IAQ	Indoor Air Quality
IDF	Input Data File
IES	Integrated Environmental Solutions
IPCC	Intergovernmental Panel on Climate Change
IEA	International Energy Agency
LHS	Latent Heat Storage
MECB	Manitoba Energy Code for Buildings
NECB	National Energy Code for Buildings
NRC	National Research Council
PCMs	Phase Change Materials
PMV	Predicted Mean Vote
RH	Relative Humidity
SPEB	Stanley Pauley Engineering Building
TES	Thermal Energy Storage
TCM	Thermochemical Materials
VAV	Variable Air Volume

1 Introduction

1.1 Problem statement

According to the IPCC report "Global Warming of 1.5°C", limiting adverse impacts of climate change requires rapid, substantial, far-reaching societal and technological transformations in energy, land, urban infrastructure (i.e., transport and buildings), and industrial systems (Myles Allen. et al., 2018). The building sector is currently one of the most greenhouse gas (GHG) intensive in Canada and is the third largest emitting sector representing around 12% of total national emissions. In Manitoba, the energy intensity and carbon footprint of the building stock are even higher due to the extremely cold winters and the use of fossil fuels such as natural gas for space and water heating, which account from 60% to 80% of total buildings' energy consumption (CaGBC, 2018). As a result, space heating for residential and commercial buildings generates approximately 11% of Manitoba's total GHG emissions (Manitoba Sustainable Development, 2017). Under the Paris Agreement, Canada committed to a 30% reduction in GHG emissions by 2030 (United Nations, 2016). As such, buildings play a vital role in the country's plan to address global warming and build a sustainable economy that benefits all Canadians over the long-term.

The need for high-performance buildings has led to more stringent building energy code requirements. In Canada, for example, National Research Council (NRC, 1978) investigated the potential for improvement of energy efficiency in buildings that would lead to the development of guidelines for designing more energy efficient buildings. As a result, a set of energy efficiency recommendations were included into National Building Code of Canada of 1983, which were culminated in the newest version the National Energy Code for Buildings (NECB) by NRC in 2015. Similarly, in Manitoba, MECB-2011 became effective via provincial Regulation 213/2013, leading to what is now known as the Manitoba Energy Code for Buildings (MECB, 2015).

The overall goal is to minimize building energy consumption, and the most compliance approach is to increase the use of insulation in building envelopes. Nevertheless, in many instances, an increase in insulation thickness may not be practical or even possible due to the space constraints and greater use of lightweight, thin façade systems such as curtain walls. Lightweight buildings are gaining popularity due to several advantages, including faster construction, higher design flexibility (Mateus et al., 2013) and cost-efficiency (Hoes et al., 2011). However, the application of lightweight façade systems increases concerns over indoor thermal comfort and energy performance of highly-glazed buildings due to their lack of thermal storage properties (Rossi, 2011; Kendrick and Walliman, 2007; Hoes et al., 2011; Kuznik et al., 2008). Phase Change Materials (PCMs) could be an effective solution in increasing the thermal mass of such buildings when integrated within building envelope elements (e.g., walls and floors) due to its ability to provide high energy storage capacity (Anisur et al., 2013). The idea is that PCM absorbs excessive heat from the space during the overheating hours (i.e., melting phase) and releases it back to space during non-operational hours when indoor air temperature drops blew a specific range (i.e., solidification phase).

Overheating is another critical problem during warm seasons in lightweight buildings, and especially those with highly-glazed external surface areas, because excessive heat gains can adversely influence the productivity and wellbeing of occupants (Lomas and Porritt, 2017). For instance, Wyon and Wargocki (2013) and Seppanen et al. (2006) have shown that there is an established quantitative relationship between internal temperature and the rate of productivity loss where the temperatures above the comfort range (i.e., 24°C to 26°C) would negatively impact general office work. Overheating, therefore, poses a risk not only to occupants' wellbeing but also to their performance. This risk is expected to escalate with the climate change, which is likely to intensify the need for auxiliary air-conditioning, thereby increasing energy use and the associated carbon emissions. In this context, the studies have explored the potential of passive cooling design (e.g., natural ventilation and solar shading systems) and management strategies to reduce cooling demand while delivering more comfortable conditions for occupants (Sun et al., 2010; Xu et al., 2011; Van Moeseke, Geoffrey, Isabelle Bruyère, 2007). The Energy Management Systems (EMS), for instance, has been commonly used to efficiently control the operation of such passive systems based on monitoring various environmental parameters such as internal-external air temperature and solar radiation level (Tzempelikos and Athienitis, 2007).

In order to evaluate the impact of energy efficient technologies on the energy and indoor environmental performance of the buildings, it is required to use whole-building energy simulation programs such as EnergyPlus. These modeling tools are able to accurately simulate the thermal behavior of buildings by considering various influential factors including climatic location characteristics, thermo-physical properties of building envelopes, technical details used during the construction, the quality of Heating, Ventilation, and Air-Conditioning (HVAC) systems installed in buildings, and occupants' activities and behaviour towards energy utilization (Page et al., 2007; Chen et al., 2015). The energy savings potential of passive strategies (e.g., integration of PCM, and control of natural ventilation, and shading devices) is then evaluated by comparing the energy use of the improved models against the reference one.

Proper design and integration of passive energy systems into highly-glazed buildings could be challenging due to the high impact of outdoor conditions on their thermal performance. This is particularly true for the highly-glazed buildings exposed to extreme weather conditions such as in Winnipeg where temperature can fluctuate from -40ºC in the winter to +30ºC in the summer. The best practices and the optimal performance of such systems require a detailed simulation-based optimization analysis to develop solutions and operation strategies that account for both energy savings and indoor environmental quality. The majority of earlier research studies typically focused on analyzing the effectiveness of passive energy techniques in improving buildings energy performance and developing design guidelines for passive system and their integration strategies. However, there is a lack of studies focused on the development of optimal integration of passive technologies with buildings' active systems, which can help designers to estimate the potential of such systems in improving building energy efficiency. Moreover, there is a limited number of studies focused on investigating the application of passive energy systems in cold climates with hot and humid summer such as Winnipeg.

1.2 Objectives and scopes

This thesis work aims to investigate the potential for optimal implementation of three hypothetical passive energy systems (i.e., PCM, natural ventilation, and solar shading systems) into the fabric of a highly-glazed graduate study room located on the 4th floor of the Stanley Pauley Engineering Building in Winnipeg. The following five objectives have been undertaken to achieve this aim:

1. Development of a detailed energy model of the Stanley Pauley Engineering Building (SPEB) using EnergyPlus software, and its verification against the SPEB model developed

in another comprehensive whole-building energy software Integrated Environmental Solutions (IES) by Stantec Consulting Ltd.

2. Selection of an appropriate case study suitable for implementation of PCM and passive cooling systems (i.e., natural ventilation and solar shading).

3. Investigation of the optimal incorporation of PCM technology into the case study under-floor hydronic heating system by performing a simulation-based optimization problem. The MATLAB programming language was used as an interface platform to couple the developed energy model of SPEB and Genetic Algorithm. Two sets of optimizations were then performed to determine the optimal design of the PCM-enhanced radiant floor system. The first set aimed to exclusively optimize the thermal properties of PCM such as thickness and melting temperature while assuming other parameters are constant. The second set intended to find an optimal solution for the entire radiant floor system by including additional design variables to the optimization problem. A set of discrete variables were included to the optimization process, namely those related to the thermo-physical properties of floor system including PCM thickness and melting temperature, insulation thickness, insulation conductivity, floor thickness, floor conductivity, and floor solar absorbance. In addition to these design variables, the impact of the radiant system on the energy performance of the case study was also evaluated by considering supply hot water temperature as a design variable.

4. Investigation of the optimal operation of the shading and natural ventilation devices using virtual Energy Management System (EMS) within EnergyPlus software. Two different sets

of control rules were developed based on internal and external environmental factors. The first control set evaluated the effect of natural ventilation on the heating and cooling energy consumptions considering the indoor-outdoor temperatures and room cooling load. The second control set evaluated the effect of the external shading management on the heating and cooling energy demands based on indoor temperature and solar radiation levels.

5. Evaluation of the proposed methods' potential to improve the energy efficiency of the highly-glazed space located in an institutional building exposed to cold climates.

1.3 Contribution to the field

The main contributions of this thesis are twofold:

- Implementation of a simulation-based optimization approach to find the optimal design of PCM-enhanced hydronic radiant floor that minimizes the total energy consumption and provide acceptable thermal comfort for the occupants of a highly-glazed study room in a cold climate. Unlike the previously studied models of electrical floor heating systems, this research work investigates the application of PCM technology when incorporated into a hydronic floor heating system. Therefore, this study provides valuable design recommendations for the optimal integration of PCM and radiant hydronic heating system to improve its energy performance as well as the indoor thermal comfort of the investigated space. Furthermore, the vast majority of the existing research studies focused on the integration of PCM into building fabrics were conducted in temperate and hot climates, and only a small number focused on cold climates. Consequently, more work is required to extend our understanding of how best to integrated PCM in buildings exposed to cold environments. Last but not least, the majority of earlier studies focused on the application of PCM in EnergyPlus software were developed using only enthalpy-temperature information of PCMs. In contrast, the constructed EnergyPlus PCM model in this research study simulates the hysteresis of the PCM, which provides more accurate information regarding the melting and freezing phase of these materials. Therefore, this study provides new knowledge and information needed for implementation and better comprehension of the recently developed hysteresis object in EnergyPlus.

- Extension of the existing knowledge related to the optimal operation of shading devices and natural ventilation system in cold climates by simulating various control strategies using Energy Management System and analyzing their impact on the thermal performance of the case study. Novel and integrated strategies were proposed using different influential environmental factors, including indoor-outdoor air temperature, cooling demand, solar radiation level, and a combination of them. This approach could be used to simulate and examine various operating strategies for each system at the early stages of design and estimate their potential in improving the thermal performance of highly-glazed buildings in cold climates. Consequently, the results and findings from this research are likely to be of interest to audiences in both academia and industry.

1.4 Thesis structure

Chapter 2

This chapter provides a comprehensive literature review on the subject of passive energy techniques and their application in buildings. This includes a detailed description of thermal energy storage methods, including PCMs, and their passive and active integration to improve energy efficiency and thermal comfort of buildings. This chapter also discusses the current development of passive cooling systems and reviews the application of Energy Management System in controlling such systems in buildings.

Chapters 3 to 5

Chapters 3 to 5 provide a research methodology detailing an optimal integration of PCM and passive cooling control systems within the case study. Chapter 3 includes the simulation of Stanley Pauley Engineering Building (SPEB) in EnergyPlus, implementation of building model verification for evaluating EnergyPlus model outputs, and selection of a proper case study. Chapter 4 introduces a research methodology aiming to (i) simulate a wide range of PCMs with various melting temperatures using hysteresis information within EnergyPlus software, (ii) simulate the radiant hydronic floor with the incorporation of PCM storage, and (iii) investigate the optimal design of PCM-enhanced radiant floor. Also, the Genetic Algorithm was employed to identify the optimal solution for PCM-enhanced radiant floor by minimizing the total energy use of the SPEB. Furthermore, chapter 5 describes the simulation of various control strategies to monitor and regulate the performance of natural ventilation and external solar shading devices. For this purpose, two sets of control strategies were developed to control their operations based on different environmental factors such as indoor air temperature, and solar radiation level.

Chapter 6

This chapter presents a detailed performance analysis to assess the effectiveness of the optimal PCM-enhanced radiant floor (chapter 4) and passive cooling systems control strategies (chapter 5) on the overall energy and thermal comfort performance of the studied case study. The EnergyPlus model of SPEB was first verified against IES model developed by a consulting company, Stantec, by comparing the models' energy consumptions and indoor air temperatures. Next, the application of PCM and passive cooling systems were evaluated by performing a detailed comparative analysis between enhanced and base-case models.

Chapter 7

This chapter summarises the main findings of the work undertaken within this thesis, lists its limitations, and offers recommendations for further research.

1.5 Dissemination

The following outcomes of this research have been disseminated:

Conference paper:

Ali Mohammadzadeh, Miroslava Kavgic, Ali Al-Janabi. 2019. *Energy Management System (EMS): The Impact of Natural Ventilation and Shading Control on Thermal Performance of University Building in Winnipeg, Canada*, 5th Building Simulation and Optimization Conference. Rome, Italy.

Journal paper:

Ali Al-janabi, Miroslava Kavgic, **Ali Mohammadzadeh**, and Afaf Azzouz. 2019. Comparison of EnergyPlus and IES to model a complex university building using three scenarios: Free-floating, ideal air load system, and detailed. *Journal of Building Engineering* 22, 262–80.

Ali Mohammadzadeh, Miroslava Kavgic. 2019. Multivariable optimization of PCM-enhanced radiant floor in highly glazed study rooms in cold climates. *Journal of Building Simulation* (Submitted).

2 Literature review

Nowadays, code requirements for the energy performance of buildings are becoming more stringent to overcome concerns of high energy consumption in buildings. The ultimate goal is to minimize buildings' greenhouse emissions as far as reasonably feasible. Therefore, the design of new buildings is required to consider the concept of sustainability by integrating appropriate energy efficient methods with building systems to achieve low carbon operation goal. The use of passive approaches in building design is a useful measure for improving the energy efficiency of buildings and reducing their reliance on fossil fuels such as natural gas, coal, and oil (United Nations, 2014; Sadineni et al., 2011).

The continuous interest in developing sustainable buildings over the last decades has required designers and engineers to more effectively utilize the concept of passive energy systems in building design. Direct solar radiation, for example, is considered to be one of the most significant sources of passive solar design, especially in cold climates. However, given the lower heat storage capacity of lightweight buildings (such as curtain wall and steel-framed construction), the natural solar gains may not be utilized efficiently during the cold months. One of the options for increasing heat storage capacity in lightweight buildings is to artificially increase the thermal mass by developing Thermal Energy Storage (TES) systems, which have high potential to save energy in buildings. This approach allows the buildings to efficiently absorb excess thermal energy and use it hours, or days later. Also, the lower thermal capacity of lightweight buildings may raise the risk of overheating issues within the occupied spaces (especially in highly glazed buildings), which requires to be encountered by using and controlling energy-intensive cooling systems, such as natural ventilation and solar shading systems.

2.1 Thermal Energy Storage (TES)

Thermal energy can be stored as a change in the internal energy of materials through three possible means: sensible heat, thermochemical, and latent heat. An overview of available techniques in thermal energy storage is demonstrated in Figure 2.1.

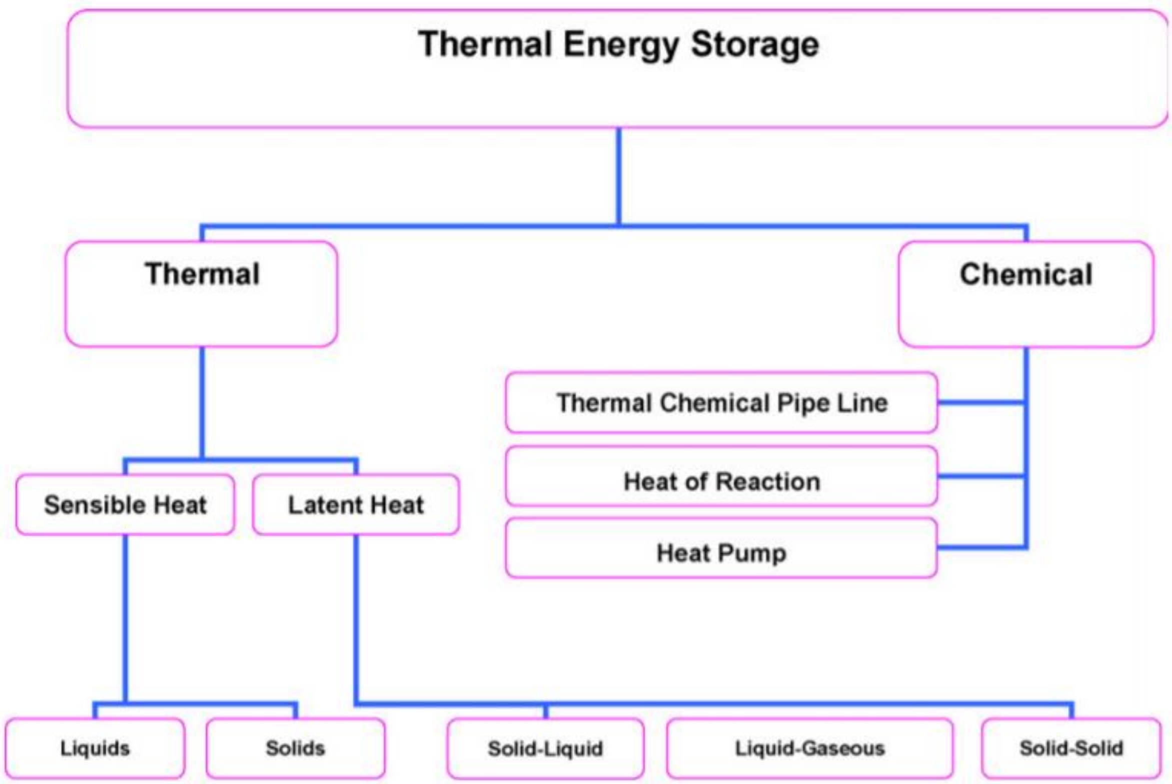

Figure 2.1: A classification of TES method (Sharma et al., 2009).

Sensible heat storage method is considered as the simplest method of thermal storage in that the heat is stored or released by directing a temperature gradient to a solid or liquid state. For example, water has been traditionally used for sensible heat storage (Hasanain, 1998), and appears to be the most significant sensible heat liquid available due to its cost efficiency and high specific heat capacity. The amount of heat stored in this method depends on the amount of storage material, the temperature, and the specific heat of the medium (Lane, 1983). The governing equation for this type of heat is:

$$Q = \int_{T_i}^{T_f} mC_p dT \qquad (2.1)$$

$$= mC_{ap}(T_f - T_i) \qquad (2.2)$$

where Q is the quantity of stored heat, m refers to the mass, C_p is specific heat at constant pressure, and T_f and T_i denote the two temperatures before and after heating.

Thermochemical materials (TCM), on the other hand, offer thermomechanical storage in which reversible chemical reaction is the critical feature in increasing energy efficiency (Rammelberg et al., 2016). This type of thermal storage method can be given as follows:

$$Q = a_r m \Delta h_r \qquad (2.3)$$

In this method, the amount of stored heat depends on the endothermic heat of reaction (Δh_r), the extent of conversion (a_r), and the mass of storage material (m). This technology has a higher potential in storing heat energy per unit of mass compared to the sensible or latent heat storage approaches as it has higher energy capacity and requires a lower volume of material, which yields a more efficient design (Saffari et al., 2017). However, studies showed that further investigations are still required to improve this method to be more viable and user attractive (Solé et al., 2015; Saffari et al., 2017).

2.1.1 Phase Change Materials (PCMs)

Phase Change Materials (PCMs) are "Latent" form of heat storage materials that transfer thermal energy based on material phase changes from solid to liquid states, or from liquid to solid states. The change in material state is called "Phase". Similar to conventional storage materials, the solid-liquid PCMs absorb heat when their temperature rises. However, unlike the sensible method, PCMs are able to store 5-14 times more heat per unit volume within a nearly constant temperature (Sharma et al., 2009). However, in order for PCMs to perform properly as latent heat storage materials, they require careful design and should meet certain requirements including: 1) minimal supercooling, 2) low cost, 3) high thermal conductivity, 4) non-flammable, 5) high availability, 6) practical melting temperature set-point suitable for the heat storage application, 7) chemically stable to not degrade over time, 8) high latent heat of fusion per unit volume, 9) non-toxic and non-corrosive (Pasupathy et al., 2008).

Contrary to the previous methods, the Latent Heat Storage (LHS) method relies on material phase change enthalpy to build up heat within a short temperature difference, which creates a possibility of achieving higher energy density compared to the sensible heat storage over the same temperature gradient. The storage capacity of the Latent Heat Storage with a Phase Change Material (PCM) medium can be formulated as (Lane, 1983):

$$Q = \int_{T_i}^{T_m} mC_p dT + ma_m \mathrm{f}\Delta \mathrm{q} + \int_{T_m}^{T_f} mC_p dT \qquad (2.4)$$

$$Q = m\left[C_{ps}(T_m - T_i) + a_m \Delta h_m + C_{\mathrm{pl}}(T_f - T_m)\right] \qquad (2.5)$$

where T_m is the melting temperature, C_{ps} is the average specific heat of the solid phase, C_{pl} is the average specific heat of the liquid phase, f is the melt fraction, and Δq is the latent heat of fusion.

2.1.2 Types of PCMs

Phase change materials (PCMs) fall into three subcategories based on their chemical composition, including organic, salt hydrate, and eutectic. Organic PCMs such as paraffin and fatty acids are capable of storing and releasing thermal energy in much higher storage capacity due to their narrow melting temperature set-point, making them reliable in fulfilling the issues discussed above. They have a high latent heat of fusion, non-toxic, non-corrosive, chemically stable, and relatively low cost. However, the main drawbacks of organic PCMs are their unacceptably low thermal conductivity and potential hazards of flammability (Zeng et al., 2010). Despite these shortages, this type of PCM still is known as the most popular PCM material (Evola et al., 2013). The salt hydrate PCMs contains a wide range of materials that also have water molecules in their crystalline structure. Some examples of these materials commonly used in PCM application are "manganese nitrite hexahydrate" ($Mn(NO_3)2.6H_2O$), "calcium chloride hexahydrate" ($CaCl_2.6H_2O$), and "lithium nitrite trihydrate" ($LiNO_3.3H_2O$). Among many benefits related to this type of PCM, the most remarkable ones include: 1) high level of latent heat of fusion, 2) low price (cheaper that paraffin-based PCMs), 3) high thermal conductivity, and 4) non-flammable. However, their main disadvantages are: 1) degradation after continuous phase change cycles, 2) prone to super-cooling, and 3) can be corrosive. Eutectic materials are produced by mixing two or more components. These materials are intended to minimize the shortages associated with the organic and salt hydrate PCM and maximize their best properties. Some studies have been carried out to investigate the organic-inorganic compounds such as myristic-stearic acid (Sari and Kaygusuz, 2006) and myristic-palmitic acid (Sarı, 2003).

2.1.3 Application of PCMs in buildings

Thermal energy storage plays a key role in building energy efficiency, which can be significantly improved by the integration of latent heat storage in different applications. Lately, PCMs with strong ability to store heat during peak power operation has been used in building envelopes as an efficient way of thermal control (Kośny, 2015). According to the International Energy Agency (IEA, 2019), "Energy Conservation through Energy Storage" Annex 16, energy storage technologies, including the PCM method, are considered as necessary and strategic components for energy conservation in buildings. PCMs are emerging latent heat materials with the potential to dramatically decrease heating and cooling energy consumption when applied properly. Published studies have investigated this potential under different circumstances, and the results showed that utilization of PCMs could substantially improve building energy conservation (Barzin et al., 2015; Castell et al., 2010; Lei et al., 2016). A wide range of studies indicated that proper incorporation of PCMs in well-insulated buildings could result in cooling and heating energy savings between 5 and 30% (Schossig et al., 2005; Feustel, 1995; Feustel and Stetiu, 1997). In the building application, PCM thermal mass can be incorporated into building envelopes (e.g., walls, floor and ceilings, the attic floor insulation) either through means of passive solar heating, active heating (Navarro et al., 2016), or night cooling (Figure 2.2).

In passive solar heating, the idea is to store heat by absorbing natural, sensible heat generated by internal heat sources (e.g., solar gain, people, lights and equipment) during the daytime and releasing the absorbed heat when there is low internal load within the space at night. As a result, the indoor temperatures become lower during the day (i.e., cooling savings) and higher during the night (i.e., heating savings) and consequently, this leads to heating and cooling energy savings.

The two most common approaches of installing PCM for passive heating and cooling of buildings include:

(i) Installing PCMs within buildings external and internal walls;

(ii) Installing PCMs within other building envelope elements such as floor and ceiling.

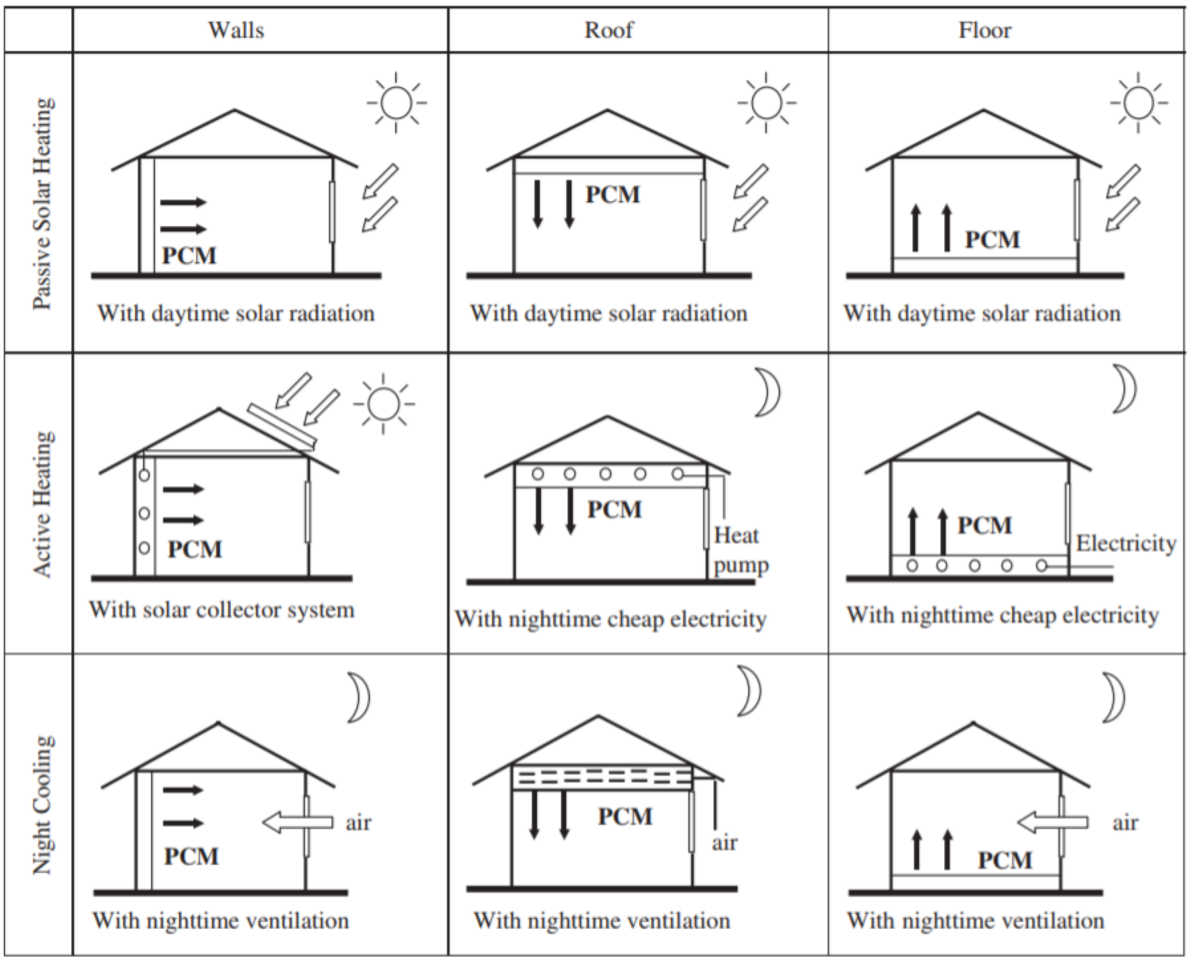

Figure 2.2: The application and effects of the PCM building envelope (Marco, 2005)

For instance, the application of PCM in building wallboards is a well-established form of passive solar heating because it is inexpensive and widely used in building applications (Soares et al., 2013). Many research studies have investigated the application of PCM-enhanced wallboards numerically (Heim and Clarke, 2004; Kuznik et al., 2008) and experimentally (Shilei et al., 2007;

Kuznik et al., 2011). Kuznik et al. (2008) developed an optimization problem using internal-external temperature evolutions within 24 hours to find the optimal thickness of PCM-enhanced wallboard to improve the thermal performance of a lightweight structure. The PCM used in this study was 60 wt% of microencapsulated paraffin with a melting temperature of around 22°C. The results showed that PCM with an optimal thickness of 1cm could avoid overheating during hot days, while in cold night, it increases the indoor air temperature by releasing the stored heat. Moreover, experimental studies have also demonstrated the benefits and limitations of using PCMs in building envelopes. In this context, Lee et al. (2015) experimentally investigated the optimal solution for the position of PCM thermal shields into west and south buildings walls to minimize peak heat flux. In another experimental study, Castell et al. (2010) evaluated an insulated house enhanced with macro-encapsulated panels RT27 (melting temperature of around 27°C), resulting in an energy savings of 15% for space cooling.

In the active mode (Figure 2.2), on the other hand, a human-made heat or cold sources would be used for charging or discharging of the energy storage in PCM using mechanical equipment. PCM can be incorporated into mechanical systems, such as a heat recovery system, solar heat pump systems, and floor heating systems, etc., to improve the heat transfer performance. In this case, the stored heat can be used to reduce the amount of heating/cooling energy use by shifting the energy demand from the peak to off-peak electricity hours (Farid and Kong, 2001).

The performance of active PCM storage for space heating and cooling has been investigated in several studies (Kaygusuz, 1995, 1999b, 1999a, 2003; Kaygusuz and Ayhan, 1999; Esen, 2000; Hammou and Lacroix, 2006; Kunping et al., 2005; Saman et al., 2005). For instance, in two studies, Kaygusuz (1999a, 1999b) numerically and experimentally studied the thermal performance of a solar-assisted heat pump with the incorporation of PCM for residential heating. These studies aimed to predict the impact of the proposed system on indoor air temperature variation, the water temperature (i.e., heat transfer fluid) in the solar collector, and temperature fluctuation of PCM in energy storage tank for parallel, dual, and series source heat pump systems. It was concluded from the results that PCM is a critical component of solar-aided heat pump systems in the moderate system, but the amount of PCM must be carefully calculated at the design stage to increase mean daily performance. The results also showed that the series system is capable of savings net energy by 9,390kWh while the parallel system can save 10,120kWh energy and dual source system can save net energy of 12,056kWh.

In addition, the PCM can be incorporated into the building under-floor heating systems to absorb heat from heater during the night when electricity cost is lower and release the stored heat during the day (peak hours). Also, PCM thermal mass offers larger latent heat storage than dense materials such as concrete, and therefore, it can improve the thermal comfort level (Zhang et al., 2007). Figure 2.3 demonstrates a schematic view of a radiant floor system enhanced with shape-stabilized PCM, including wood floor, air layer, PCM, electric heater, and insulation (Lin et al., 2004).

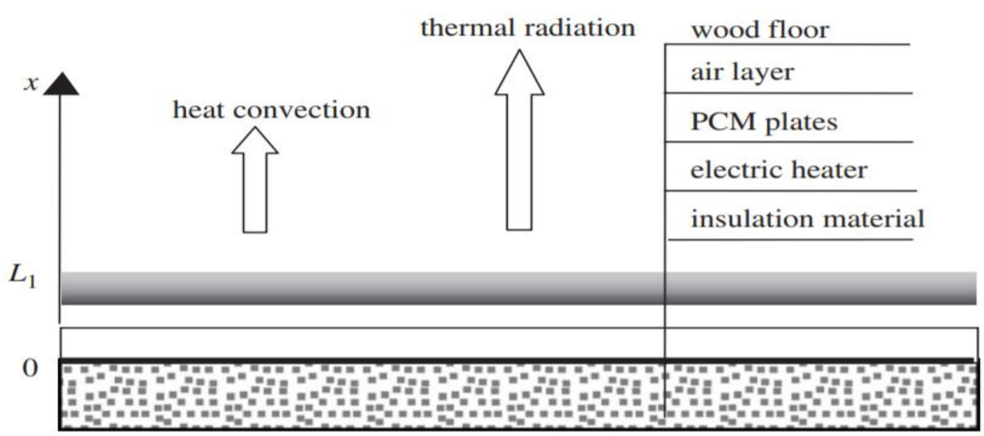

Figure 2.3: Schematic view of the slab heating system enhanced with shape-stabilized PCM plates (Lin et al., 2004).

Performance of the slab heating systems with the incorporation of PCMs have also been analyzed in several studies (Farid and Chen, 1999; Lin et al., 2007; Farid and Kong, 2001). For example, Farid and Chen (1999) proposed a novel electrical floor heating system containing encapsulated PCM (paraffin wax) to shift the use of electricity from the peak hours to the off-peak period. Figure 2.4 illustrates a sketch of PCM-incorporated floor heating system in which a 30 mm layer of PCM with a melting point of 40°C was located between the heated surface and the 30 mm floor tiles. The findings indicate that although it is possible to maintain constant heating throughout the day, however, the heat output could be considerably raised from 30 to 75W/m^2 when a uniform layer of PCM storage is placed at the top of the heat source. In another study, Farid and Kong (2001) constructed two concrete slabs ($0.5\ m \times 0.5\ m \times 0.095\ m$) with a hydronic heating system (i.e., hot water pipe) embedded in both of them where one of the concrete slabs contained a 75 mm layer of PCM storage. The results showed that the concrete-PCM slab could ensure uniform heating throughout the day and also reduce surface temperature fluctuation and could maintain the floor surface temperature close to the acceptable temperature of 24°C. It was also suggested that in order to achieve high thermal storage, the system variables (e.g., concrete thermal conductivity, PCM type, and thermal properties) must be designed properly. Another numerical (Lin et al., 2007) and experimental (Kunping et al., 2005) studies of incorporating PCM with floor heating system were performed where an electric radiant floor system was integrated with shape-stabilized phase change material (PCM) plates. In these studies, PCM was thermally charged by cheap nighttime electricity heating and distributed the stored heat at pick-hours. The results indicated that this system could perform well only if the PCM melting temperature and thickness are chosen properly. The active system discussed in above studies has demonstrated that the integration of PCM storages with mechanical systems are thermally efficient and technically feasible if the system is designed properly before implementing in practice (Zhu et al., 2009).

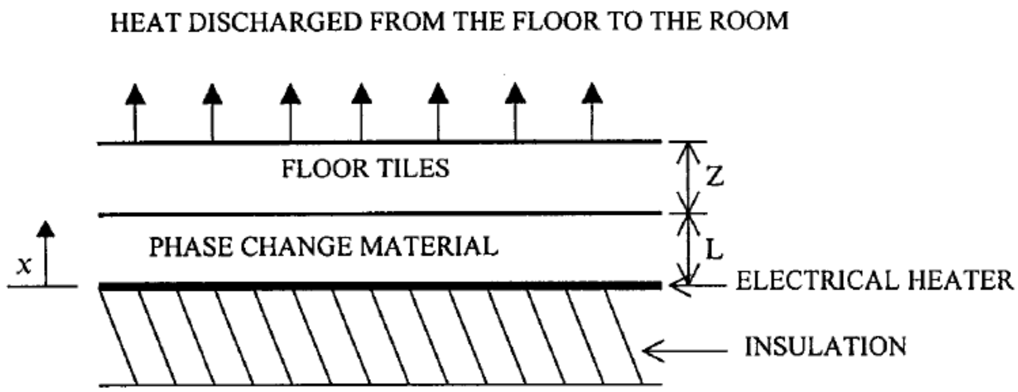

Figure 2.4: Sketch of the underfloor heating system incorporating PCM (Farid and Chen, 1999)

2.2 Passive cooling

As mentioned previously, the passive solar design can benefit buildings in cold climates by minimizing heating energy demand and improving the indoor environmental quality of buildings (e.g., daylight and thermal comfort) without additional construction or maintenance costs (Stevanović, 2013). However, in cold climate regions with hot summers such as Winnipeg, excessive solar energy may result in overheating in summer, which in turn leads to increased use of the cooling system. Therefore, the incorporation of passive cooling technologies into building design can be an effective solution in such climates for reducing cooling demand and overheating hours during summer. Passive cooling refers to energy efficient and eco-friendly measures that aim to control heat gains and heat dissipation in buildings in order to maintain comfortable conditions with no or low energy consumption (Samuel et al., 2013; Santamouris and Asimakopoulos, 1996). This method is used to either prevent heat from entering the space (heat gain prevention) or remove heat from the building. Classification of passive cooling systems are summarized in Figure 2.5 (Givoni, 1994).

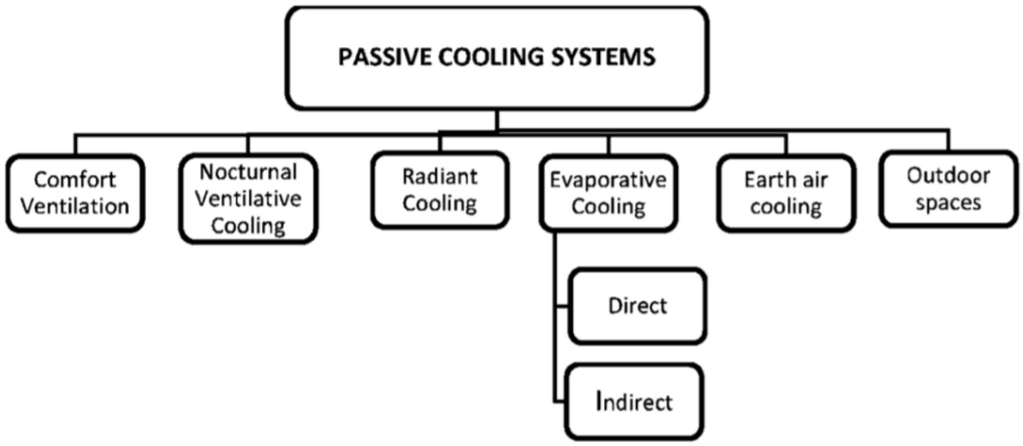

Figure 2.5: Classification of passive cooling systems (Givoni, 1994).

There is a wide range of passive cooling techniques that are classified based on their applications and performance (Samuel et al., 2013). Natural heat sinks such as ground, water, and air when incorporating into building systems can be effectively used to account for partial or total cooling energy demand during summer or throughout the year. The earth-air cooling, for example, takes advantage of the natural thermal inertia of earth to achieve energy efficiency and comfort in buildings (Kumar et al., 2007) through earth tunnel cooling (Sharan and Jadhav, 2003) or earth sheltering (Anselm, 2008) (earth as a heat sink). Underground water with low temperature (hydro geothermal cooling) or from surface water bodies such as ocean or lake could be another efficient source of cooling due to its cost efficiency and reliability (Saaly et al., 2019; Maryam Saaly, Pooneh Maghoul, 2019). Passive cooling can also be achieved by removing sensible heat from an interior space (such as using natural ventilation (Sekhar and Goh, 2011) or by decreasing heat transfer into the building using thermal insulation or shading devices.

The efficiency of passive cooling systems depends significantly on local climatic characteristic and is closely related to the outdoor temperature gradient daily (Pacheco et al., 2012). Many studies have shown that specific techniques such as natural ventilation and solar shading systems are immediately useful in improving comfort conditions and reducing building cooling energy use in hot and tropical climates (Gómez-Muñoz et al., 2003; Givoni, 1994; Al-Obaidi et al., 2014; Meng and Zhang, 2006). However, there is a lack of research focused on the application of such systems in cold climate regions with warm and humid summers such as Winnipeg.

2.2.1 Natural ventilation system

The term “natural ventilation” refers to the process of providing and removing air to or from an interior space during occupied hours without the need for mechanical systems. Generally, it allows external air flowing to an indoor space caused by pressure differences between the outdoor and indoor environment. The pressure differences are created either by wind driving forces or stack effect (or buoyancy), which can be applied to the building system separately or simultaneously. Wind-driven ventilation can be achieved through pressure differences made by wind around the building, and openings structured on the perimeter that allow air flow through the building. Stack effect, on the other hand, corresponds to the movement of air into and out of the building as the result of air buoyancy (Linden, 1999). In other word, buoyancy-driven ventilation occurs due to the difference between indoor and outdoor air density, which in large scale is due to the difference in temperatures. When there is a temperature difference between two adjacent volumes of air, the warmer air rises above cold air as the result of density stratification and creates an upward air stream. This type of ventilation is more feasible in colder climates (Asfour, 2015) since there is a high difference between internal and external air temperatures. A basic concept of natural ventilation strategy in the building application is demonstrated in detail in Figure 2.6 (Actual, 2015). Ideal conditions for effective implementation of natural cooling in buildings are: external façades with the inclusion of windbreak, spaces with high solar heat gains; external solar shading

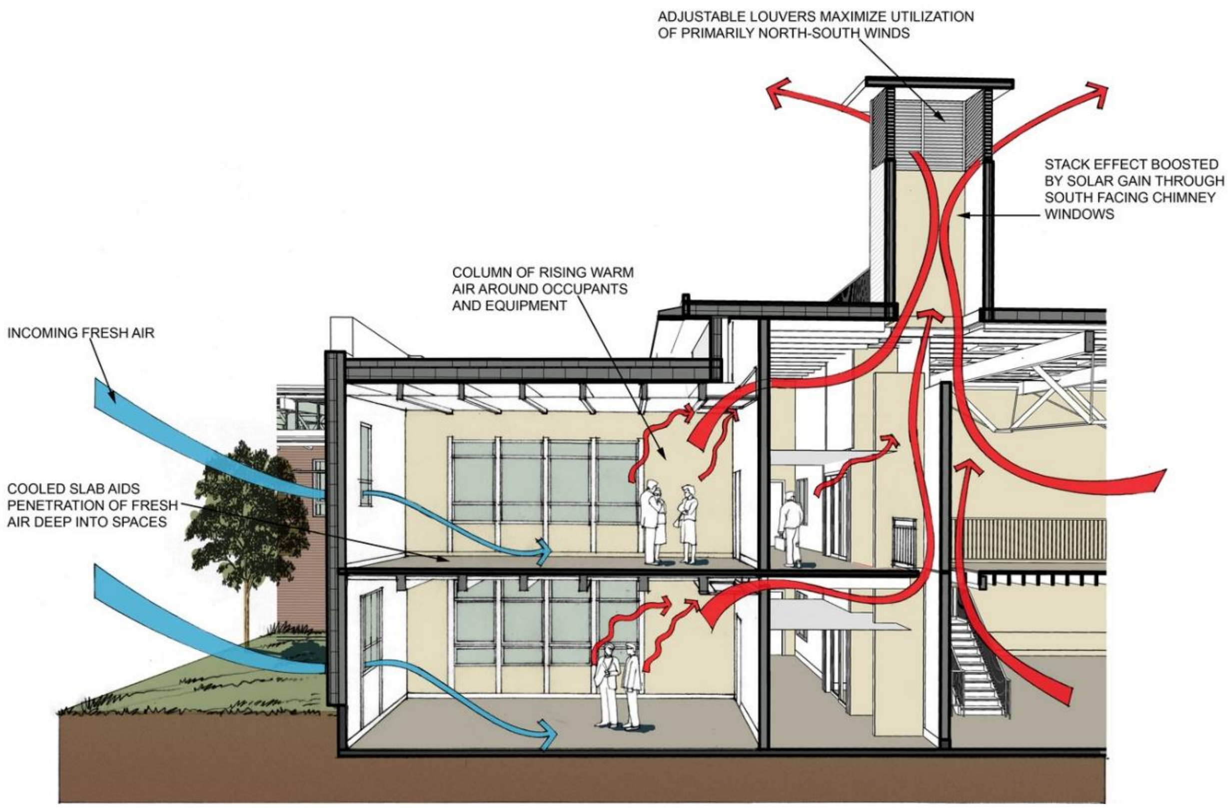

Figure 2.6: Basic Natural Ventilation Concept for Office Type Buildings (Actual, 2015)

attached to the south-facing windows; use of glazing with low thermal conductivity (U value); and effective use of Building Energy Management Systems (BEMS) (Brittle, 2017).

As discussed above a major factor in designing natural ventilation is the external climate, and in particular, the way hot and cold outdoor temperatures influence naturally ventilated buildings. For example:

- In summer, when the outdoor air temperature is lower than indoor air temperature, airflow into the building can remove internal heat gain and improve occupants' thermal comfort. In contrast, if the indoor air temperature is lower than the outdoor air temperature, natural ventilation can have a negative impact on indoor thermal conditions as it may bring warmer air into the building (overheating risk during the summer).

- If both indoor and outdoor air temperatures are equal, natural ventilation is not able to improve thermal comfort, while it is still beneficial in supplying fresh air to the interior space.

- In winter, when the indoor air temperature is higher than comfort set-point (particularly during the day when solar gain rises), natural ventilation can be used to reduce the effect of overheating nearly at noon.

The negative effect of climatic conditions on naturally ventilated spaces can be mitigated by applying different control strategies (Schulze and Eicker, 2013). In the basic form of control in conventional buildings, the indoor thermal conditions are usually controlled by occupants when opening or closing openable windows, for example Roetzel et al. (2010). In such buildings, occupants can manually modify the sizes of opening windows in order to create a positive thermal sensation. Therefore the interaction of occupants with ventilation provisions (such as a window) for providing necessary thermal comfort, may add extra heat to space. More intelligent controls over the thermal environment that are responsive to the outdoor conditions can be obtained by using more complicated control systems. In these advanced methods, natural ventilation system automatically adjusts its area via damper in response to the internal environmental factors such as internal dynamic temperatures and humidity. The means of such controls can be carried out by some form of Building Energy Management Systems (BEMS). For example, the air flow rate entering the interior space can be regulated by changing the position of a damper in response to the indoor air temperature or CO_2 emission concentration.

Nevertheless, uncontrollable factors such as high exterior air temperature during summer can limit external supply air temperature to be lower than a set-point temperature. Therefore, for average outdoor air temperatures greater than specified criteria, auxiliary passive solar techniques such as external solar shading could be useful in moderating indoor thermal conditions. As recommended by Iqbal and Al-Homoud (2007), other strategies include the use of alternative mechanical ventilation techniques such as Variable Air Volume and Constant Air Volume (VAV and CAV), increase of set-point temperature, or nighttime cooling.

2.2.2 Solar shading

Solar heat gain is created as the result of short wave radiation naturally coming from the sun that heats a building either directly through an opening (such as a window), or indirectly through physical components of buildings (Gupta and Tiwari, 2016). Additionally, natural lighting provided by sunlight can be beneficial in improving occupants' visual comfort, and in reducing the need for necessary artificial lighting. Studies have shown that natural lighting can have positive psychological benefits by improving occupants' productivity in the work environment and their well-being (Boyce et al., 2003; Edwards and Torcellini, 2002). In a survey collected from office workers, results indicated that more sunlight penetration could result in higher job satisfaction (Leather et al., 1998). Despite advantages of natural lighting mentioned above, an excessive amount of solar radiation entering an interior space can cause overheating (thermal discomfort), which may require additional energy-intensive cooling, or can result in glare, a form of visual discomfort when lighting is excessively bright. Therefore, solar shading could be used to restrict excessive solar radiation effectively.

Solar shading is a form of solar control that, when applied effectively, aims to minimize the amount of solar heat during overheating hours without adversely affecting visual comfort (Littlefair, 1999). This strategy can significantly improve energy efficiency in buildings and provide thermal and visual comfort for occupants by preventing overheating and glare entering the space, particularly during summer (Hammad and Abu-Hijleh, 2010). As shown in Figure 2.7, solar shading can be divided into three primary classifications including fixed (such as trees, canopies, and external louvres), moveable (such as internal and external blinds, and Internal or external shutters), and other types of solar shading (such as combination of electrochromic windows and overhangs) (Bellia et al., 2014). Figure 2.8 also demonstrates the different shapes of solar shading systems.

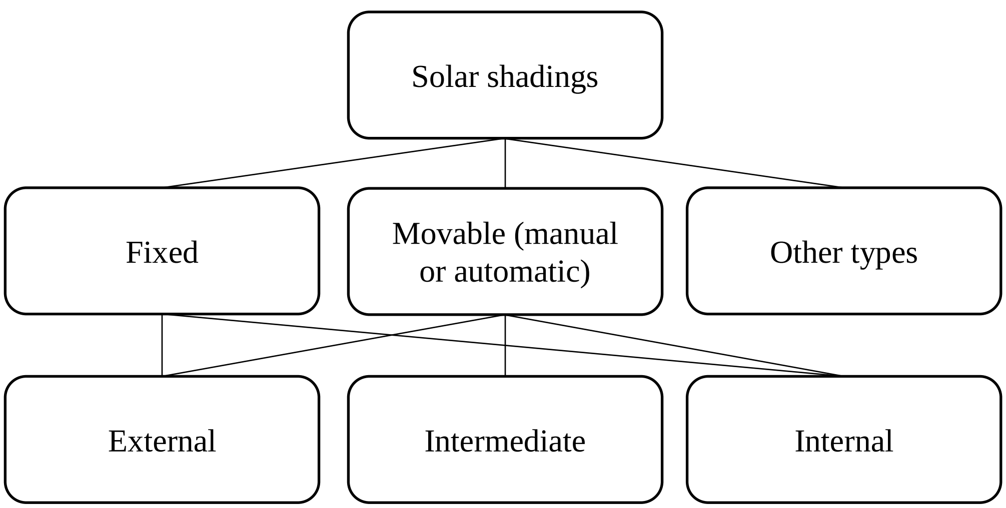

Figure 2.7: Classification of solar shading systems for building (Bellia et al., 2014).

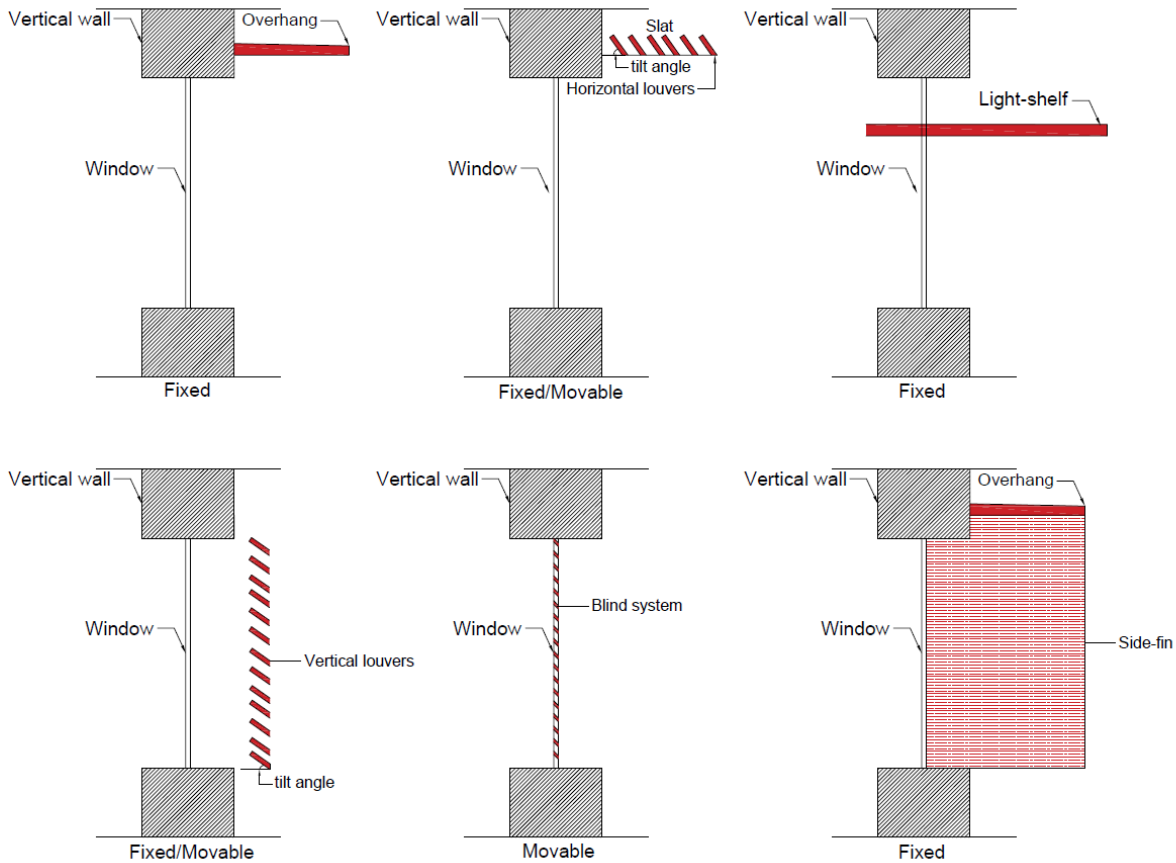

Figure 2.8: Shading types, adapted from Bellia et al. (2014).

Earlier studies completed for estimating the impact of fixed solar system on energy and thermal comfort performance of different building types indicate that proper design of such a system can reduce both lighting and cooling energy demand under different climate conditions (Ochoa and Capeluto, 2006; Wong and Istiadji, 2004; Claros and Soler, 2001; Datta, 2001; Bellia et al., 2014). For example, Datta (2001) analyzed the influence of fixed horizontal louver shading devices on the energy performance of buildings using energy simulation program (TRNSYS) in four different cities in Italy. The results showed that the effective use of fixed solar shadings could reduce the heat gain by 70% in summer and 40% in winter. However, compared to the fixed solar shading approaches, automated shading systems can continually adjust the length and size in response to the various internal (e.g., indoor air temperature, daylighting level) or external (e.g., solar radiation level) conditions. Therefore, while using such control can considerably reduce cooling energy demand in buildings, at the same time, it has minimum negative impacts on occupants' visual comfort, as recommended by Nielsen et al. (2011). In this study, they evaluated the potential of different solar shading façade elements (including fixed solar shading and dynamic solar shading) in improving energy demand, indoor air quality, daylighting level, and visual comfort. The results showed that compared to the fixed solar shading systems, the use of dynamic solar shading could considerably reduce cooling energy use while provides a sufficient amount of daylight in the space.

The introduction of dynamic solar shading control to the building fenestrations raised the possibility of achieving more beneficial resources, such as daylight and insulation, concerning both occupant comfort and energy demand requirements (Lee et al., 1998). There have been previous studies in this field that provide more insight into the relation between automated shading system and building energy consumption and occupants' comfort level (Lollini et al., 2010; Tzempelikos and Athienitis, 2007). For example, Tzempelikos and Athienitis (2007) performed an integrated lighting-shading control using an advanced window system with motorized shading to investigate the impact of dynamic shading control on building energy demand and daylight illumination in Montreal, Canada. The results of simulation showed that significant energy savings for cooling and lighting could be achieved if an integrated approach for control of shading and lighting systems is used. In another study, Lollini et al. (2010) studied the impact of dynamic solar shading control on annual and monthly cooling energy use in an office building. They developed a dynamic glazing system with the incorporation of a controllable shading device to actively respond to the external environmental loads. Analysis of simulation results showed that compared to the model without a shading device, the dynamic control of external shading element can cause significant energy savings. Regarding occupants' visual comfort, Koo et al. (2010) developed an innovative control method for automated blinds, which aimed to maximize the amount of daylight level in space while preventing direct solar glare. The results showed that the proposed control method can compromise between energy savings and occupants' visual comfort. However, it was mentioned that excessive daylight could adversely influence cooling energy efficiency in summer. Therefore the maximization of daylighting level and cooling energy savings requires further investigations. Choosing the optimal control for solar shading system, however, is a complex discipline with many interdependence input parameters such as indoor air temperature, daylighting level, and solar radiation level, which often are contradictory to one another (Nielsen et al., 2011).

2.2.3 Control of natural ventilation and solar shading systems

The control of natural ventilation systems either focuses on improving Indoor Air Quality (IAQ), indoor air temperature or a combination of both (Schulze and Eicker, 2013); while control of solar shading system focuses on reducing the amount of glare entering the space and improving daylight availability. The main objective of both controls is to maximize energy savings while reducing discomfort conditions (including thermal, air quality, or visual discomfort) within the occupied spaces. In most basic control systems (such as unity feedback control) a single sensor is used to monitor internal environmental condition (e.g., indoor air temperature or CO_2 emission) and apply mechanical cooling or heating energy accordingly whenever the measured variable exceeds a maximum target criteria. For example, the cooling control is turned off when the indoor air temperature drops below the specified threshold to ensure the difference between the measured air temperature and given set-point (error) is equal to zero (or is at the minimum value). This strategy offers a beneficial and powerful tool when designing a control system due to its ease of installation and effectiveness of regulation (Stefanopoulou and Kim, 2015).

However, in more complicated modes, system outputs (such as building energy use) are affected by both internal and external environmental factors such as indoor-outdoor air temperatures or solar radiation level. For example, in naturally (or hybrid) ventilated spaces, energy use is affected by multiple variables including internal and external air temperature, wind speed and direction, dynamic indoor conditions, or other control flow variables. Therefore the complexity of controlling various variables recommends the use of an integrated rule-based control system that concurrently takes all or most of these variables into account (Khatami et al., 2013). It was proven that introducing greater domain of inputs and strategies into the controller algorithm can improve the results in terms of thermal comfort and energy savings (Dounis et al., 1996, 1995; Marjanovic and Eftekhari, 2004).

The implementation of such integrated control strategies requires a sophisticated system that can minimize building energy use in response to a large variety of environmental aspects while maintaining comfort conditions. In this context, the role of Building Energy Management Systems (BEMS) as a useful tool in minimizing building energy demand and providing a comfortable environment for occupants is known and significant (Doukas et al., 2007). The following sections discuss the concept of BEMS and in particular reviews its application in Building Energy Simulation Tools (BEST).

2.3 Building Energy Management System (BEMS)

Building energy management system (BEMS) is a sophisticated computer-based method for monitoring and controlling the building's mechanical and electrical equipment that can significantly improve its energy performance. However, the majority of recent developments in BEMS are related to the active systems, i.e., heating, ventilation, and air-conditioning (HVAC) systems (Doukas et al., 2007). Earlier studies used different techniques for controlling HVAC systems ranging from adaptive control, optimal regulator, and pole-placement (Zaheer Uddin, 1993; Zaheer Uddin, 1994). In addition, more advanced methods such as a neural network (Kanarachos and Geramanis, 1998), and genetic algorithm (Huang and Lam, 1997) for controlling the HVAC system were also developed. Integrated control systems coupling optimized fuzzy controllers and genetic algorithm for the indoor environmental management have also been developed, implemented, and tested (Kolokotsa et al., 2002). Also, the development of BEMS in controlling "intelligent buildings" have shown ongoing interest among research community on this topic (Kua and Lee, 2002; Wong et al., 2005; Kolokotsa et al., 2002). Kolokotsa et al. (2002) proposed a new architecture incorporating the application of BEMS into newly-built and existing buildings to monitor the overall performance of building systems including building energy use and occupants' comfort level. The results showed that the integration of BEMS with building system could reduce building energy use and occupants' discomfort.

Recent research studies on BEMS problems and their associated technical solutions have shown that simulation tools play an essential role in implementing and evaluating the application of EMS in buildings (Clarke et al., 2002). Building energy modeling (e.g., EnergyPlus) can be used to imitate the thermal behavior of buildings and simulate their response to the BEMS commands.

These tools can be used for developing control products, tuning of control systems, training of BEMS operators, and detecting fault patterns (Kelly et al., 1994). Also, energy modeling programs can be utilized to evaluate the efficiency and feasibility of possible control strategies. In such a case, a detailed model of the building with its associated active and passive systems is developed, and various control strategies are tested in terms of energy efficiency and comfort acceptability (Haves et al., 1998; Lebrun, 1992).

2.3.1 Energy Management Systems (EMS) in EnergyPlus

Conventionally, the control algorithms in building energy simulation tools (such as EnergyPlus) were intended to simulate typical operational strategies such as thermostatic control, daily and annual schedules, flow control, equipment load staging, and daylighting control. Most simulation inputs have predefined control sequences hard-coded in the software and only provide users with access to schedules and set-points. As a result, the interactions between different elements in the simulation program are limited (Ellis et al., 2008).

The built-in EMS function is an advanced control approach available in EnergyPlus that allows users to implement customized controls and modeling routines. EMS provides users with a high-level, generalized, and supervisory control to override specified aspects of EnergyPlus modeling (EnergyPlus, 2018). The main objective of EMS is to imitate the energy management systems commonly used in real buildings inside the EnergyPlus. Thus, EMS can use a large variety of "sensors" (e.g., indoor temperature and pump energy use) to direct various types of control actions by controlling the "actuators" such as roller shade, or pump valve. All these "sensors" and "actuators" are nodes provided within the EnergyPlus model. For example, similar to the high-level control objects available in EnergyPlus, EMS can turn on and off fans and pumps (AvailabilityManager objects), as well as can change the set-point (DemandManager objects) on the system nodes. A simple instructive language called EnergyPlus Runtime Language (Erl) is used to define the logic of the control algorithms. The program uses Erl to perform the calculation by linking the Erl variables to the EnergyPlus output variables and meters. The EMS then initiates control actions by sending the command to the intended "actuator" and accordingly changes the value of this variable through the Erl program. Figure 2.9 shows the general scheme for the control of building systems in EMS models, which can be divided into three general categories including: (i) sensors level (building internal boundary, climatic boundary condition, and occupants preferences), (ii) control logic level, and (iii) actuators level (any building elements that can be controlled). For further information about the EMS in EnergyPlus, one can refer to the Application Guide for EMS provided by EnergyPlus documentation (EnergyPlus, 2018).

Previous research studies have investigated the application of EMS in EnergyPlus. Ellis et al. (2008) reviewed the inventory of controls in EnergyPlus, and in particular, explored some of the possible capabilities of the EMS module. Many standard controls in EnergyPlus, including low-level (e.g., schedule) and high-level (e.g., EMS) controls were examined, and their limitations were discussed. It was concluded that the built-in EMS feature in EnergyPlus and its flexible Erl language allow designers to simulate a wide range of control strategies that are not possible with low-level standard control objects. Favoino et al. (2015), in another research, studied the application of built-in Energy Management System (EMS) tool of EnergyPlus in developing an alternative control approach for adaptive glazing and validated the model by comparing the numerical results against experimental data. Results showed negligible difference arise between the simulated and actual modeling approaches. Dutton et al. (2012) also implemented a binary stochastic window-opening model using EnergyPlus's EMS feature to evaluate the predictive capacity of new window-opening features in EnergyPlus. The results showed both excellent potentials for the incorporation of occupant behavior models in EnergyPlus and the need for further development of the tool. In the same context, Gunay et al. (2016) used EMS to investigate the accuracy of EnergyPlus in predicting occupants' behavior in using operable windows, lighting, and blinds. Various occupancy models from the literature were used, and a comparison of heating, cooling, and lighting energy use predicted by each model was presented. The results showed that in general, the model prediction of window, blind and lighting use could considerably vary from that model to another.

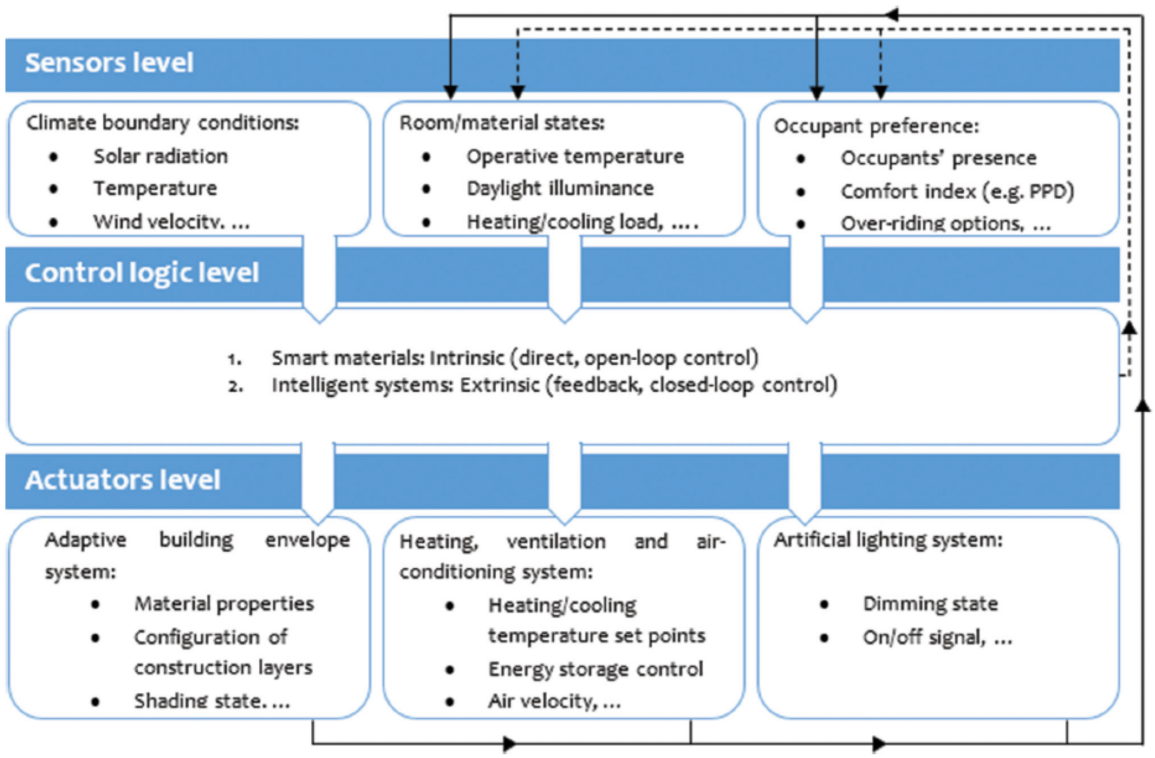

Figure 2.9: Control architecture for building systems (Loonen et al., 2017)

2.3.2 Energy Management System control type

The control of the building systems can fall into two categories, namely known as (i) *intrinsic* and (ii) *extrinsic* (Loonen et al., 2013). The term *intrinsic* corresponds to the adaptive capacity that is automatically activated by environmental stimulus (such as indoor temperature, humidity, and solar radiation). This type of autonomous control (dashed arrows in Figure 2.9) is also known as "direct" or "open loop" controls (Fox and Yeh, 2000) and the materials used in this process are known as "smart" (such as PCM) (Loonen et al., 2017), since environmental factors are directly converted to the control actions without use of external control elements. These "intelligent" materials can switch their mechanism by a variation in their internal energy. In contrast, *extrinsic* control types require feedbacks from external decision making components to be able to activate the adaptive capacity (continuous arrows in Figure 2.9). Feedback indicates that the impact of the present actions (configuration) can be contrasted with the level of set-point (desired state), and the behavior of the building system can be adapted accordingly. This type of control is also known as "closed loop" or "feedback" controls (Loonen et al., 2017). Therefore, a control management system is required to provide feedback in an adaptive way, which includes three principal components: sensors, processors, and actuators (Teuffel, 2004).

In order to analyze the reliability and effectiveness of innovative control technologies in BEMS, and to optimize their control design for building integration in the early design stage, whole-building energy simulation programs can be used (Dutton et al., 2012; Favoino et al., 2015). These tools can accurately simulate the dynamic behavior of such control systems when integrated at the building level (Favoino et al., 2015).

2.4 Summary

The main goal of this literature review was to introduce and compare the application of three passive energy techniques when incorporated into the building system and discuss the current findings regarding the potential of each technique in improving the thermal performance of buildings. The three techniques were (i) passive and active application of PCM in building envelopes, (ii) passive cooling systems including natural ventilation and solar shading devices, and (iii) current investigations regarding BEMs, and in particular the simulation of EMS in EnergyPlus. In general, earlier research studies have identified many benefits from the application of passive energy systems including lower heating and cooling energy demand (Barzin et al., 2015; Castell et al., 2010; Lei et al., 2016), enhanced thermal (Gómez-Muñoz et al., 2003; Givoni, 1994; Al-Obaidi et al., 2014; Meng and Zhang, 2006) and visual (Koo et al., 2010 comfort, and improved indoor air quality (Ben-David and Waring, 2016). However, a wide range of these research studies focused on the integration of passive energy systems in moderate and hot climates. As a result, their findings can be utilized by designers and building service engineers for similar types of buildings and climates, but they may not be as effective in buildings exposed to cold climates with hot and humid summers such as Winnipeg. Furthermore, the majority of the earlier studies have analyzed the performance of PCM integrated within the under-floor electrical heating system, and further studies are required to investigate the performance of PCM integrated into the hydronic radiant floor system.

3 Building energy modeling

3.1 Chapter outline

This chapter sets out a research methodology for simulating the Stanley Pauley Engineering Building (SPEB) in EnergyPlus software. Verified base case SPEB model was thereafter used for energy performance assessment of the passive energy systems, PCMs, natural ventilation, and shading. This chapter provides brief information about the EnergyPlus program (section 3.2). Then it outlines the design approach used to simulate the base case model (section 3.4) and model verification method (section 3.5). Next, it explains the selection of the case study for further implementation of PCM and passive cooling technologies (section 3.5). The final section of this chapter provides a summary (section 3.6).

3.2 EnergyPlus

Whole-Building Energy Modeling (BEM) is a multipurpose approach that provides a powerful tool for designers to replicate the thermal behavior of buildings using the computer-based simulation for retrofit design, green certification, code compliance, and real-time building control. EnergyPlus is a "new generation" whole-building simulation tool that can simulate multiple building systems using a network of nodes, which offers considerable flexibility in the modeling of building energy system (EnergyPlus, 2018). EnergyPlus is a thermal load simulation and energy analysis program designed for simulating buildings with all their related design elements, including building physical components, heating, ventilating, and air conditioning equipment. It can calculate the heating and cooling demand necessary to maintain desired thermal comfort (thermal control set-point), the energy consumption of plant equipment, and many other detailed simulation results that are required to verify the simulation performance.

EnergyPlus is a command-line program that takes input files and generates output files. In many situations, EnergyPlus requires two main input files in order to simulate the building model:

- IDF building model description file: Input Data File (IDF) provides a primary pathway by which model inputs can interact with the EnergyPlus engine (EnergyPlus, 2018). This file is a text file that contains a set of objects representing the building geometry and its associated operational systems.
- EPW weather file: Weather has a critical impact on the building thermal performance, and is required by EnergyPlus simulations to be able to run the model successfully. EnergyPlus Weather (EPW) file is a plain text file providing key weather information for different locations such as latitude, longitude, elevation, outdoor dry-bulb air temperature, peak heating, and cooling design conditions, daylight savings period, and solar radiation.

3.3 Numerical study: Simulation of Stanley Pauley Engineering Building (SPEB) in EnergyPlus

3.3.1 Building description

The newly-built Stanley Pauley Engineering Building (SPEB) is located at the Fort Garry campus of the University of Manitoba, Winnipeg, Canada. This building has been operational since 2019 and provides spaces for engineering programs and related research activities by accommodating up to 25% of enrolled students. In addition, the new and open-concept laboratories can be used by a variety of groups within the faculty. Figure 3.1.a shows that the orientation of the building is 26° to the west of true north. As illustrated in Figure 3.1.b, the SPEB consists of one-floor below-grade and three floors above-grade, with a total floor area of 4,200 m^2. A bridge link connects the building to the Engineering and Information Technology Complex (Figure 3.1.a). On the East side, the building is adjacent to the existing Stanley Pauley Centre. Window to wall ratio is around 60%, with the most glazing on the South and West sides of the building (Figure 3.1.b). The building design incorporates multiple envelope systems, which consists of double glazed, argon filled, insulating, low-E curtain wall glass, and well insulated external walls. Table 3.1 summarizes and describes the details of the main building's materials and constructions.

A high-energy performance combination of hydronic and air systems serves the SPEB to meet the building's heating and cooling load requirements. Furthermore, a frost resistant, dual-core energy recovery ventilation system provides 100% of the fresh air to the building. The outside air is primarily distributed throughout the variable-air-volume units, whereas two-pipe fan coil units circulate a mixture of direct outside air and local recirculated air within the space as needed. Heating or cooling water is flowing through cross-linked polyethylene piping embedded in the concrete floor of specific areas (e.g., mainly perimeter zones) to assist in heating or cooling. In heating mode, the radiant system provides the baseline heating while the air system provides the trim. Because of the thermal lag of the concrete slab, in heating mode, the fan coil units satisfy any temporary changes in the room temperature. The active floors serve areas where direct sunlight strikes the floor. The floors flow cooled water derived from the central campus chilled water system. Central high-pressure steam and pumped condensate return is provided to SPEB through a new connection routed through the lower level of the Engineering and Information Technology Complex. The presence of multiple systems in one zone varies upon the location, occupancy type, and the internal loads of that particular zone. Both the radiant floor system and the fan coil units are supplied with hot and chilled water by the central physical plant at the University of Manitoba.

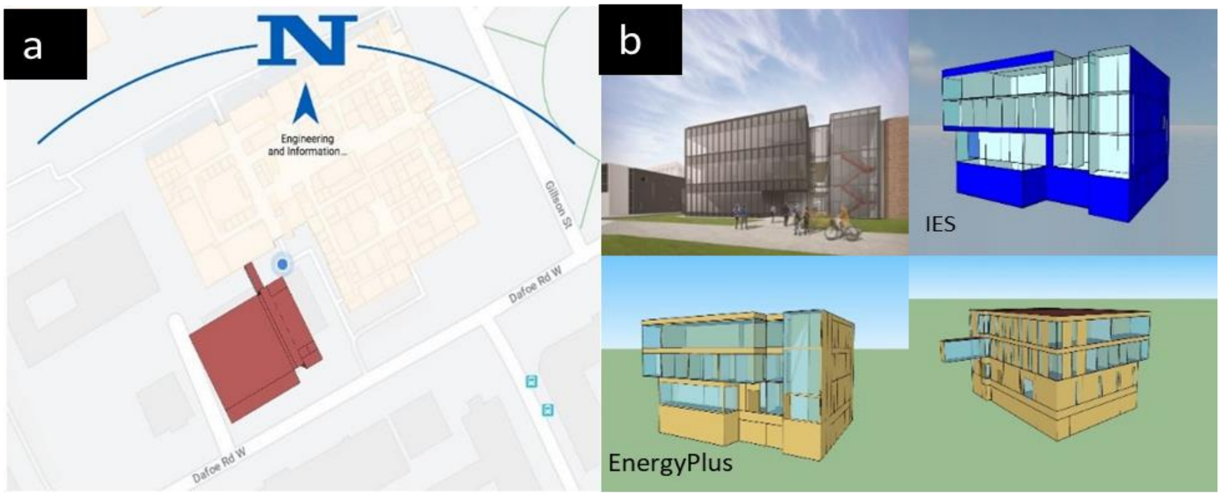

Figure 3.1: (a) Top view of the SPEB, (b) Front and back sides of the SPEB (Al-janabi et al., 2019).

Table 3.1: Stanley Pauley Engineering Building constructions and materials (Al-janabi et al., 2019).

Construction type	Constructions and materials	
Exterior wall	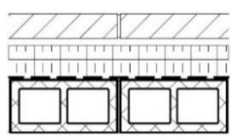	- 90 mm x 90 mm x 590 mm concrete masonry (outer layer) - 25 mm air gap - 125 mm 2 layers (50 mm + 75mm) board insulation - Air/vapor barrier membrane - 200 mm concrete masonry unit (inner layer)
Roof	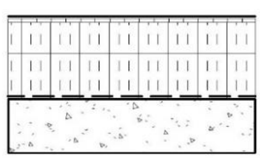	- Roofing membrane (outer layer) - Styrene-butadiene-styrene modified bitumen cap sheet - Styrene-butadiene-styrene modified bitumen base sheet - 250 mm 2 layers (150 mm + 100mm) board insulation - tapered board insulation for back slopes - Vapor retarder - Concrete slab (inner layer)
Floor		- 150 mm concrete slab

Interior partition		- 12.5 mm Plasterboard - steel studs / furring @ 400 mm O.C. - 12.5 mm Plasterboard
Window	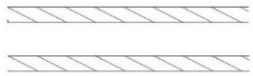	- 6 mm low-E outer glazing layer - Spacer: stainless steel finish: black - 13 mm argon filled gap - 6 mm inner glazing layer

3.3.2 Weather data

In order to evaluate the feasibility of passive energy systems in cold climates, and perform the simulations, this thesis work uses the Canadian Weather for Energy Calculations (CWEC, 2017). The CWEC file contains 12 typical meteorological months composed of hourly weather data records that are selected from a 30-year database of Canadian Weather Energy and Engineering Datasets to predict the average heating and cool loads in buildings (NRC, 2014). Figure 3.2 shows CWEC's monthly average hourly maximum, minimum, and average temperatures. It is evident that Winnipeg experiences extreme temperature fluctuations that range from +35°C in summer to -35°C in winter. Consequently, the construction of low-energy buildings, and in particular, commercial and institutional buildings, which typically have higher energy requirements, is challenging.

Additionally, Figure 3.2 shows the monthly average hourly solar radiation level in Winnipeg. As illustrated, Winnipeg experiences high solar radiation throughout the year with global average solar radiation of 4695.4Wh/m^2 (CWEC, 2017). This provides great photovoltaic potential of 1277kWh/kW per annum, which is suitable for application of solar heat panels. Furthermore, in cold months (including swing and winter seasons), the high level of solar radiation with a global monthly average ratio of 3232.6Wh/m^2 indicates excellent potential for heating energy savings when the outdoor air temperature can be quite low. However, during the summer, the higher amount of solar radiation with a global monthly average of 6330Wh/m^2 may increase the risk of overheating problems, which requires to be encountered with passive cooling systems.

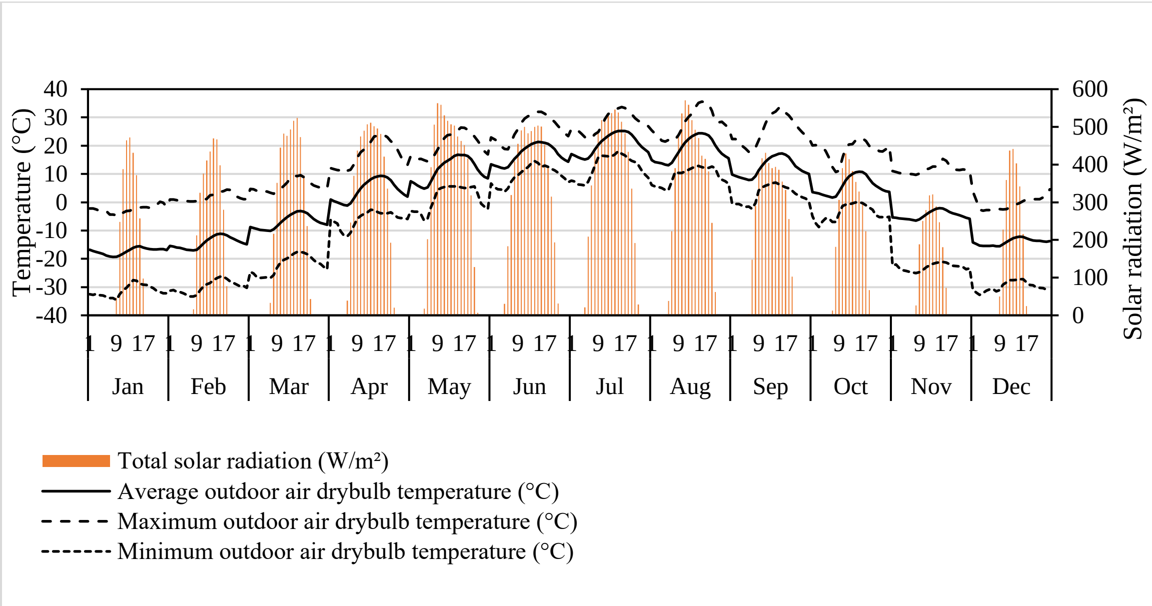

Figure 3.2: Monthly average hourly outdoor air temperatures and solar radiation in Winnipeg (CWEC, 2017).

3.3.3 Zoning approach

According to the ASHRAE standard 90.1-2010, thermal zones may be combined into thermal blocks when three main conditions are met. First, all the zones in the block should have the same load and scheduling characteristics. Second, to accurately model solar heat gains, the glazing for all zones included in the thermal block must have the same orientation, or at least their orientations must be within 45 degrees of each other. Third, to accurately model the performance of the system(s) serving the block, the same type of HVAC system must serve all the zones within the block. Therefore, to simplify the EnergyPlus model without compromising its accuracy and robustness, zones with the same orientation, served by the same HVAC system(s) and with the same occupancy schedules were grouped. This approach reduced the number of zones by approximately 30% and resulted in 98 thermal zones in total. Free 3D modeling program SketchUp

Make/Euclid 0.9.3 is used to develop the EnergyPlus model. In this program, the surrounding buildings are modeled as simple cuboids to consider the effect of shading. Figure 3.3 illustrates the implemented zoning approach.

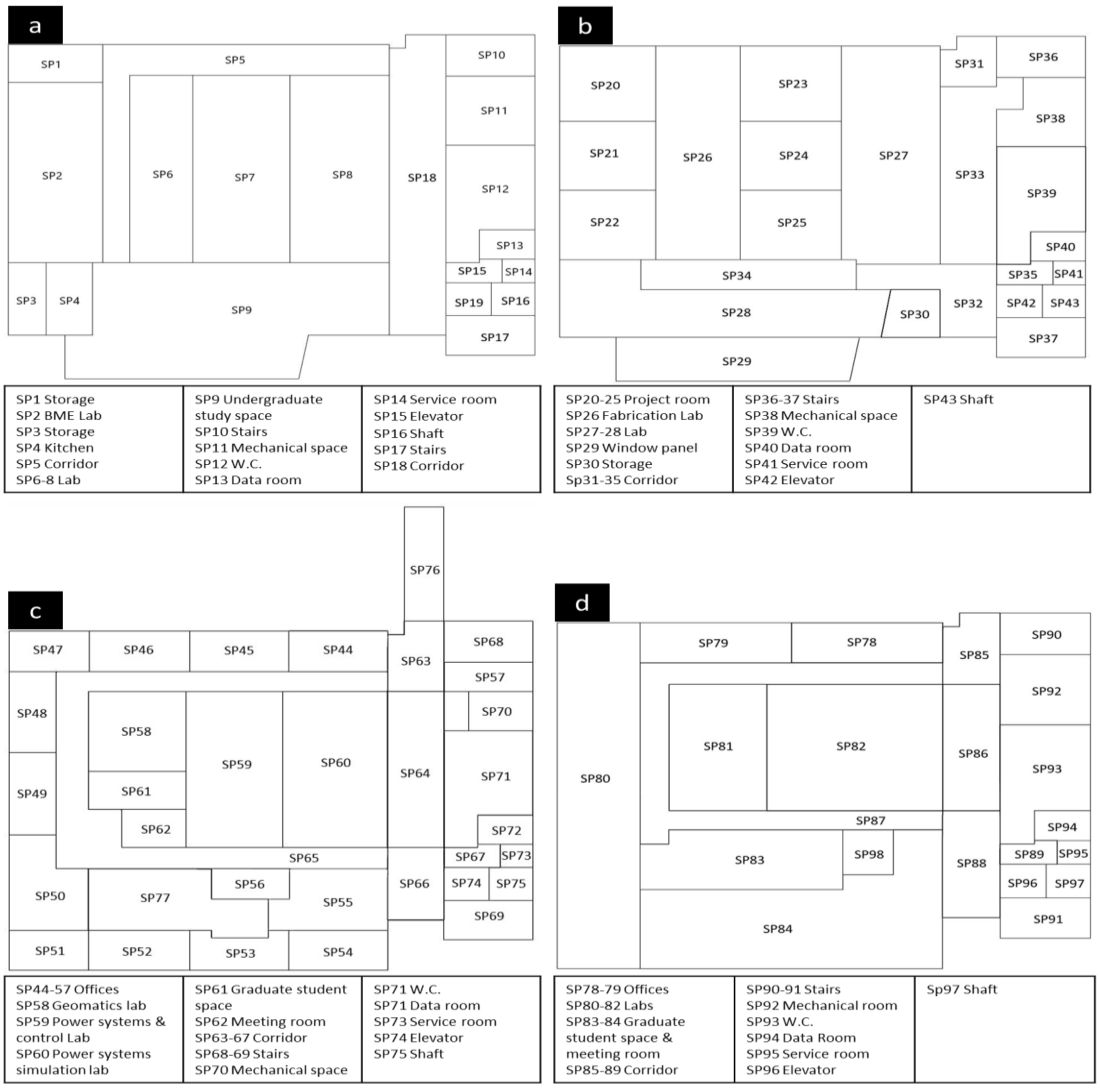

Figure 3.3: Thermal zones of the SPEB: (a) Basement, (b) First Floor, (c) Second Floor, and (d) Third Floor (Al-janabi et al., 2019).

3.3.4 Materials and constructions

In EnergyPlus software, envelope construction is the assembly of multiple layers defined from outside to the inside where each layer represents a specific material defined based on its physical properties (e.g., thickness, thermal conductivity, density, and specific heat). The thickness of each layer was taken from the final construction drawings provided by the developer, whereas the thermophysical properties were taken from the Manitoba Energy Code for Buildings (MECB, 2011). Similarly, windows are created by defining two layers of glazing separated by a gap filled with argon. There are two main limitations related to the modeling of complex envelopes and façades in EnergyPlus. First, EnergyPlus performs only one-dimensional heat transfer through multilayered construction calculations (Simões et al., 2014), and thus, all materials are defined as flat layers regardless of their actual shape. Second, because EnergyPlus assumes that highly conductive and thin materials do not contribute to the overall thermal resistance or heat capacity of the construction, they have to be omitted from the simulation (EnergyPlus, 2018). Therefore, developed models exclude all thin metal sheets. The U-values of different envelope elements are provided in Table 3.2.

Table 3.2: U-values of the envelope elements in IES and EnergyPlus (Al-janabi et al., 2019).

Construction type	U-value (W/m^2K)
	EnergyPlus
Exterior wall	0.263
Roof	0.135
Floor	3.445
Interior partition	1.789
Window	1.379

3.3.5 Internal loads and schedules

Internal gains have a considerable impact on energy consumption (Ward et al., 2016). Therefore, people, internal lights, equipment, and plug-loads were defined as internal gains following realistic schedules. People are modeled by defining the occupancy density based on the occupancy category such as labs, offices, and study areas, whereas the design team established the density values for each category. Since people's activities differ depending on the occupancy type, the people's activity level was defined to reflect each zone (EnergyPlus, 2018). For instance, a higher activity level is assigned to labs and student spaces than offices. Each type of internal gain is controlled by detailed schedules for weekdays and weekends, which are created by modifying the operating schedule D for school and university proposed by the National Energy Code of Canada for Buildings (NECB, 2015) to match the observed occupancy in the existing engineering buildings on campus. Figure 3.4 illustrates the schedules of internal lights, plug-loads, and occupancy.

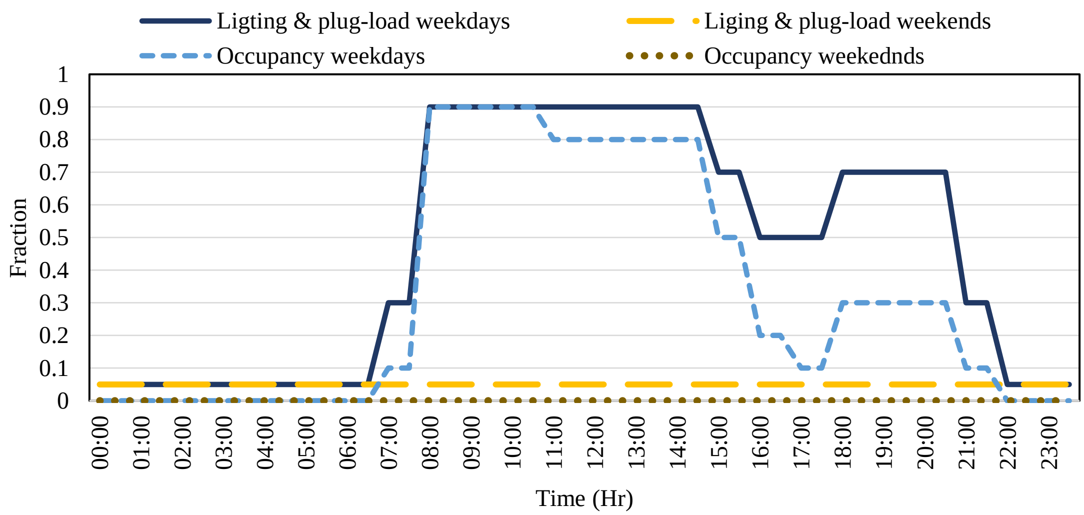

Figure 3.4: Internal lights, plug-loads, and occupancy schedules (Al-janabi et al., 2019).

Furthermore, the building's lighting power density was defined based on the requirements provided by the design team, and it varies upon the space type from 0.323 to 24.43W/m^2 and day (e.g., weekday or weekend). Equipment power consumption and sensible heat gains were defined based on the equipment available in different zone types (e.g., data centers in data rooms, welding equipment in the welding shop). Table 3.3 lists the zone types with high sensible gains, their power consumption, and period of operation. Additionally, plug-loads such as computers, printers, and monitors energy use intensity (W/m^2) were specified according to the NECB, (2015).

Table 3.3: Zones' types, their sensible gains, power consumption and period of operation (Al-janabi et al., 2019).

Zone type	Sensible heat gain (KW)	Power consumption (KW)	Operation period (Hr)
Data rooms	20	54	24 (every day)
BME Lab	9.7	51.9	1 (weekdays only)
Spray Paint Booth	0.35	4.8	1 (weekdays only)
Mech/Elect Room	9	9	24 (every day)
Welding Shop	0.23	64	0.5 (weekdays only)
Electric Vehicles Lab	1.2	229.1	1 (weekdays only)

3.3.6 Simulation of HVAC systems in EnergyPlus

Modeling of a sophisticated HVAC system is challenging in EnergyPlus and in particular when thermal zones are served by more than one system (e.g., fan coil units and radiant systems). In this case, HVAC templates in EnergyPlus cannot be used to present a system, and each component must be created individually using the IDF Editor and connected to other components using the node system. This approach increases the flexibility of the BPS tool and allows modeling of more complex and diverse HVAC systems. However, it also increases modeling efforts as well as the need for knowledge of each HVAC system component and its connection with other equipment. Therefore, several hot and chilled water loops were defined to supply the radiant floor systems and coils with hot and chilled water. The DOAS was modeled to deliver 100% outdoor air through VAV units, which were modeled using the AirTerminal:SingleDuct:VAV:NoReheat object. To model the energy-recovery ventilator (ERV), the air-to-air heat exchanger object HeatExchanger:AirToAir:SensibleAndLatent was added to the air loop of DOAS. Heating and cooling coils were defined as a part of DOAS to maintain a temperature of 12.8°C. The hydronic radiant system in EnergyPlus was modeled by defining internal source construction and by creating the low-temperature variable flow radiant using

ZoneHVAC:LowTemperatureRadiant:VariableFlow object. The radiant floor system is connected to a separate water loop because the supplied chilled and hot water temperatures differ between the coils that serve radiant floor heating and those that serve the fan coil units, AHU and ERV. The ZoneHVAC:FourPipeFanCoil object was used to model fan coil units with recirculation fans at a constant speed (EnergyPlus, 2018).

3.4 Building model verification

In the context of computer simulation, model verification is the process of confirming that the model is correctly implemented concerning the assumptions made and specifications used during the simulation phase (Carson and John, 2002). Therefore, in order to verify the reliability of the developed model, it is crucial to verify its accuracy in detail. In this regard, a possible approach is to compare the various results of a simulation model to the results of other models (Sargent, 2010). To accomplish this, a comparative analysis is performed between energy prediction made by EnergyPlus model and the existing energy model of SPEB developed by Stantec Ltd. using IES VE (2015); a whole-building energy simulation that estimates building energy demand on an hourly basis (Crawley, Drury B., et al., 2006). Figure 3.5 shows a flow chart for the verification of the EnergyPlus model.

As illustrated in Figure 3.5, the model developed in IES software used the same approach for simulating the thermal performance of SPEB. However, IES software differs regarding its architecture and algorithms used to model buildings and their energy systems (Abdullah et al., 2014). For example, IES combines several modules to perform dynamic whole-building energy analysis (IES VE, 2015). ModelIT is the single central 3D data model at the core of the IES that provides geometry data shared by all modules. ApacheSim is a central simulation processor, which enables assessment of building's thermal performance as well as shares results and input across other IES modules, such as ApacheHVAC for modeling of HVAC systems, MacroFlo for airflow analysis, and SunCast for advanced 3D solar analysis. Therefore, different inputs may be required to model the same building envelope elements or HVAC system components.

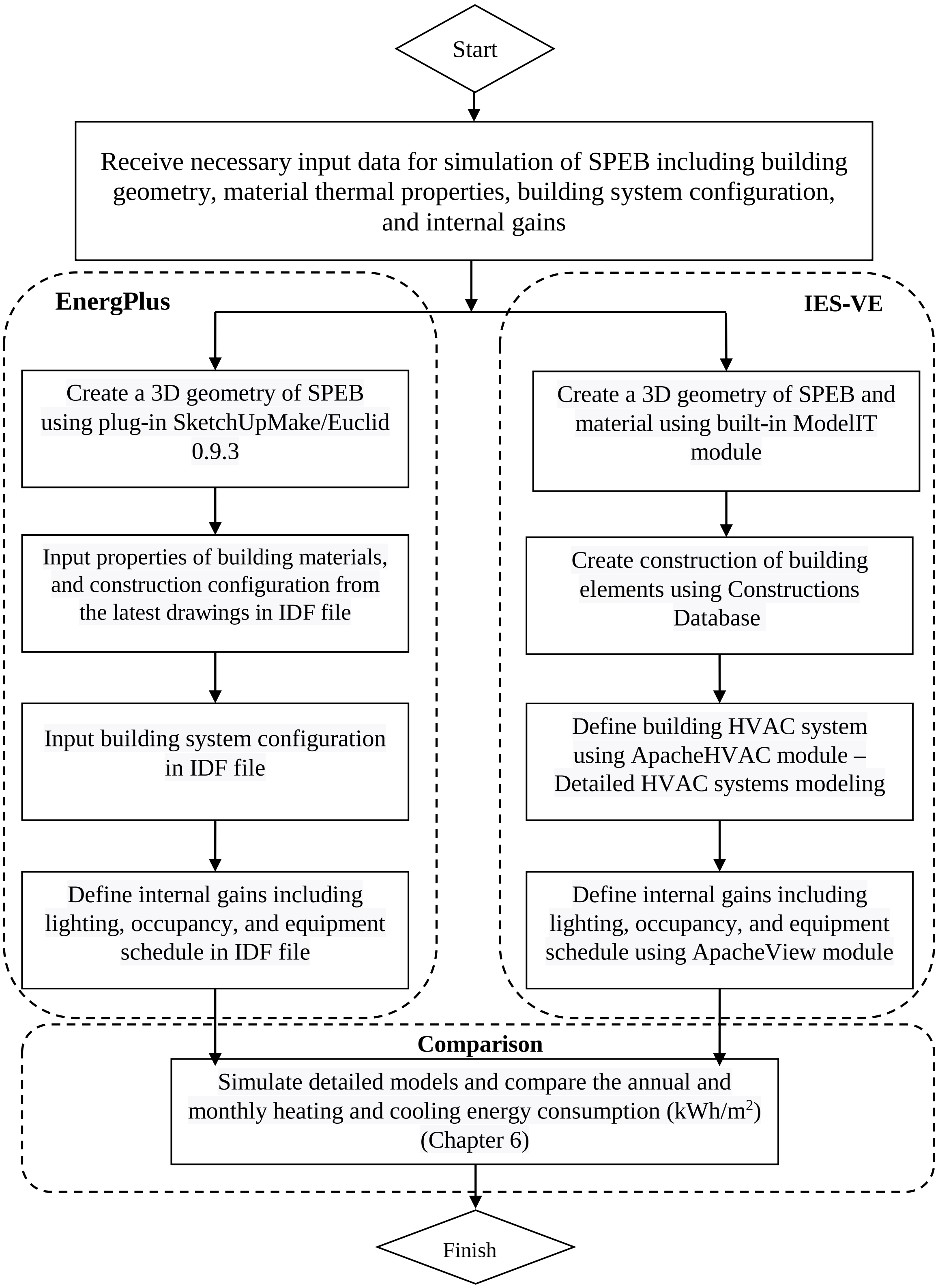

Figure 3.5: Theoretical building model verification flow diagram

3.5 Case study

Because this research aimed to investigate the feasibility for the applications of Phase Change Materials (PCMs) and passive cooling systems (i.e., natural ventilation and solar shading), a south-orientated study room at the top floor of the SPEB was chosen for a case study. This study room was selected due to the following specific reasons:

- It has high heating and cooling energy consumptions because of its perimeter location and south orientation.
- It is a large zone that needs to provide adequate thermal comfort and air quality to a large number of students.
- Glazing surfaces of the study room constitute around 95% of the exterior walls, which allows a high amount of solar radiation to enter the space.
- The study room experiences high internal gains due to its high occupancy and equipment patterns.

Figure 3.6 presents 3D models of the reference graduate study room as the case study in this research. Additionally, Table 3.4 summarizes the main characteristics of the graduate study room, whereas Table 3.6 provides the thermophysical characteristics of the case study envelope materials.

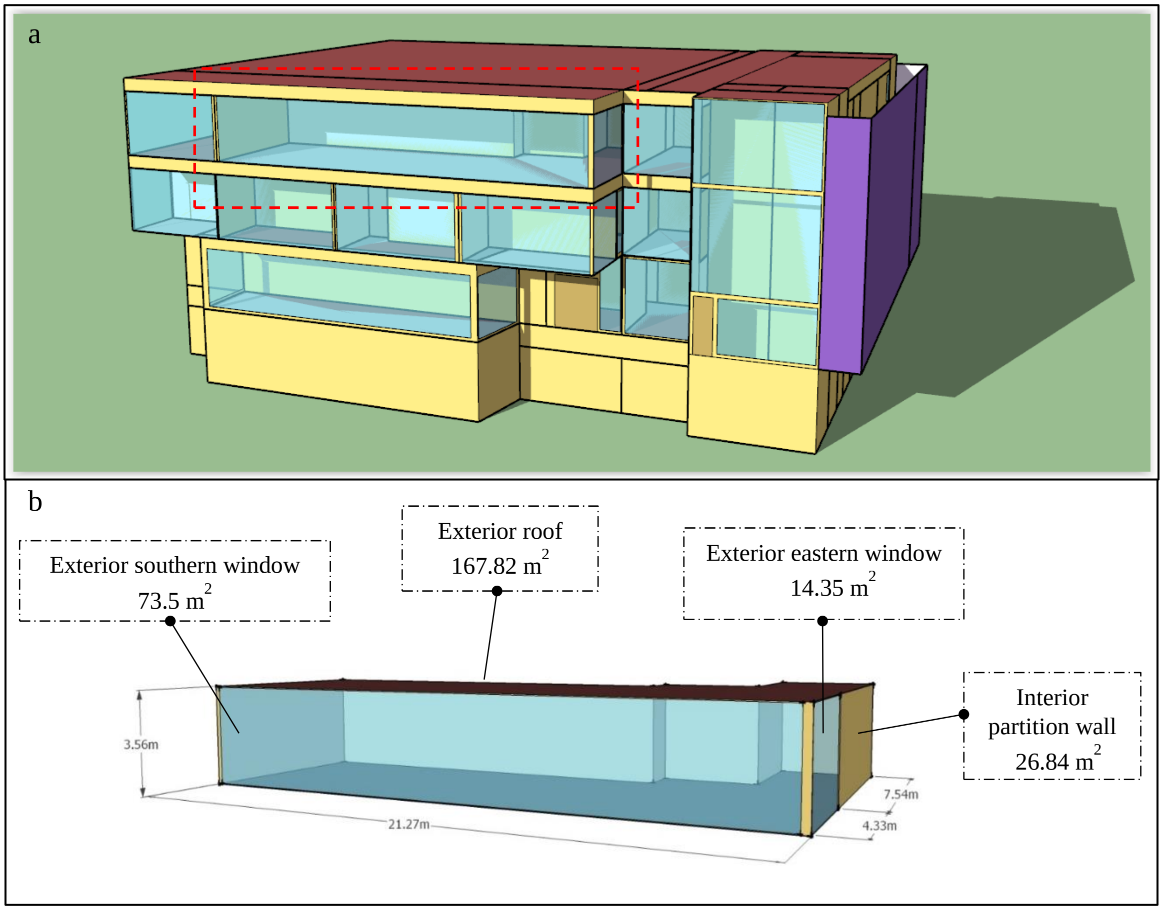

Figure 3.6: A schematic view of (a) Stanley Pauley Engineering Building, and (b) sketch of the case study graduate study room model, the southern façade.

Table 3.4: Graduate study room characteristics.

Characteristic	**Graduate study room**
Floor area (m^2)	167.8
Volume (m^3)	597.4
Height (m)	3.5
Total glazing area (m^2)	87.8
South glazing (m^2)	72.3
East glazing (m^2)	15.4
Total EUI (kWh/(m^2·year))	350
Heating EUI (kWh/(m^2·year))	279.2
Cooling EUI (kWh/(m^2·year))	70.8

Table 3.5: Reference envelopes construction.

Material	Thickness (m)	Conductivity (W/m·K)	Density (kg/m^3)	Specific heat (kg/m^3)	Solar absorptance
Gypsum board	0.0125	0.21	700	1000	0.4
Acoustic tile	0.0191	0.06	368	590	-
Glazing	0.25	0.9	-	-	-
Interior floor concrete	0.125	1.73	837	837	0.65
Exterior floor concrete	0.125	1.73	837	837	-
Floor insulation	0.1693	0.05	265	836	-

3.6 Summary

In summary, this chapter discussed a research methodology for developing a detailed energy model of the SPEB in EnergyPlus and selecting an appropriate case study for further implementation and optimization of PCM and passive cooling systems. To accomplish this, the SketchUp/Euclid plug-in was first used to develop a 3D geometry and perform thermal zoning of SPEB. Afterward, the EnergyPlus software was used to develop all other required information necessary for simulation of the model including thermal properties of building materials and construction configuration, HVAC systems, and internal loads and schedules (section 3.3).

Also, to investigate the accuracy of the developed model in EnergyPlus, a model verification approach was proposed based on comparing the predictions made by EnergyPlus against the results of another model, i.e., IES model (section 3.4). This approach allowed gaining more confidence in the estimations of the developed SPEB model.

4 Optimal design of PCM-enhanced radiant floor system in cold climates using EnergyPlus and MATLAB

4.1 Chapter outline

This chapter details a research methodology for energy performance assessment of optimal PCM design when integrated with the radiant floor system of the studied case study. The methodology is approached by (i) simulating PCM-enhanced radiant floor in EnergyPlus using newly introduced hysteresis object, and (ii) finding the optimal solution for PCM-enhanced radiant floor design by coupling the developed thermal model and Genetic Algorithm. In this regard, this chapter first describes the simulation of the radiant floor system enhanced with PCM storage using EnergyPlus software (section 4.2). Afterward, it details the simulation approach used for modeling PCM in EnergyPlus (section 4.3). Next, it introduces the optimization method, including the optimization algorithm and its objective function (section 4.4). Last, this chapter provides a summary of the proposed methodology (section 4.5).

4.2 PCM integration

The PCM storage is integrated into the hydronic radiant floor system, which in the heating mode provides the baseline space heating, and the air system provides the trim. In cooling mode the air system covers the main cooling energy demand, and the radiant system provides the trim (Al-janabi et al., 2019). Consequently, the energy consumption of the hydronic radiant system is significantly larger (~70%) in winter than in summer. Furthermore, the majority of research studies focused on the implementation of PCM for cooling applications (Cabeza and de Gracia, 2015), and there is a limited number of studies focused on the potential of PCM in improving heating performance (Osterman et al., 2015). Therefore, more work is required to demonstrate PCMs' capabilities to reduce heating energy consumption in cold climates.

The HVAC systems are modeled in detail and parameters such as set-point temperatures, airflow rates, water flow rates, and capacities of the system components are specified according to the final mechanical drawings. The radiant floor system installed in the graduate study room is made of a hard plastic tube with 1.27cm inside tubing diameter and length of 1091 m (Table 4.1). The tubes are embedded between the concrete slab and the interior finishing construction, as shown in Figure 4.1. As earlier discussed in section 3.3.6, the baseline model of the radiant system (hydronic) was developed in EnergyPlus using Low-Temperature Radiant system with the variable flow. This system contains a central loop and pump that provides water at a specific temperature to all of the systems connected to the loop (Strand and Baumgartner, 2005). Valves are then used to control the amount of water flowing through each system to maintain the water temperature based on some particular thresholds associated with the comfort conditions within the space (e.g., indoor mean air temperature). For this study, a separate water loop and pump with similar temperature and flow rate set-points were developed to evaluate the heating and cooling performance of the radiant system in the graduate study room. This discrete system allows us to directly control the hot water temperature and calculate the heating energy used in the graduate study room to maintain comfort.

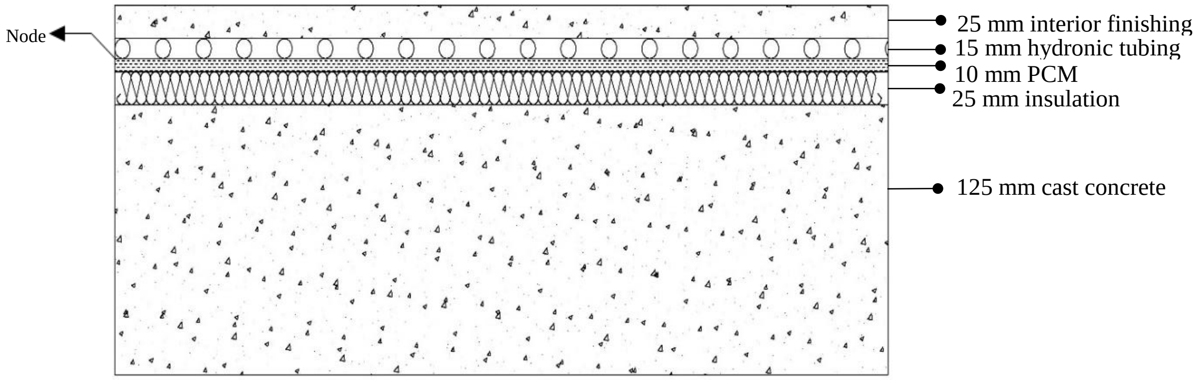

Figure 4.1: Cross section of the radiant floor construction elements considered in the EnergyPlus model.

Table 4.1: Physical properties of radiant floor system used in the graduate study room

	Inside diameter (cm)	Tubing length (m)	Heating design capacity (W)	Cooling design capacity (W)	Maximum hot water flow rate (cm^3/s)	Maximum cold water flow rate (cm^3/s)	Temperature control type
Radiant floor system	1.27	1091.03	22550	17310	690	930	Mean Air Temperature

The latent heat storage used in the present simulation is assumed to be a single homogeneous layer of pure PCM laid under the heater system. Figure 4.1 illustrates a cross-section of the radiant floor construction containing a layer of PCM storage. The proposed construction shown in Figure 4.1 implies a possible temperature variation at the lower surface of radiant tubes. However, since EnergyPlus uses one-dimensional conduction calculation (Strand and Baumgartner, 2005), the surface temperature between the heater and the PCM layer is assumed to be at a uniform temperature for the entire floor. Another limitation of the one-dimensional analysis is related to the location of the PCM layer when incorporating with a radiant floor system. A preliminary study on the location of PCM storage showed that adding a layer of pure PCM at the upper face of the heater could significantly increase the heating energy provided by hot water pipes by 35%. A possible explanation for this behavior might be that the embedded PCM layer is assumed to be distributed uniformly throughout the floor and therefore, the radiant system needs to supply more heat to maintain the required comfort within the space. Hence, this study assumes that PCM storage is placed at the lower face of the heater to extract heat from heating pipes during the day by natural conduction and release the stored heat within the space during off-peak hours through the means of convection (Farid and Chen, 1999). In addition to the assumptions mentioned above, for an efficient heating system, an insulation layer is installed at the bottom of the radiant system to minimize the heat loss to the lower room (Figure 4.1) as suggested by Farid and Chen (Farid and Chen, 1999). Another potential benefit of using insulation at the lower face of the radiant system might be the reduction of PCM thickness due to the improvement of thermal insulation performance.

For this simulation, a commercially available phase change material, suitable for floor heating application with 100% bio-based material was selected. In order for PCM to be effectively utilized, it is essential to achieve a full phase transition cycle day-after-day (Kośny, 2015), which is greatly dependent on the PCM melting temperature (Kauranen et al., 1991). Therefore, as illustrated in Figure 4.1, a monitoring node is used to continuously measure the surface temperature between the PCM layer and heating pipes. Figure 4.2 demonstrates the daily average surface temperature distribution at the lower face of the heater for the coldest months, November to March. As illustrated in Figure 4.2, the surface temperature of the radiant floor with PCM could vary between 23ºC and 29ºC with the highest frequency of 27ºC. Analyzing the floor surface temperature implies that the PCMs with melting temperatures of 23 to 29ºC would be suitable to be integrated with the under-floor radiant heating system. The manufacturer, "PureTemp" has provided the thermo-physical information of PCM23, PCM25, PCM27, PCM28, and PCM29 necessary for simulation in EnergyPlus. This wide range of melting temperature covers almost the entire variation of surface temperature and therefore is considered for further modeling in EnergyPlus.

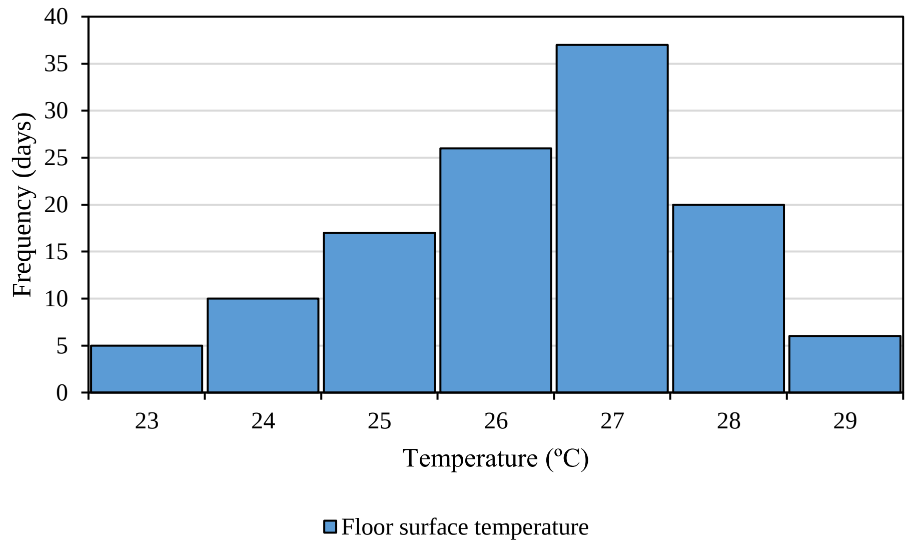

Figure 4.2: Surface temperature distribution between the PCM layer and the heater.

Earlier research studies on the optimization of PCM using EnergyPlus software only considered enthalpy-temperature information to create a simplified model of PCM (Saffari et al., 2017; Soares et al., 2014), as the PCM model in EnergyPlus did not simulate hysteresis effect due to the complexity of these materials. Therefore, as concluded by Tabares-Velasco et al. (2012), the accuracy problems could arise when simulating PCMs with strong hysteresis. In contrast, the methodology proposed herein considers the hysteresis effect of the PCM, which, unlike the enthalpy method, uses two curves to define freezing and melting phases, thus significantly improving the accuracy of the simulation. Table 4.2 summarizes the hysteresis properties of the five PCM types defined in EnergyPlus.

Table 4.2: Hysteresis properties of the pure PCM (PureTemp, 2018).

Physical properties	PCM 23	PCM 25	PCM 27	PCM 28	PCM 29
Latent heat (J/kg)	227000	187000	202000	190000	202000
Liquid state thermal conductivity (W/mK)	0.15	0.15	0.15	0.15	0.15
Liquid state density (kg/m^3)	830	860	860	860	850
Liquid state specific heat (J/kgK)	1990	2290	2630	2540	1940
Solid state thermal conductivity (W/mK)	0.25	0.25	0.25	0.25	0.25
Solid state density (kg/m^3)	910	950	950	950	940
Solid state specific heat (J/kgK)	1840	1990	2460	2340	1770

4.3 PCM modeling in EnergyPlus

Modeling of the PCM in EnergyPlus requires the use of the one-dimensional conduction finite difference (CondFD) solution algorithm (EnergyPlus, 2018). The user can choose between two solution schemes, CrankNicholsonSecondOrder (before version 7) and FullyImplicitFirstOrder (as of version 7) to be used by the CondFD model throughout the simulation. A fully implicit, first-order scheme was used in this research due to its robustness and unconditional stability over time (Versteeg and Malalasekera, 1996). The FullyImplicitFirstOrder scheme equation for the internal node can be formulated as follows:

$$C_p \rho \Delta x \frac{T_i^{new} - T_i^{old}}{\Delta t} = \left(K_W \frac{(T_{i+1}^{new} - T_i^{new})}{\Delta x} + K_E \frac{(T_{i-1}^{new} - T_i^{new})}{\Delta x} \right) \tag{4.1}$$

where

$$K_W = \frac{(k_{i+1}^{new} + k_i^{new})}{2} \tag{4.2}$$

$$K_E = \frac{(k_{i-1}^{new} + k_i^{new})}{2} \tag{4.3}$$

where C_p denotes the specific heat capacity, ρ is material's density, T is temperature, K is thermal conductivity, Δx is the space between nodes used as the finite difference layer thickness, and Δt is time step. These formulations are related to the node positions and appropriate time step, where the node i refers to the node being modeled, and nodes i+1 and i-1 are the adjacent nodes to the internal and external surfaces of construction, respectively (EnergyPlus, 2018). In this regard, K_w and K_e refer to the thermal conductivity for interface between nodes i and i+1, and between nodes i and i-1, respectively. The *new* and *old* time steps also indicate the present and previous time steps, respectively. In the CondFD model, all surface components are discretized using Equation 4.4 in which Δx relies on the space discretization constant (C), thermal diffusivity of the material (α), and time step (Δt), as shown in the following equation:

$$\Delta x = \sqrt{C\alpha\Delta t} \tag{4.4}$$

Equation 4.1 is coupled with Equation 4.5 and Equation 4.6 to account for enthalpy (h) and the thermal conductivity (k) of the PCM concerning the temperature (T).

$$h_i = h(T_i^{new}) \tag{4.5}$$

$$k_i = k(T_i^{new}) \tag{4.6}$$

Before EnergyPlus 8.8, the specific heat (C_p) at each time step is calculated using the tabulated input data of temperature/enthalpy pairs (Equation 4.7) which particularly accounts for only the heating mode (Property:PhaseChange object).

$$C_p = \frac{h_i^{new} - h_i^{old}}{T_i^{new} - T_i^{old}} \tag{4.7}$$

The main limitation of the enthalpy/temperature approach is the use of single enthalpy curve, which arises accuracy issues when simulating PCM with a pronounced hysteresis (Versteeg and Malalasekera, 1996). As of EnergyPlus version 8.8, this issue is approached with a new MaterialProperty:PhaseChangeHysteresis object, which models the hysteresis physics existing between the melting and freezing processes by considering both the current and previous state of the model to determine the specific heat of the PCM. The iterative process is used to assure that the correct enthalpy, and therefore the correct specific heat (C_p) is calculated accurately in each time step. Also, the hysteresis object requires more information regarding thermal conductivity, density, and specific heat capacity of PCM in both solid and liquid states compared to the enthalpy/temperature approach (EnergyPlus, 2018). Equation 4.8 describes the calculation method of specific heat at each time step in EnergyPlus using hysteresis method.

$$C_p = f\left(T_i^{new}, T_i^{previous}, PhaseState^{new}, PhaseState^{previous}\right) \tag{4.8}$$

4.4 Optimization

Simulation-based optimizations were performed to find the optimal design of PCM-enhanced radiant floor by coupling the EnergyPlus's model with a Genetic Algorithm developed in the MATLAB environment. The simulations were performed on cluster 6 core Intel® Xenon® processors using parallel computing approach provided by Western Canada Research Grid (West-Grid Canada) (Yi and Malkawi, 2009) to run EnergyPlus 8.9.0 CentOS release 6.3–2.6.32 X 86_64 GNU/Linux and MATLAB 2017b.

4.4.1 Problem description and design parameters

An innovative multivariable optimization approach is proposed based on coupling a building energy simulator (i.e., EnergyPlus) and a generative optimization algorithm developed in MATLAB environment. Because inputs in EnergyPlus are written in text format, MATLAB can easily read and automatically rewrite the individual variables according to the best solutions derived from the optimization algorithm. The optimizer then collects the results from the EnergyPlus output file and solves the cost function. A new vector of best solutions is then identified by which the optimizer prepares a new EnergyPlus IDF file for the next run. This iterative approach continues until the predefined stopping criteria is met, or the maximum number of iteration is reached. Figure 4.3 presents an overview of the methodology workflow for the simulation-based optimization of PCM-enhanced radiant floor system.

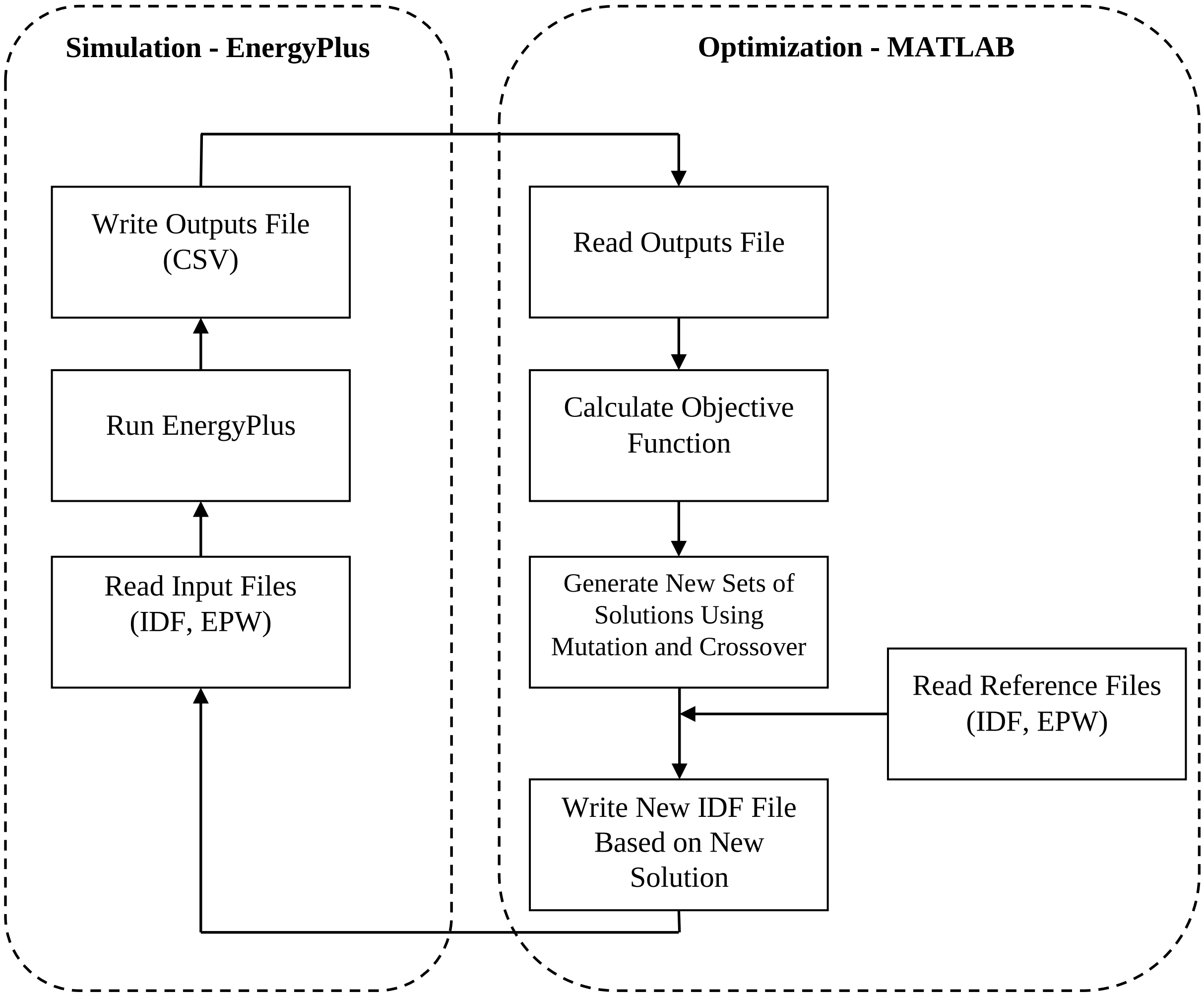

Figure 4.3: Methodology workflow of the simulation-based optimization, coupling MATLAB and EnergyPlus.

Two optimization scenarios are proposed to optimize the energy performance of the case study enhanced with PCM radiant floor. The first scenario aims to exclusively optimize the thermal properties of the pure PCM, including the melting temperature (PCM_{MT}), and thickness (PCM_T), while assumes other parameters to be constant during the optimization. The objective of the second scenario, on the other hand, is to investigate the non-linear interactions of the PCM storage with other interconnected parameters such as the insulation material and the interior concrete finishing. Therefore, it includes five additional parameters related to the thermal properties of the insulation and interior finishing, including: insulation thickness (I_T), insulation conductivity (I_k), floor thickness (F_T), floor conductivity (F_k), and floor solar absorbance (F_α). It should be noted that in both scenarios, the optimization is applied for the coldest months of the year, November-March, because of the following vital reasons. First, the case study is located in heating predominant climate, whereas due to the narrow phase change temperature range, the same PCM cannot be equally effective in winter and summer, and in particular when integrated with the HVAC system. Second, according to the Physical Plant at the University of Manitoba, the heating energy is produced from the carbon-intensive natural gas generated by the gas boilers with the efficiency of approximately 90%, whereas cooling energy is produced from low-carbon electricity using chillers with a Coefficient of Performance (COP) of around 4. Last but not least, considering the large number of inputs that describe the physical properties of SPEB, the iterative simulation of SPEB is computationally expensive and dramatically increases the convergence time for the optimization algorithm to find the global optimal solution. Nevertheless, to evaluate the impact of the proposed method on the overall energy performance of the SPEB, this study performed an annual performance analysis by applying the optimized values to an annual simulation.

Both scenarios are considered as single objective multivariable optimization problems with three (first scenario) and eight (second scenario) variables. Design parameters are divided into continues (i.e., PCM_T, I_T, I_k, F_T, F_k, F_α) and discrete (i.e., PCM_{MT}) categories, where continues variables can vary within a specified range (Table 4.3), and the discrete variable can assume one of the five possible values, i.e., PCM_{23}, PCM_{25}, PCM_{27}, PCM_{28}, and PCM_{29} as a fixed object. As it is shown in Table 4.3, PCM_T-value is assumed to vary between 0.01 and 2.5cm; I_T between 0 and 2.5cm; I_k between 0.02 and 1W/m·K; F_T between 0.01 and 2.5cm; F_k between 0.02 and 2 W/m·K; and F_α between 0 and 1.

Table 4.3: Continuous design variables range.

Design variable	Unit	Minimum value	Maximum value
PCM thickness (PCM_T)	cm	0.01	2.5
Insulation thickness (I_T)	cm	0.01	2.5
Insulation conductivity (I_k)	W/m·K	0.02	1
Interior concrete thickness (F_T)	cm	0.01	2.5
Interior concrete conductivity (F_k)	W/m·K	0.02	2
Interior surface solar absorptance (F_α)	-	0	1

In addition to the above design variables, the amount of heat generated by the under-floor hydronic system can directly influence the performance of PCM, and it should be considered as a design variable into the optimization process. Therefore, in order to evaluate the impact level of each parameter (i.e., hot water flow rate, and hot water temperature) on the studied outputs and identify the most influential parameter, the following local sensitivity analysis is carried out.

4.4.2 Local sensitivity analysis

In addition to the above design variables, parameters of the hydronic heating system such as hot water flow rate and hot water temperature can directly influence the performance of PCM. Therefore, the local sensitivity analysis is performed to assess the impact of small changes in the water flow rate and hot water temperature on the total energy consumption of the graduate study room. The local sensitivity analysis is based on a central finite-difference approximation approach, which determines the partial derivatives of the response of the system regarding the input parameters around their initial values (Firth et al., 2010; Lomas and Eppel, 1992). Equations 1 and 2 are used to calculate the sensitivity coefficients $\Phi_{i,j}$, and the normalized sensitivity coefficients $S_{i,j}$, respectively.

$$\Phi_{i,j} = \frac{\partial y_i}{\partial x_i} \approx \frac{y_i(x_j + \Delta x_j) - y_i(x_j - \Delta x_j)}{2 \times \Delta x_j} \tag{4.9}$$

$$S_{i,j} = \frac{x_i}{y_i} \times \frac{\partial y_i}{\partial x_i} \tag{4.10}$$

where i = 1 to n and j = 1 to m; y_i is the i^{th} output variable, x_i is the j^{th} input parameter, and $y_i(x_j+\Delta x_j)$ and $y_i(x_j-\Delta x_j)$ are the values of y_i when the input parameter x_i is increased and decreased, respectively, by a small amount Δx_j.

As recommended by the literature Saltelli et al. (2000), a change of ± 1% has been executed on each both parameters, whereas to extend the analysis each parameter was allowed to vary within the four levels. As summarized in Table 4, the supply water temperature had four discrete values starting from 45.6 °C (base case) to 46.9 °C (level four), whereas supply water flow rate had four discrete values between 690 cm^3/s (base case) and 710.7 cm^3/s (level four).

Table 4.4: Radiant water design variables for thermal performance.

Supply water	Reference model	Level 1: 1% increase	Level 2: 2% increase	Level 3: 3% increase	Level 4: 4% increase
Temperature (°C)	45.6	46.05	46.51	46.9	47.4
Flowrate (cm^3/s)	690	696.9	703.8	710.7	717.6

Table 4.5 summarizes the results of the local sensitivity analysis and shows that supply water temperature has a more significant impact on both heating and cooling energy use than water flow rate. For example, a 1.0% rise in water temperature would result in approximately 0.3% and 0.65% increase in heating and cooling demand, respectively, whereas the same increases in supply water flow rate would increase heating and cooling energy demand for approximately 0.1% and 0.32%, respectively. Therefore, this study considers supply water temperature as a design variable for the further optimization process. It is important to note that the local sensitivity analysis is performed for the same period as the optimization analysis from November to March.

Table 4.5: Local sensitivity analysis of radiant water design variables.

Design variables	Level*	Heating EUI (kWh/m^2)	Cooling EUI (kWh/m^2)	Total EUI (kWh/m^2)	$S_{i,j}$
Base case	-	205.17	8.36	213.53	-
Water flow rate	1	205.46	8.38	213.84	0.14
	2	205.73	8.42	214.14	0.27
	3	205.98	8.45	214.43	0.39
	4	206.23	8.48	214.71	0.51
Water temperature	1	205.80	8.41	214.21	0.30
	2	206.38	8.46	214.85	0.59
	3	206.85	8.50	215.36	0.82
	4	207.32	8.54	215.86	0.95

*Note: Acceptable level of increase for each design variable is provided in Table 4.4.

A comprehensive feasibility analysis required the calculation of the optimal solutions for the six supply water temperatures ranging from 35.6 ºC (minimum temperature recommended by Djuric et al., 2007) to 45.6 ºC (reference temperature) with a 2 ºC step. This wide temperature range enabled a better understanding of the impact of supply water temperature on the performance of the PCM-enhanced hydronic radiant floor system. The minimum cost function value associated with each supply water temperature is then determined by post-processing of the outputs.

4.4.3 Objective function

An optimization model based on Genetic Algorithm (GA) is developed in MATLAB to minimize the objective function for different radiant floor temperatures as shown in Equation 4.13. Where $E_{Total,ref}$ and $E_{Total,PCM}$ are total energy use of the graduate study and correspond to the conditions that model is simulated before and after including pure PCM, respectively. An appropriate objective function in the field of thermal optimization should be able to reduce energy use to the lowest level while ensuring thermal comfort is maintained within an acceptable range (Keeney and Braun, 1996). Therefore, in this study, a penalty function is used to implement thermal comfort constraint during the optimization using the commonly utilized thermal comfort index, Predicted Mean Vote. PMV was developed by American Society of Heating Refrigerating and Air Conditioning Engineers (ASHRAE 55, 2017) is able to predict the mean thermal sensation vote on a standard scale for a large group of people based on various comfort-related factors including indoor air temperature and speed, occupants' clothing insulation (I_{cl}), occupants' metabolic rate (M), and relative humidity (Fanger, 1984; Fanger and others, 1970). It is important to note that it is difficult to evaluate the thermal comfort accurately using PMV, due to the uncertainty regarding subjective parameters, such as clothing thermal insulation, and metabolic rate. In this study, I_{cl} varies between 0.5 and 0.9 based on the daily outdoor temperature, and M is equal to 1 for a medium office activity (ASHRAE 55-2017).The seven-point thermal sensation scale shows the comfort level in the space, which varies between -3 for cold,-2 for cool,-1 for slightly cool, 0 for natural, +1 for slightly warm, +2 for warm, and +3 for hot space. According to ASHRAE 55-2017, compliance for thermal comfort is achieved if measured PMV for majority of occupants (80% and more) falls between -0.5 to +0.5 on the PMV scale during the occupied hours.

Additionally, the results from the preliminary study on the implementation of PCMs with different melting temperatures showed that non-restrictive integration of PCM with the under-floor heating system can adversely affect the cooling demand and result in a substantial increase of cooling energy consumptions (~20-30%) during the winter months (i.e., October to April). Therefore, to gain control over the increase of the cooling energy demand, additional penalty function was added to the objective function to ensure that space cooling does not exceed a threshold level. The constraint level for the acceptable cooling increase should be chosen based on the case by case basis. For instance, although SPEB has cooling demand during the winter, it is very small and presents less than 5% of the heating energy demand. Moreover, the supplied cooling energy to the

SPEB is sourced from hydroelectricity, which is considered to have lower embodied energy compared to the gas that is used to provide space heating. Therefore, a 10% threshold is assumed to limit the increase in cooling energy use.

The objective function for the optimization problem can then be formulated as follows:

$$\min f(x) = E_{Total,PCM} - E_{Total,ref}$$

Subject to (4.11)

$$E_{cool,PCM} < 1.1 \times E_{cool,ref}$$

$$-0.5 < PMV_i(x) < 0.5 \quad \forall i \in I$$

For the first and second optimization scenarios, with respect to each radiant water temperature, $x_i^* \in X$ indicate the best design solutions resulted in the lowest cost function, which can be defined as:

$$x_1^* = \{PCM_{mt}, PCM_t\}_{opt}$$
$$x_2^* = \{PCM_{mt}, PCM_t, I_t, I_k, F_t, F_k, F_\alpha\}_{opt}$$

Studies have shown that the selection of an appropriate algorithm with proper properties can highly influence the efficiency of an optimization algorithm (Saffari et al., 2017; Soares et al., 2014). In order to avoid the full enumeration (exhaustive search) of the design variables that yields a large computational effort, the Genetic Algorithm (GA) is employed as an approach to extract more intelligent solutions from entire design domain. GAs are classified into the class of mathematical approaches that utilize the principle of natural selection in which the processes of crossover, mutation, and selection are employed to improve a set of solutions towards an optimal solution. The GA can be divided into three main parts: generation of a new population, evaluation of new population, and reproduction. It begins the process by creating a random vector of individuals (initial population) of the entire available domain. In this study, the initial populations are created by defining $x_1 \in X$ as a vector of independent variables where X is the constraint set described in section 4.4.2. For the first and second scenarios, the initial population is defined as $x_1^1 = \{PCM_{mt}, PCM_t\}_{int}$, and $x_2^1 = \{PCM_{mt}, PCM_t, I_t, I_k, F_t, F_k, F_\alpha\}_{int}$, respectively. Afterward, the algorithm calculates the objective function and evaluates the initial population by comparing the cost function value for each individual. The GA then sorts the population based on their cost function value, and the individuals with better performance (lower cost function) are selected for reproduction (through the means of crossover and mutation). The better performing generation then takes the place of lower performing individuals; this process is called "breeding" of the previous population. This iterative process continues until some number of iterations are finished, or other stopping conditions are satisfied. Table 4.6 presents the Genetic Algorithm parameters used in the optimization process. Appendix A provides further information about the implementation of the optimization process including a code section that illustrates how the EnergyPlus simulation model can be interfaced with the MATLAB for data exchange at each evaluation step as well as how the optimization problem is developed. According to Caldas and Norford (2002), the appropriate population size for GAs can range from 30 to 200. Considering this recommendation and the existing computational limitations, this study used population of 30 individuals.

Table 4.6: Genetic Algorithm parameters used in the optimization problem.

Optimization parameter	Value
Maximum number of evaluations	1000
Initial population size	30
Selection procedure	Disregard the worst 50% of the population
Mating operator	Tournament selection
Crossover operator	Single-point crossover
Crossover percentage	85% of the new population
Mutation rate	15% of the new population
Maximum number of generation	40

In order to evaluate the energy performance of the optimized PCM-incorporated radiant floor, three energy indices are developed including the Indices of Energy Savings for Cooling (IESC), for Heating (IESH), and for Total energy (IEST). These indices of energy are defined as follows:

$$IESC = 1 - \frac{E_{tot,PCM}}{E_{tot,ref}} \tag{4.12}$$

$$IESH = 1 - \frac{E_{heat,PCM}}{E_{heat,ref}} \tag{4.13}$$

$$IEST = 1 - \frac{E_{cool,PCM}}{E_{cool,ref}} \tag{4.14}$$

where $E_{heat,PCM}$ and $E_{heat,ref}$ refer to the heating, $E_{cool,PCM}$ and $E_{cool,ref}$ refer to the cooling, and $E_{tot,PCM}$ and $E_{tot,ref}$ refer to the total energy consumption for the PCM-enhanced and reference rooms, respectively.

4.5 Economic analysis

In order to evaluate the impact of optimized PCM and insulation materials on the total price of the analyzed case study, this thesis also presents a general cost analysis according to the PCM, insulation, and energy prices. Therefore, all of the other costs remain constant throughout the optimization for the simplification. The studied total cost is described as follow (Baniassadi et al., 2016):

$$Total\ cost = PCM\ price + Insulation\ price + Energy\ price \tag{4.15}$$

4.5.1 Price of phase change material

The PCMs cost is highly dependent on the classification of the PCM (i.e., organic or inorganic) (Kosny et al., 2013). Organic PCMs are usually made of organic materials such as paraffin, fatty acids, and sugar alcohols, which are more expensive than their inorganic counterparts such as salt hydrates. According to the PuteTemp website, the cost for the organic PCM products is around \$20/lb for small quantities (PureTemp, 2019). However, this cost is projected to reduce to \$5/lb for commercial amounts of more than 1,000 pounds. The PCM price is then calculated as follows:

$$PCM\ price = 1.2 W_{PCM} C_{PCM} \tag{4.16}$$

where W_{PCM} corresponds to the amount of given PCM, by weight, which depends on the PCM volume and density: $W_{PCM} = A_{PCM} \delta_{PCM} \rho_{PCM}$, where A_{PCM} (m^2), δ_{PCM} (m), and ρ_{PCM} (lb/m^3) refer to the PCM floor area, thickness, and average density, respectively; C_{PCM} denotes the ratio of PCM cost which is equal to \$5/lb for large quantities. It also should be noted that the PCM price is calculated only based on the average material price and the other factors (e.g., transport and installation) are assumed to be constant throughout the simulation. Therefore, an additional estimation of 20% is added to Equation 4.15 for the installation and transport costs.

4.5.2 Price of insulation material

The insulation material selected in this study is a commercially available material (i.e., stone wool batt insulation with R-value of 25) that meets thermal regulations in floor constructions for “Very Cold” climate zone 7A recommended by National Energy Code of Canada for buildings (NECB, 2015). The insulation layer is assumed to be continuous under the PCM layer covering the entire floor area. The insulation price is calculated as follow (Djuric et al., 2007):

$$Insulation\ price = 1.2 A_I C_I \tag{4.17}$$

where A_I (m^2) is the insulation surface area, and C_I (\$/m^2) is the insulation price per unit of surface that depends on the insulation thickness: $C_I = 1.9\delta_I$, where δ_I (cm) is the insulation thickness. The additional cost of 20% is also considered for installation and transport related costs.

4.5.3 Price of energy

In order to find the energy cost, current local prices for cooling (electricity) and heating (natural gas) energy are required. According to the official data from the local energy supplier in the province of Manitoba (Manitoba Hydro, 2019), the average commercial rate for natural gas and electricity is equal to 0.089$/kWh.

4.6 Summary

In summary, this chapter presents a research methodology to investigate the optimal design of hydronic floor heating system with the incorporation of PCM storage by performing a simulation-based multivariable optimization problem. First, a model of hydronic radiant floor system was developed in EnergyPlus using Low-Temperature Radiant system. Next, a single homogeneous layer of pure PCM desirable for the under-floor heating application was added to the lower face of hydronic pipes. In order to study an appropriate range of PCMs, the surface temperature of the radiant floor was measured and based on the variation of surface temperature, five PCMs with melting temperatures of 23, 25, 27, 28, and 29°C were selected accordingly. Afterward, selected PCMs were defined in EnergyPlus using hysteresis information for further analysis in the optimization process. Once the base-case model of PCM-enhanced radiant floor system is created, two sets of optimizations problems were introduced to optimize the thermal properties of PCM with respect to different radiant water temperatures. The first set aimed to exclusively optimize the thermal properties of PCM (i.e., PCM thickness, and PCM melting temperature) while assuming other design variables to be constant. The second set intended to optimize a wider range of design variables by including the thermal properties of insulation (i.e., thickness and conductivity) and interior finishing (i.e., thickness, conductivity, and solar absorptance) to the optimization process.

Accordingly, in both sets of optimization, an objective function was formulated to minimize the total energy consumption of the case study based on the results derived from the simulation. In addition, a general cost analysis of PCM-enhanced radiant floor was proposed to evaluate the feasibility for each of individual optimization scenarios.

5 Optimal operation of natural ventilation and solar shading devices

5.1 Chapter outline

This chapter presents a research methodology to investigate the optimal control of natural ventilation and solar shading devices in Winnipeg using EnergyPlus's Energy Management System (EMS) function (section 5.2). The proposed methodology is approached by (i) simulating natural ventilation and external solar shading in EnergyPlus (section 5.3 and 5.5), and (ii) implementing various control strategies in EMS based on different environmental factors (section 5.4 and 5.6). In order to determine the most effective form of passive controls, two sets of control rules are proposed to regulate the natural cooling and solar gains. In the first set, the natural ventilation management was used to control natural cooling during the operational hours based on indoor-outdoor air temperatures, and cooling load; whereas the second set regulated solar gains through the control of the external shading during the day based on indoor air temperature, and amount of solar radiation.

5.2 Energy Management System (EMS) in EnergyPlus

5.2.1 Overview

EMS is a more advanced adaptive control system that provides users with a script-based control system, which can be coded directly within EnergyPlus. Script-based control, corresponding to the capability of changing the behavior of building systems during the simulation enables implementation of a specific control strategy, such as control of shading or natural ventilation systems. The fundamental steps required for modelling a script-based control in EMS, include (i) selection of state variables (e.g., indoor air temperature) from available sensors (using energy Management System: Sensor object), (ii) selection of buildings systems that need to be controlled by available actuators (using energy Management System: Actuator object), and (iii) coding of a control algorithm (using energy Management System: Program object) that converts sensor signals into control commands and applies them onto actuators. These basic objects of the EMS can be explained as follows:

Energy Management System: Sensor object is used to declare an Erl variable that is linked to EnergyPlus output variables or meters (EnergyPlus, 2016). In other word, this object collects information from everywhere in the model for use in control calculations. eplusout.rdd and eplusout.mdd output files provide a listing of variables and meters that can be used as sensors.

Energy Management System: Actuator object is used to connect an Erl variable to a control actuator in EnergyPlus. Actuator variables correspond to the nodes within EnergyPlus model, which can be controlled such as external shading roller. EnergyPlus then changes the value of these variables to initiate control actions. eplusout.EDD output file contains a listing of the actuator variables available for specific simulation.

Energy Management System: Program object is the central processor of the EMS and main source of the EnergyPlus Runtime Language or Erl.

5.3 Simulation of natural ventilation in EnergyPlus

In this study, auxiliary natural cooling is applied through an opening in the plenum, which directly connects indoor air to the outside and allows the outdoor air to cool down the room according to the active strategy. One of the general approaches to model natural ventilation in EnergyPlus is ZoneVentilation:DesignFlowRate object, which is intended for simplified ventilation calculation. In this method, natural ventilation can be controlled by either a specified schedule or by specifying minimum, maximum, and average temperature. The temperature can be defined either as a constant value throughout the simulation or as schedules that can be changed over time. However, complex zone ventilation control strategies that are controlled by other environmental factors such as external temperature require a control algorithm that is manually programmed in a script-based platform (such as EMS). Following inputs are needed for simulating the natural ventilation system using ZoneVentilation:DesignFlowRate object (Figure 5.1).

- *Field: Name:* this field determines the name of the ZoneVentilation:DesignFlowRate object

- *Field: Zone or ZoneList Name:* this field determines the name of the zone or zone list assigns a specific ventilation statement to a thermal zone(s) in the building.

- *Field: Schedule Name:* This field requests the name of the predefined schedule that determines the maximum design volume flow rate. This value can vary between 0.0 and 1.0. In another word, this object helps us determine the status of the natural ventilation system, where 0 and 1 indicate that the natural ventilation damper is fully closed and opened, respectively. In this study, this key object was used as the actuator object in EMS for controlling the natural ventilation system.

- *Field: Design Flow Rate Calculation Method:* This field specifies the calculation method used for measuring the design flow rate.

- *Flow/Zone:* This method requires a direct insertion of the design volume flow rate. This research uses this method (i.e., empirical power law (Swami and Chandra, 1987)) to calculate the amount of airflow across the opening in the building façade as follows:

$$Q_v = C_d \cdot A \cdot V \tag{5.1}$$

  where Q_v is volumetric flow rate through the opening (m^3/s); A is the free area of inlet openings (m^2); V is air velocity leaving the opening (m/s), and C_d is the discharge coefficient (effectiveness of openings). C_d is calculated based on the direction of the wind and can vary between 0.3 for the condition that wind hits an opening at a 45º angle and 0.6 for wind hitting directly at a 90º angle of incidence. Assuming Winnipeg average wind speed of 4.7 m/s (Environment Canada, 2017) and average wind incident normally on the wall (C_d = 0.45), the quantity of airflow for 0.1 m^2 opening is equal to 0.21 m^3/s.

- *Field: Ventilation type:* this field determines the types of ventilation that could be applied to the thermal zone. Natural ventilation used in this thesis assumes that air movement/exchange is due to opening in the building plenum and uses an intake fan to bring in a specific amount of air based on a specific control, which results in the removal of excess heat and contaminant from the space. This type of fan enables us to control the air movement entering the space by changing the position of fan damper. Values related to the fan pressure and efficiency of this type of natural ventilation are chosen from the software default. For this ventilation type, it is assumed that the condition of the air entering the space is equivalent to outside air condition.

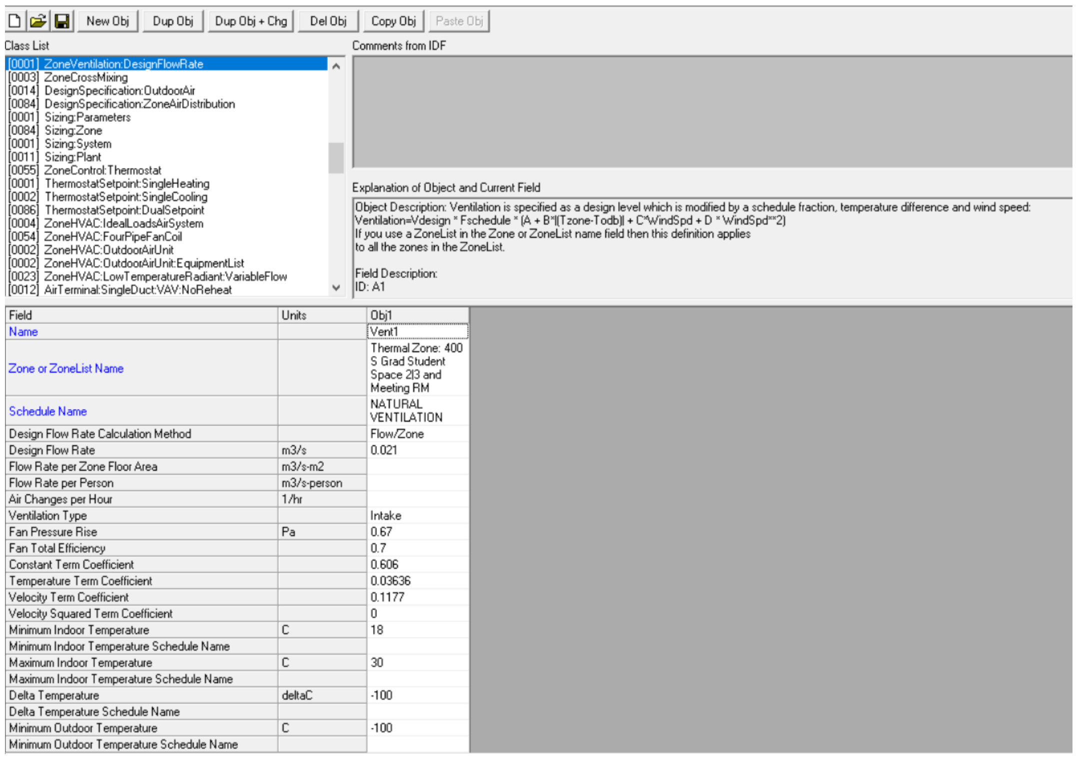

Figure 5.1: Required inputs for simulation of natural ventilation in EnergyPlus

5.3.1 Simulation of natural ventilation control in EMS

The control strategies applied to the EMS are based on the four scenarios: (i) mean zone air temperature, (ii) combination of mean air temperature and the difference between internal-external temperatures, (iii) couple measurement of cooling load and internal-external temperatures, and (iv) combination of the three control strategies. In all of these control strategies, the natural ventilation can take one of the following positions: on (damper is fully open) or closed (damper is fully closed). The applied control strategies aim to maximize thermal comfort and reduce cooling loads by limiting overheating hours and bringing free cool air to the study room directly from the outside. Table 5.1 provides an overview of the following four types of management schemes:

- *Only inside mean air temperature level*: The damper (or actuator) opens when the mean air temperature (or sensor) reaches the higher set-point and closes when it falls under the lower set-point. The set-point varies between 22°C to 26°C, with 0.5°C step.

- *Inside mean air temperature and internal-external temperatures*: Natural cooling starts working when the indoor temperature exceeded a predefined set-point (i.e., 22°C to 26°C with 0.5°C step), and the outdoor temperature is lower than the indoor temperature.

- *Cooling load and internal-external temperatures*: Damper switches to opens mode if there is a need for cooling in the zone and the outdoor temperature is lower than the indoor temperature

- *Inside mean air temperature, internal-external temperatures, and cooling load:* Natural ventilation is used if all three conditions (i.e., indoor temperature, indoor-outdoor temperature, and cooling load) are met and it is turned off if one of above conditions is not satisfied. As an example, Figure 5.2 shows the simulation of natural ventilation control in EnergyManagementSystem:Program object.

Table 5.1: Overview of the applied natural ventilation strategies.

Scenarios	Parameter set-points	IF function defined in EMS
Case 1: activated indoor air temperature.	T_{set} = 22 - 26°C with 0.5°C step	$T_i > T_{set}$
Case 2: activated based on indoor-outdoor temperature.	T_{set} = 22 - 26°C with 0.5°C step	$T_i > T_{set}$ and $T_i - T_o < 0$
Case 3: activated based on cooling load and indoor-outdoor temperature.	-	$Cooling > 0$ and $T_i - T_o < 0$
Case 4: activated if Cases 1-3 are met.	-	$T_i > T_{set}$ and $T_i - T_o < 0$ and $Cooling > 0$

Where
T_i = Indoor temperature, T_{set} = Temperature set-point, T_o = Outdoor temperature

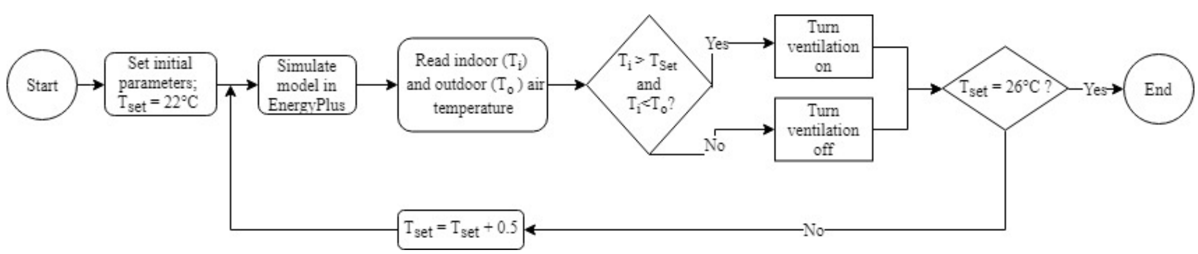

Figure 5.2: Flowchart of natural ventilation control simulation in EMS based on indoor-outdoor temperature set-point

5.4 Simulation of exterior solar shading in EnergyPlus

External solar shading was simulated in EnergyPlus by assuming two exterior window shading devices attached to the external side of the southern and eastern glazing in the case study (see Figure 3.8). The shading device selected for this study is an exterior roller shade with thermal conductivity of 0.1W/m·K for all scenarios. Thermal properties of the selected shading device are defined in EnergyPlus using WindowMaterial:Shade object, which can be used for diffusing materials such as drapery and translucent roller shades (EnergyPlus, 2018). Furthermore, transmittance and reflectance values for solar shading material can be obtained from ASHREA Fundamentals, Chapter 30 (ASHREA, 1995).

The following steps were undertaken to assign exterior shades to the southern and eastern windows in EnergyPlus program:

(i) Defining the construction of windows without considering the external shades.

(ii) Referencing the defined construction in FenestrationSurface:Detailed object as a window.

(iii) Defining shading thermal and visual properties in WindowMaterial:Shade object.

(iv) Using WindowProperty:ShadingControl object to (a) assign the defined shades to the windows and (b) specify the desired control method for the shades.

WindowProperty:ShadingControl object allows users to specify the type and location of the shading devices, which is the key object affecting control deployment of the shading devices, and the set-point. However, similar to the control of natural ventilation system, implementation of complex control strategies for shading devices that are based on various environmental parameters can be made only through EMS (EnergyPlus, 2018). Exterior shading device can have two discrete conditions: (1) retracted (i.e., the window is fully closed), or (2) activated (i.e., the window is fully opened). Whether the shading device is open or closed during a particular time step depends on the EMS control strategy (section 5.6).

The following inputs are required for the simulation of the exterior solar shading system using WindowProperty:ShadingControl object (Figure 5.3):

- *Field: Name*: this field determines the name of window shading control.

- *Field: Shading Type:* This field determines the type and location of solar shade. Since the shading device is attached to the exterior side of windows, therefore this field must be "ExteriorShade".

- *Field: Construction with Shading Name:* This field requires the name of the window construction that has the shading in place.

- *Field: Shading Control Type:* This field specifies how the shading device is controlled. However, the EMS control strategies override this predefined field.

- *Field: Schedule Name:* This field specifies whether the shading is scheduled or not. If schedule value is more than zero, shading control is active, otherwise, it is off. This field is used as an actuator in EMS to manually control the shading device.

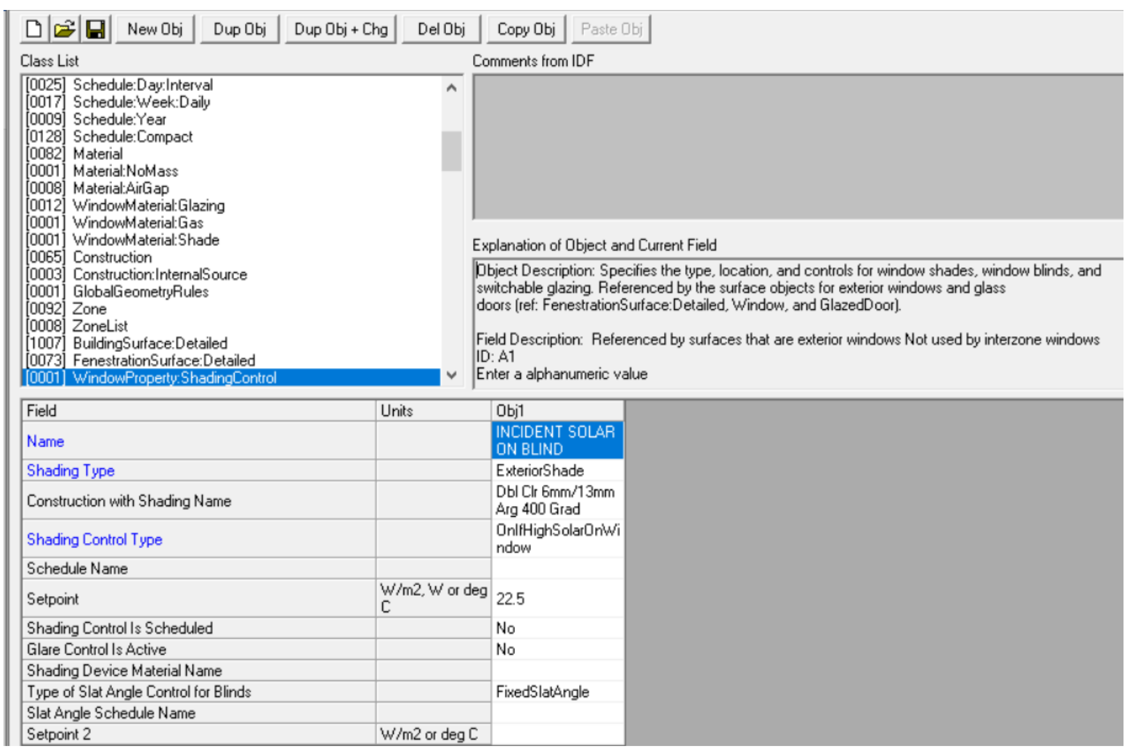

Figure 5.3: Required inputs for simulation of solar shading in EnergyPlus

5.4.1 Effects of external solar shading devices on daylighting

External solar shading device can affect the contribution of daylight in the space. This mainly depends on the type, size, angle of incidence, and window coverage (Breitenbach et al., 2001; Tzempelikos and Athienitis, 2007). Best practice in controlling the shading device is to minimize excessive solar gain while maximizing daylight level in the space. Maximization of daylight level can improve visual quality, and occupants' productivity and reduce electricity consumption. The average daylighting level can vary for each orientation with a desired level of 500 lux required for reading the text in a study room (CIBSE, 1999). Tzempelikos and Athienitis (2007) reported that in order to provide 500 lux daylight in the workplace, the visual transmittance for the external shading device should be around 20%. Therefore, to balance between the energy savings, occupants' thermal comfort, and daylighting this study assumed 35% visual transmittance for the external shades in all of the scenarios. Figure 5.4 shows the annual illuminance analysis of the study room using EnergyPlus DElight tool (Radiosity technique). It can be seen that for approximately 95% of daily hours the selected shading device provided daylighting of 500 lux, which satisfies the recommendations of National Research Council Canada (NRC, 2011).

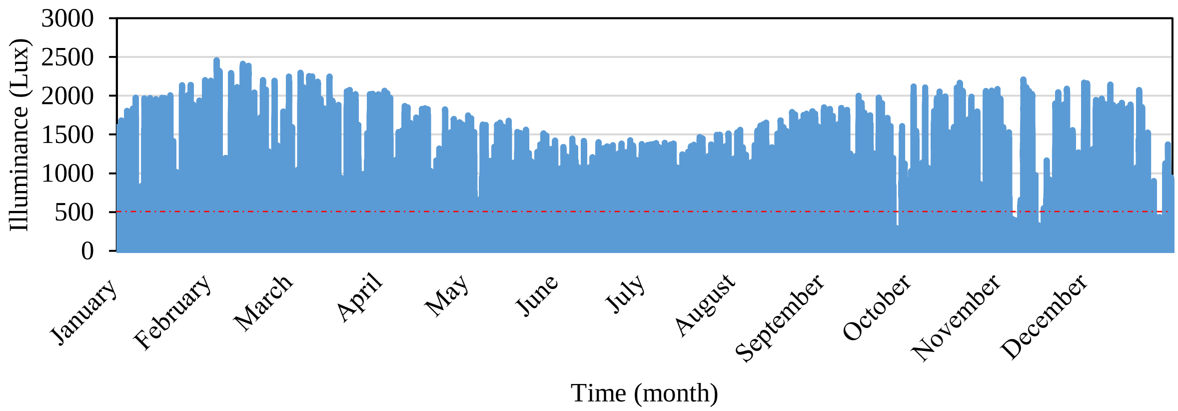

Figure 5.4: Annual room daylighting when shading with 35% transmittance is used.

5.4.2 Simulation of exterior solar shading control in EMS

Defined shading control strategies are based on three parameters: (i) the radiation level on the façade, (ii) the mean air temperature, and (iii) the coupled radiation level and indoor temperature. An efficient strategy should minimize the room's energy demand while ensuring adequate vision to the outside and daylight in the room. Table 5.2 summarizes the applied shading control strategies. Three types of management schemes are modeled:

- *Only window transmitted radiation level*: The screen closes when window transmitted radiation on the vertical south side of the external shading exceeds a specified set-point. The set-point can vary between 0kW and 12kW, with a 1kW step. As an example, Figure 5.5 shows the simulation of shading control strategy in EnergyManagementSystem:Program object for different radiation level.

- *Only inside mean air temperature level*: Shading closes when internal mean air temperature exceeds a chosen set-point. Set-point temperature can vary between 22°C and 26°C, with a 0.5°C step.

- *Window transmitted radiation and inside mean air temperature*: The shading is activated when both conditions (i.e., window transmitted radiation level and inside mean air temperature) are met, and disabled if one of the above opening conditions is not satisfied.

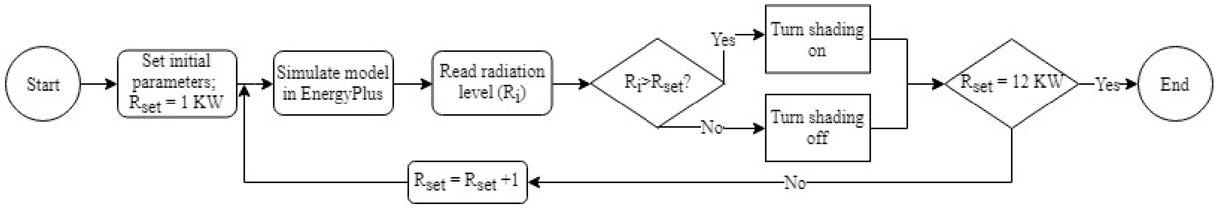

Figure 5.5: Flowchart of shading device control simulation in EMS based on radiation level set-point.

Table 5.2: Overview of the applied shading strategies.

Scenarios	Parameter set-points	IF function defined in EMS
Case 1: activated based on radiation level.	R_{set} = 1 – 12kW with 1kW step	$R_i > R_{set}$
Case 2: activated based on indoor air temperature.	T_{set} = 22 - 26°C with 0.5°C step	$T_i > T_{set}$
Case 3: activated if Cases 1-2 are met.	-	$R_i > R_{set}$ and $T_i > T_{set}$

Where
R_i = Radiation level passing through the window, R_{set} = Radiation level set-point
T_i = Indoor temperature, T_{set} = Temperature set-point

5.5 Summary

In summary, this chapter presented a new methodology for further energy performance investigation of optimal automated natural ventilation and solar shading devices using built-in EMS function of EnergyPlus. To enable this, a brief overview of EnergyPlus's EMS feature was first presented. Next, natural ventilation and solar shading devices were numerically simulated in EnergyPlus using ZoneVentilation:DesignFlowRate and WindowMaterial:Shade objects (section 5.3 and 5.4). Afterward, two sets of integrated control strategies were developed to find the optimal operation of each system based on various environmental factors (section 5.3.1 and 5.4.2). The first set of control rules aimed to investigate the impact of free cooling on the annual heating and cooling use and thermal comfort of the case study. In this case, the air movement is regulated based on monitoring the internal-external air temperature, and the cooling demand in the space. The second control set evaluated the impact of external solar shading management on the energy and thermal comfort performance based on indoor temperature and solar radiation levels.

6 Results and discussion

6.1 Chapter outline

The objective of this chapter is to analyze the effectiveness of the developed passive solar design strategies on the energy and indoor environmental performance of the case study. Section 6.2 provides model verification analysis that included a comprehensive comparative study between the SPEB model developed in EnergyPlus and the SPEB model developed in IES. Section 6.3 analyzes the optimal design of PCM-enhanced radiant floor for each scenario and evaluates the effect of each design on the energy and thermal comfort performance of the case study. Section 6.4 provides a performance analysis on the impact of optimal control of natural ventilation and solar shading devices on reducing excessive heat gains, energy consumption, and indoor environmental quality.

6.2 Results analysis of detailed building model verification

Overall there is a very good agreement between the predictions of the SPEB model developed in EnergyPlus model and the SPEB model developed in IES models. Figure 6.1 provides a comparison of total energy consumption by end use between the EnergyPlus and IES model. As it is shown, the discrepancy between the total energy consumption is less than 2.1%, whereas the percentage differences between the annual heating, cooling, lighting and plug-load predictions are around 0.7%, 7.6%, 0.6%, and 0.13%, respectively. Furthermore, the Energy Use Intensity (EUI), which expresses energy use as a function of the building size (kWh/m²/year), shows that EnergyPlus model's EUI of 386kWh/m²/year is approximately 1.8% lower than IES model's EUI of 393kWh/m²/year. Additionally, Table 6.1 compares the mean, maximum, minimum, and standard deviation of the heating and cooling energy consumption between the two models. There is a very good agreement between the EnergyPlus and IES models' aggregated energy predictions, and in particular in comparison to several similar studies. For example, Abdullah et al. (Abdullah et al., 2014) reported a difference of 36% between the EUIs' of 4,740 m² university building modeled in Vasari/GBS (505kWh/m²) and Sefaira (324kWh/m²) software.

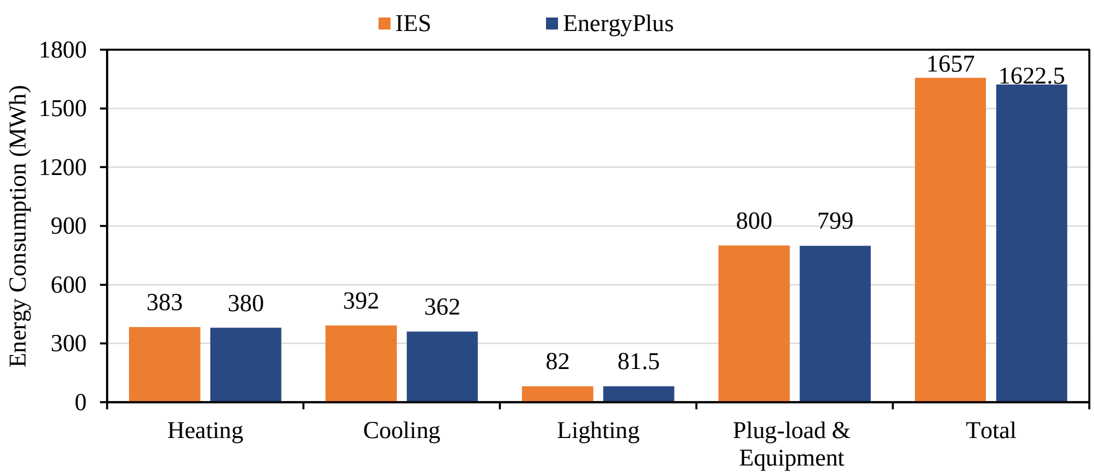

Figure 6.1: EnergyPlus and IES annual energy consumptions by end-uses (Al-janabi et al., 2019).

Table 6.1: Descriptive statistics for EnergyPlus and IES heating and cooling energy consumptions (Al-janabi et al., 2019).

Energy use (kW)	**Heating**			**Cooling**		
	EnergyPlus	IES	Percentage difference (%)	EnergyPlus	IES	Percentage difference (%)
Mean	43.4	43.7	0.7	41.3	44.8	8.1
SD	47.4	40.4	15.9	36.8	36.8	0
Minimum	0	0	0	17.4	18.0	3.4
Maximum	239.7	202.8	16.7	208.9	266.3	24.2

Figure 6.2 shows that better accordance exists between the models' heating than cooling energy consumption profiles. For cooling energy consumption, the difference between the EnergyPlus

and IES model predictions is particularly pronounced during the summer months. Considering that the cooling load calculations are inherently more complicated as they involve solving unsteady equations with unsteady boundary conditions and internal heat sources, a more significant discrepancy between the models' predictions are anticipative. Furthermore, these findings are in agreement with the results of some previous studies, which also reported higher discrepancies for cooling than heating energy consumption. For instance, Schwartz, and Raslan (2013) modeled a 32-story student residential hall, located in London, UK in EnergyPlus and IES and showed that EnergyPlus predicted around 21% lower heating energy consumption and more than 4 times higher cooling energy consumption.

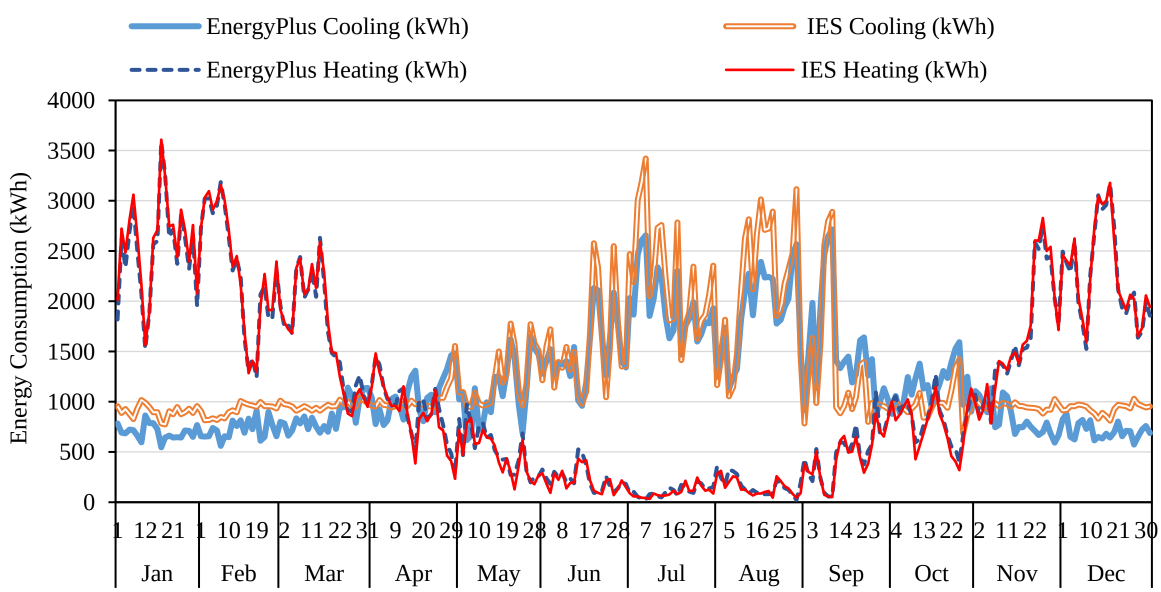

Figure 6.2: EnergyPlus and IES total daily heating and cooling energy consumptions (Al-janabi et al., 2019).

Figure 6.3 illustrates the total monthly heating and cooling energy consumption of the EnergyPlus and IES models along with their average indoor air temperatures during an occupied (06:30 am-10:30 pm) and unoccupied (10:30 pm-06:30 am) hours over the year. During the occupied winter hours, the EnergyPlus model calculated higher heating and lower cooling energy consumptions than the IES model, whereas during the unoccupied winter hours the IES model predicted higher heating energy consumptions that the EnergyPlus model, whereas the cooling energy consumptions were almost equal between the two models. Furthermore, during the occupied summer hours, the IES model calculated higher cooling energy consumptions compared to the EnergyPlus model. Figure 6.3 also shows that the EnergyPlus model predicted 0.65°C (November) to 1.2°C (March) lower monthly average indoor air temperatures that the IES model during the unoccupied winter hours, whereas it maintained higher indoor air temperatures than the IES model during the summer months. Consequently, the tighter air temperature range of the IES model might be the reason for higher energy consumptions of the IES model compared to the EnergyPlus model. The EnergyPlus model, on the other hand, predicted higher cooling energy consumption during the shoulder seasons (i.e., March, April, September, and October). A possible reason for this might be the shoulder seasons' weather conditions, which differ from the rest of the year as they are characterized by the quick temperature changes from day to day as well as warmer and longer days with cold nights. For example, Figure 6.4 shows that the EnergyPlus model consumed more cooling energy during the days with daily average outdoor air temperatures below 20°C, whereas the IES model used more cooling energy during the days with daily average outdoor air temperatures above 20°C.

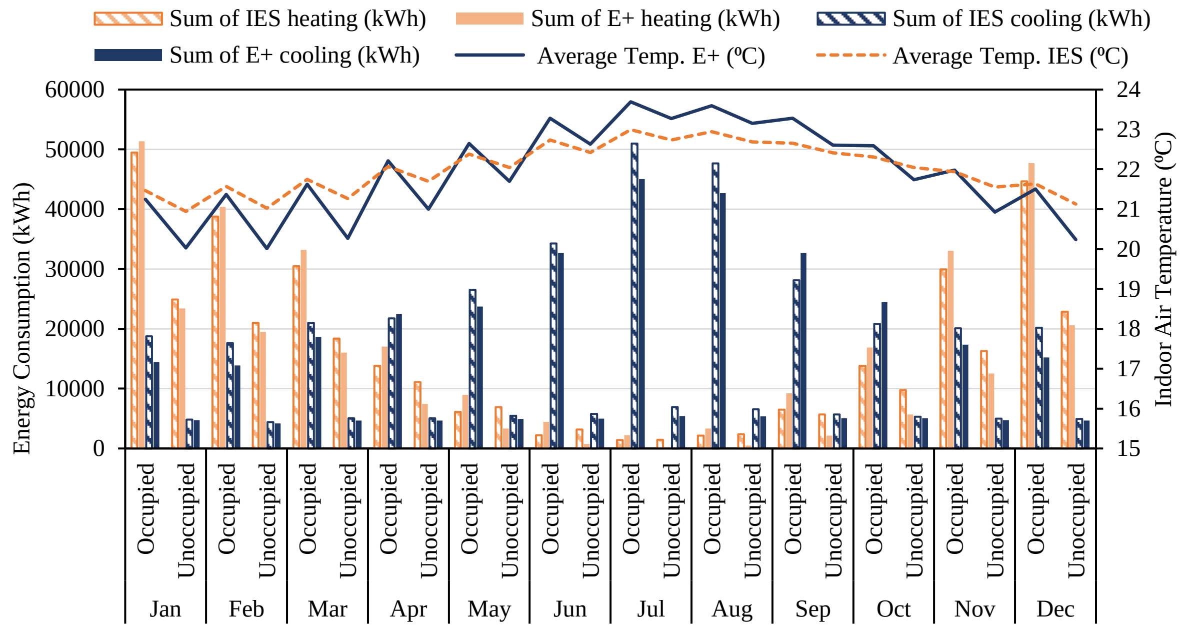

Figure 6.3: EnergyPlus and IES heating and cooling energy consumptions and average monthly indoor air temperatures during the occupied and unoccupied hours throughout the year (Al-janabi et al., 2019).

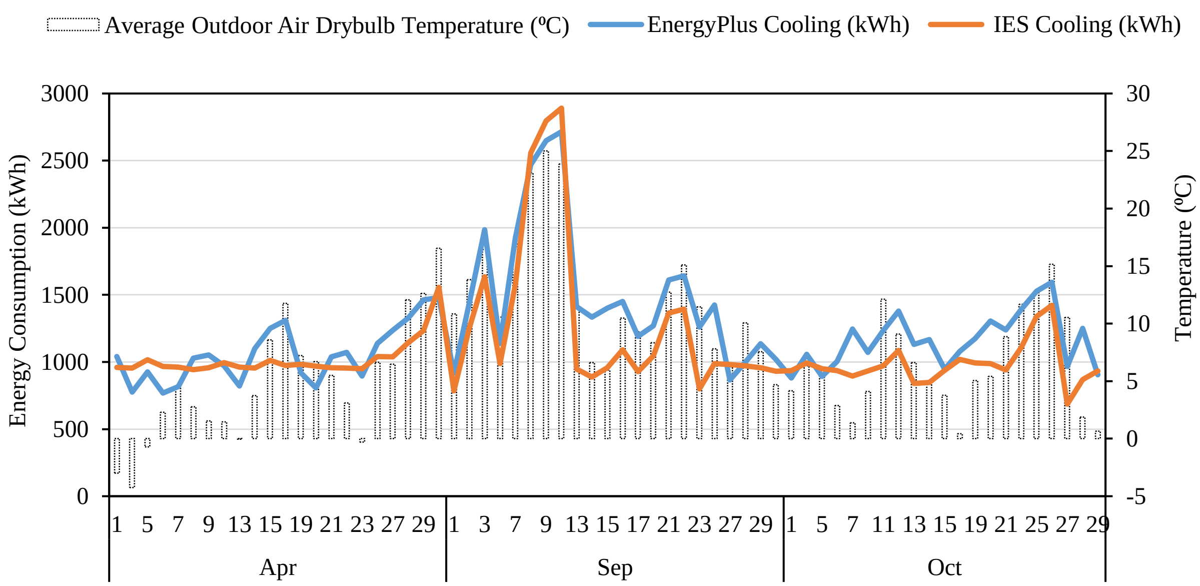

Figure 6.4: EnergyPlus and IES cooling energy consumptions and outdoor air temperatures during April, September, and October (Al-janabi et al., 2019).

To better illustrate the differences in the indoor air temperature variations between the models, Figures 6.5 and 6.6 compare the indoor air temperature distributions during occupied and unoccupied hours, respectively. Additionally, Table 6.2 summarizes the temperatures' mean, standard deviation, minimum and maximum values, whereas Table 6.3 shows the percentage of time EnergyPlus model over- and under-predicted indoor air temperatures compared to IES model. It is evident that the indoor air temperatures of the EnergyPlus model have higher variability than the indoor air temperatures of the IES model across all floors. Considering the operation of the HVAC systems in a reality where indoor air temperatures vary within the specified temperature range (i.e., dead-band) to improve the efficiency of the system and reduce energy consumption, the variations of the indoor air temperatures within the EnergyPlus model are expected. The largest discrepancies between the models' calculations of the indoor air temperatures exist for the below-grade and top floor. Also, in the EnergyPlus model, the standard deviation increases with floor level, whereas in the IES model it is the lowest for the top floor and basement and the highest for the first floor (see Table 6.2).

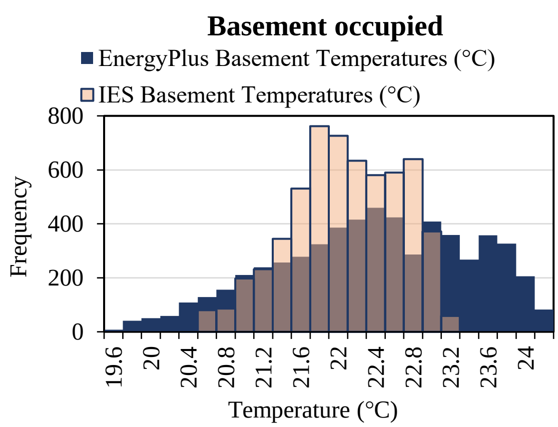

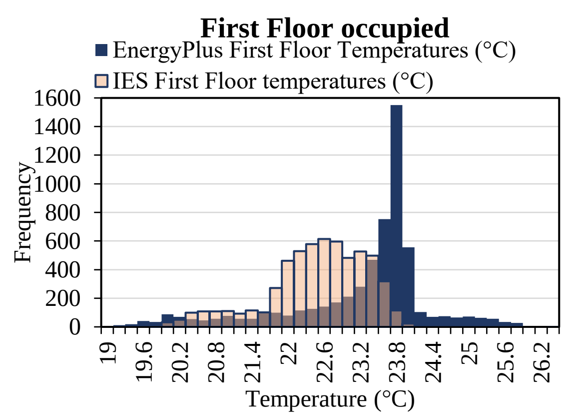

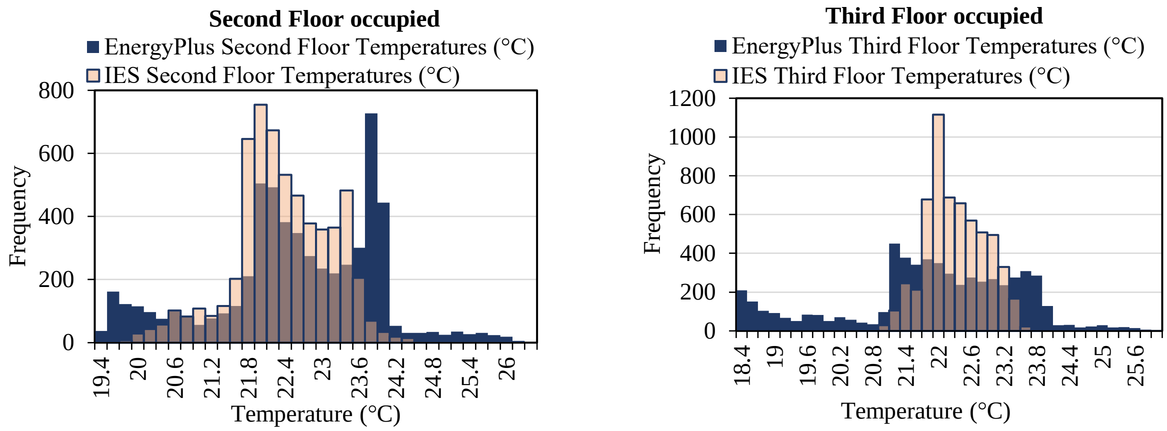

Figure 6.5: EnergyPlus and IES indoor air temperature distributions during the occupied hours (06:30 am-10:30 pm) by floor (Al-janabi et al., 2019).

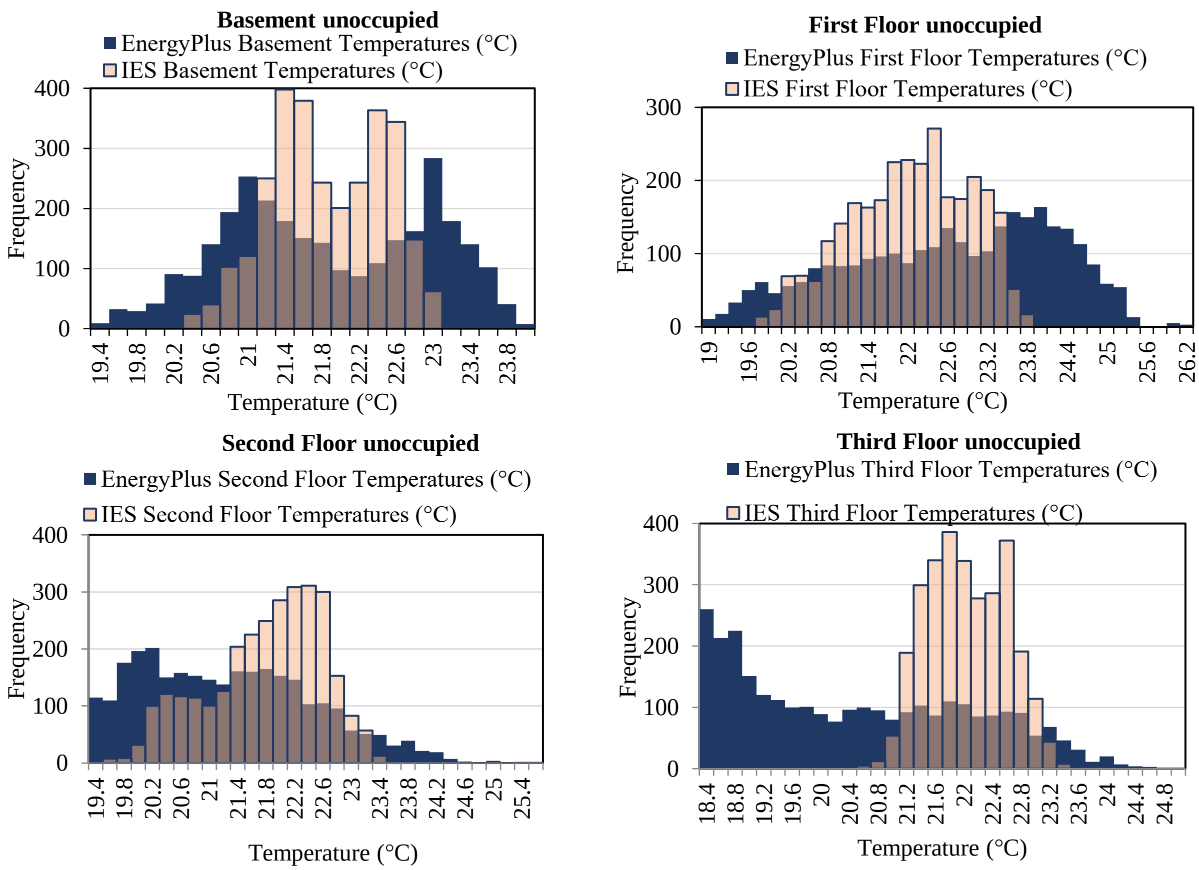

Figure 6.6: EnergyPlus and IES indoor air temperature distributions during the unoccupied hours (10:30 pm-07:30 am) by floor (Al-janabi et al., 2019).

Table 6.2: Descriptive statistics for EnergyPlus and IES indoor air temperatures by floor (Al-janabi et al., 2019).

Temperature (°C)	Basement		First floor		Second floor		Third floor	
	EnergyPlus	IES	EnergyPlus	IES	EnergyPlus	IES	EnergyPlus	IES
Mean	22.10	21.91	22.95	22.23	22.04	22.07	21.33	22.12
SD	1.08	0.60	1.37	0.88	1.44	0.84	1.73	0.56
Minimum	19.34	20.25	18.89	19.58	19.21	19.45	18.29	20.33
Maximum	24.19	23.19	26.37	23.95	26.15	24.67	25.88	23.61

Table 6.3: Percentage of time EnergyPlus model over- and under-predicted indoor air temperatures compared to IES model (Al-janabi et al., 2019).

EnergyPlus	Basement%		First Floor%		Second Floor%		Third Floor%	
	Occupied	Unoccupied	Occupied	Unoccupied	Occupied	Unoccupied	Occupied	Unoccupied
Over-predicts total	**74**	**50**	**94**	**76**	**84**	**27**	**45**	**17**
≤ 1°C	89	97	73	48	96	68	100	72
1°C – 2°C	11	3	27	46	4	30	0	24
≥ 2°C	0	0	0	6	0	2	0	4
Winter months	*48*	*35*	*47*	*35*	*47*	*10*	*25*	*1*
≤ 1°C	90	100	63	81	99	100	100	100
1°C – 2°C	10	0	37	19	1	0	0	0
≥ 2°C	0	0	0	0	0	0	0	0
Summer months	*52*	*65*	*53*	*65*	*53*	*90*	*75*	*99*
≤ 1°C	88	97	82	29	94	66	100	71
1°C – 2°C	12	3	18	61	6	32	0	25
≥ 2°C	0	0	0	10	0	2	0	4
Under-predicts total	**26**	**50**	**6**	**24**	**16**	**73**	**54**	**83**
≤ 1°C	100	100	100	100	85	70	84	26
1°C – 2°C	0	0	0	0	15	30	10	21
≥ 2°C	0	0	0	0	0	0	6	53
Winter months	*54*	*65*	*98*	*99*	*40*	*36*	*71*	*60*
≤ 1°C	99	99	100	100	84	64	85	8
1°C – 2°C	1	1	0	0	16	36	8	15
≥ 2°C	0	0	0	0	0	0	7	77
Summer months	*46*	*35*	*2*	*1*	*60*	*64*	*29*	*40*
≤ 1°C	100	100	100	100	87	80	83	54
1°C – 2°C	0	0	0	0	13	20	13	31
≥ 2°C	0	0	0	0	0	0	4	15

Figure 6.7 illustrates the breakdown of the heating and cooling energy consumptions between the radiant system and air system for the IES and EnergyPlus models. There are significant differences

regarding the utilization of the air and radiant systems between the two models. Thus, the radiant system meets approximately 23% of the total cooling energy demand in the EnergyPlus model and only around 9% in the IES model. In heating mode, the difference in the utilization of the radiant system is less, as the radiant system covers approximately 75% of the total heating energy demand in the EnergyPlus model and around 60% in the IES model.

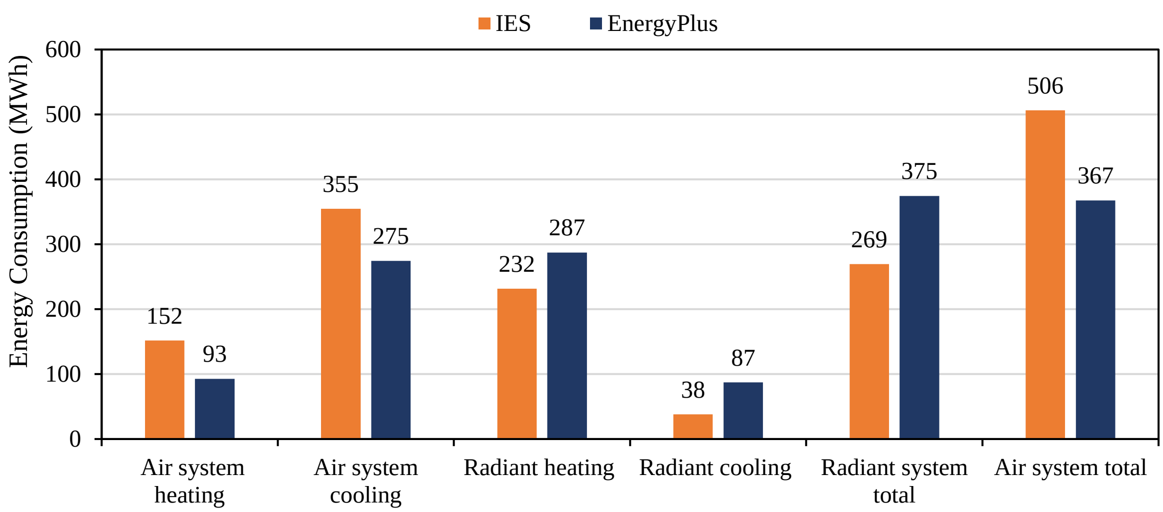

Figure 6.7: EnergyPlus and IES model comparison of heating and cooling energy consumptions on the system level (Al-janabi et al., 2019).

Figure 6.8 provides further insight into the models' utilization of the radiant and air systems throughout the year. It shows that the discrepancy between the utilization of the air system occurred during the summer months when the air cooling system within the IES model consumed around 26% more energy than the air cooling system within the EnergyPlus model. Furthermore, the air cooling system within the IES model consumed nearly 27% more energy during the winter season compared to the air cooling system within the EnergyPlus model. Similarly, the air heating system within the IES model consumed nearly 30% more energy during the winter season than the air heating system within the EnergyPlus model. Higher utilization of the air system in the IES model is the likely reason for the differences in the predictions of the indoor air temperatures between the models as well as smaller indoor air temperature variations in the IES model compared to the EnergyPlus model. Furthermore, Figure 6.8 also shows that the EnergyPlus model on average maintained lower indoor air temperatures during the winter season and higher indoor air temperatures during the summer season than the IES model, which is the likely reason for the higher heating and cooling energy consumptions of the IES model compared to the EnergyPlus model.

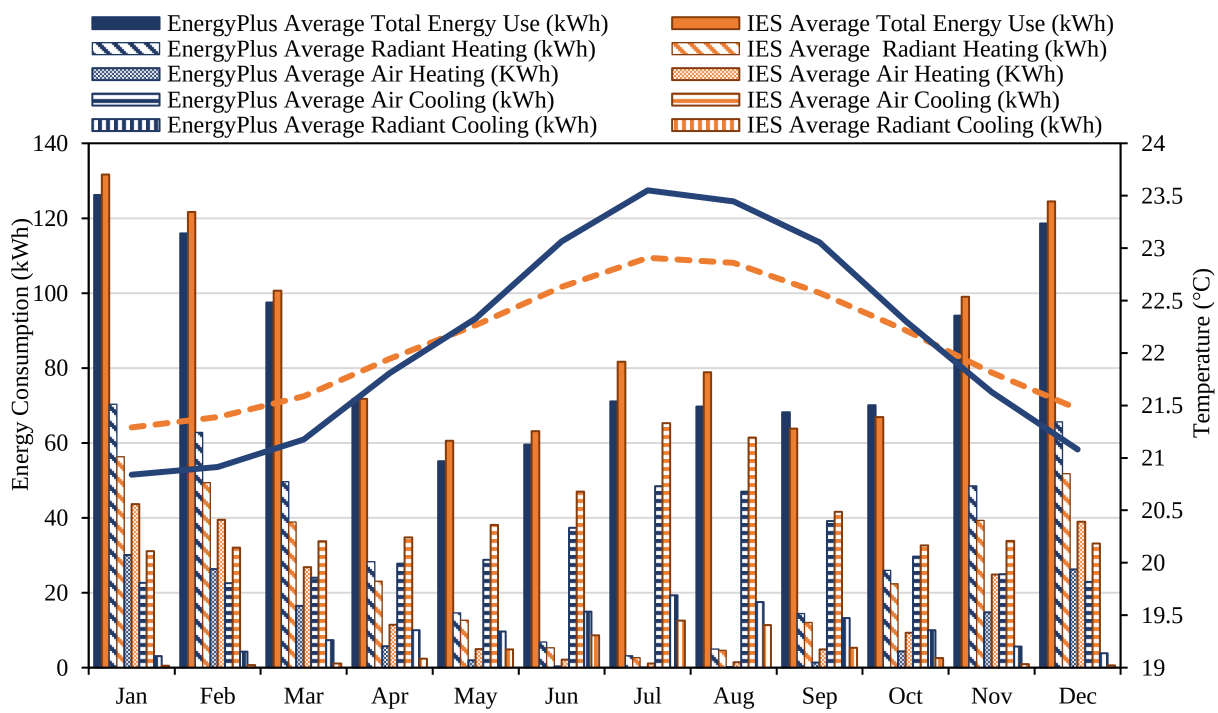

Figure 6.8: EnergyPlus and IES monthly average total energy consumptions, cooling, and heating energy consumptions by the system and indoor air temperatures over the year (Al-janabi et al., 2019).

Figures 6.9 and 6.10 compare the models' peak heating and cooling loads. As in the ideal air load scenario, both models calculated the peak heating loads at 8 am on January 18th (see Figure 6.9). On the other hand, the IES model calculated the peak cooling load at 12 pm on August 17th, while the EnergyPlus model calculated the peak cooling load at 17 pm on September 10th (see Figure 6.10). As in the previous results, Figure 6.9 demonstrates that the EnergyPlus model relied more on the radiant system, which has a slow thermal response time, whereas the IES model mostly used the fast response air system to meet the building's heating demand. Figure 6.10 shows a similar behavior of the two models in cooling mode. Consequently, the energy profiles of the two models have different peaks and valleys as the IES model maintained the indoor air temperatures within the tighter range compared to the EnergyPlus model.

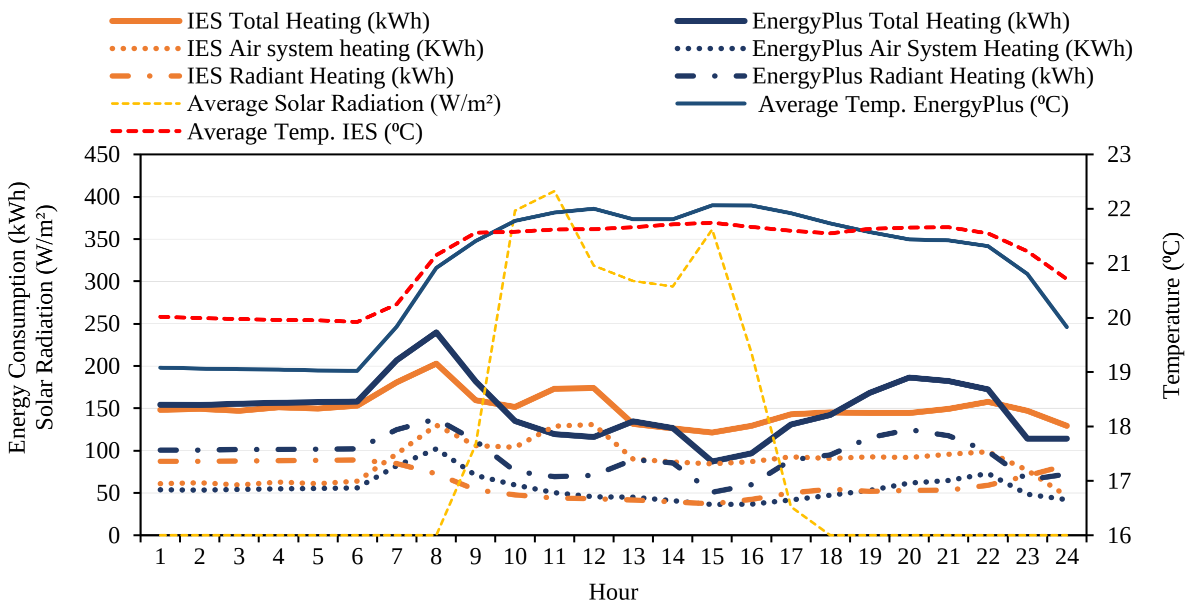

Figure 6.9: EnergyPlus and IES total hourly heating energy consumptions, heating energy consumption by the system, indoor air temperatures and solar radiation on January 18th (Al-janabi et al., 2019).

The disparity between the energy consumption and operation of the models' HVAC systems are most likely related to some differences in the modeling approach. For instance, in the IES model, the air system is simulated using templates, whereas in the EnergyPlus model the air and radiant systems are built from the individual components (e.g., each coil of the fan coil units is defined individually). Consequently, it was not possible to model the same controls. For example, in the EnergyPlus model the sequencing of the HVAC equipment is applied on the zone level (e.g., radiant system or the fan coil), while in the IES model it is implemented on the system level (e.g., hot water loops).

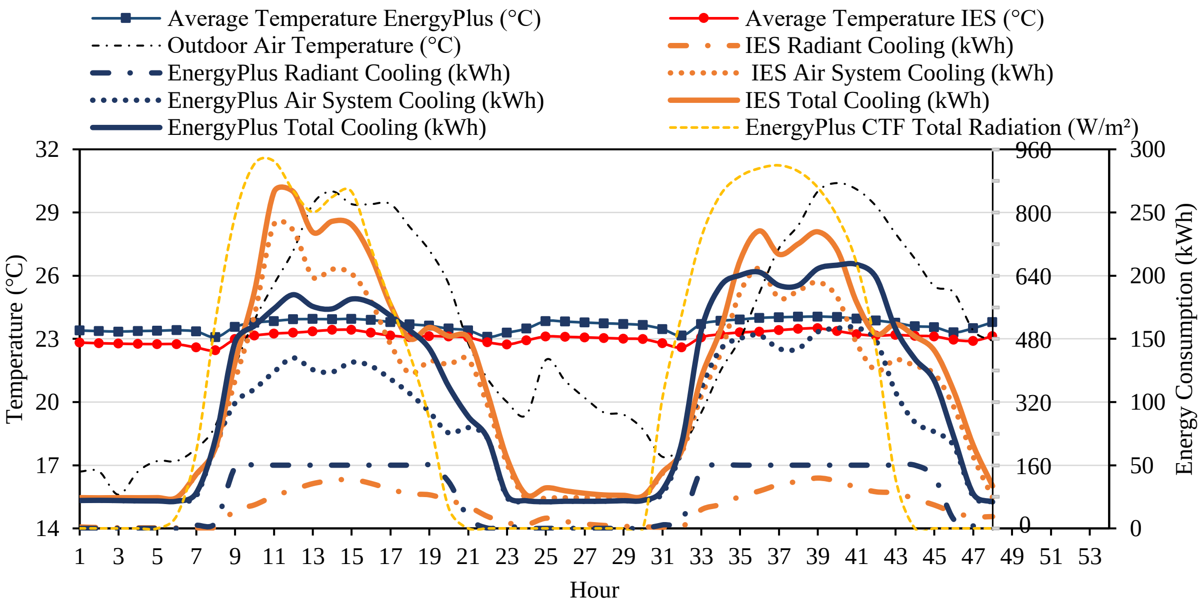

Figure 6.10: EnergyPlus and IES total hourly cooling energy consumptions, cooling energy consumption by the system, indoor air temperatures, outdoor air temperatures, and solar radiation on August 17th and September 10th (Al-janabi et al., 2019).

Therefore, as per the final construction drawings, in EnergyPlus the radiant system is the first system intended to serve the load and the air system second, which might be the reason for the more extensive utilization of the radiant system in the EnergyPlus model compared to the IES model. There is a limited body of literature that compares predictions of building performance simulation tools on the HVAC system level and especially for complex buildings such as the SPEB. One study created an ideal building model to investigate the constant air volume and variable air volume systems of EnergyPlus, DeST, and DOE-2.1E and compared them in detail to assess their similarities and differences (Zhou et al., 2014). The study concluded that the main influencing factors for HVAC discrepancies are the algorithms used for the HVAC component models and their control strategies. Furthermore, it was also revealed that differences between the

HVAC systems' energy consumption could be within a 10% range only if all component models are chosen to be similar, and the same or equivalent inputs for the HVAC systems are used and sometimes there is no way to map between the user inputs directly.

6.3 Results analysis of optimal PCM-enhanced radiant floor system

This section evaluates the impact of the PCM-enhanced hydronic radiant floor system on the overall performance of the studied case study by analyzing three essential parameters, i.e., energy consumption, predicted mean vote (PMV) index (thermal comfort), and economic perspective. Furthermore, thorough understanding about the impact of the incorporated PCM on the space heating and cooling energy consumptions as well as thermal comfort of the occupants required a comprehensive analysis of the data using three different resolutions, including annual, monthly, and hourly.

6.3.1 Optimized design variables of scenario 1 and scenario 2

Table 6.4 summarizes optimized design variables of the two scenarios for six water supply temperatures ranging from 45.6°C to 35.6°C, with a 2°C difference. Under both scenarios, PCM_{28} with a peak melting temperature of 28°C is the optimal solution for all the supply water temperatures. This finding is not surprising considering that the majority of the time (~57%), surface temperatures were within the working temperature range of PCM_{28} of 26-28 ºC (Figure 6.11). Similarly, Farid and Kong (2001) concluded that PCMs with a melting temperature of 28°C achieved the most considerable heating reductions for supply water temperatures of approximately 50°C. The results also show that the addition of the insulation layer in the second scenario reduced the thickness of PCM_{28} for more than 70% compared to the first scenario. For instance, optimal PCM_{28} thickness for the highest supply water temperature of 45.6°C was 15 mm in the first scenario and only 4 mm in the second scenario. Similarly, optimal PCM_{28} thickness for the lowest supply water temperature of 35.6°C was 10 mm in the first scenario and only 2 mm in the second scenario.

In both scenarios, the thickness of PCM_{28} decreases with the decrease of the supply water temperature. The positive correlation between PCM_{28} thickness and the supply water temperature suggests that an optimal amount of PCM_{28} that undergoes a complete phase transition cycle day-after-day to a great extent depends on the amount of heat generated by the hydronic radiant heater. Moreover, a decrease in heat transfer caused by a decrease in the supply water temperature explains a reduction in insulation thickness. The results also show that the supply water temperature reduction has a more pronounced impact on the decrease in PCM_{28} thickness of second than the first scenario. For example, the reduction of the water supply temperature of 10°C resulted in more than 55% decrease in the PCM_{28} thickness in the second scenario and nearly 30% in the first scenario. The likely explanation of these results is the reduced heat dissipation through the floor due to the inclusion of an insulation layer to the lower face of the PCM_{28} layer within the second scenario.

The findings also indicate that the floor thickness with the lower values (approximately 20 mm) and floor conductivity with the higher values (approximately 2 W/(m·K)) performed better compared to other solutions due to the increased heat transfer. Table 6.4 also shows that α-value (F_α) tends to take higher solar absorptance surface values for all supply water temperatures, and it tends to increases with the decrease in water temperature. The negative correlation between water temperature and surface solar absorptance values suggests that an increase in solar absorptance properties of PCM-enhanced hydronic radiant floor system compensates for the decrease in water temperature.

Table 6.4: Optimal values of the design variables that result in the most efficient performance for each radiant hot water temperature.

	$Radiant_{ST}$ (°C)	PCM_{mt} (°C)	PCM_t (mm)	I_t (mm)	I_k (W/m·K)	F_t (mm)	F_k (W/m·K)	F_a
Case 1	45.6	28	15.08	-	-	-	-	-
	43.6	28	13.7	-	-	-	-	-
	41.6	28	12.9	-	-	-	-	-
	39.6	28	11.7	-	-	-	-	-
	37.6	28	11.03	-	-	-	-	-
	35.6	28	10.6	-	-	-	-	-
Case 2	45.6	28	4.5	6.1	0.025	20.3	1.79	0.62
	43.6	28	4.1	6.0	0.026	20.1	1.83	0.74
	41.6	28	3.8	5.7	0.031	20.0	1.99	0.93
	39.6	28	3.50	5.2	0.034	20.0	1.97	0.90
	37.6	28	3.21	4.8	0.037	20.7	1.92	1.00
	35.6	28	2.50	4.6	0.041	20.0	2.00	1.00

6.3.2 Energy consumption analysis

Figure 6.12 depicts, and Table 6.5 lists total EUI (i.e., heating and cooling) of scenario 1 and scenario 2 against the reference case for six supply water temperatures. Overall the findings show that total EUI of both scenarios reduced compared to the reference case for all supply water temperatures. Furthermore, in both scenarios, the lowest supply water temperature of 35.6°C achieved the most significant total annual energy savings, whereas the highest supply water temperature of 45.6°C achieved the lowest total annual energy savings. For instance, under the first scenario, PCM_{28} achieved the total annual energy savings of approximately 13% and 17% for the maximum and the minimum supply water temperatures, respectively. Under the second scenario, the application of PCM_{28} resulted in total annual energy savings of approximately 18% for the maximum supply water temperature and nearly 20% for the minimum supply water temperature. These results also suggest that the addition of the insulation layer increased the total annual energy savings of scenario 2 compared to scenario 1 for approximately 3% to 5%.

Figure 6.12 also illustrates that heating rather than cooling energy savings contribute to the total energy reductions. Thus, the reference heating energy consumption of 279.2 kWh/(m²·year) reduced for approximately 17% in scenario 1 and approximately 24% in scenario 2 for the highest supply water temperature of 45.6°C. Similarly, the reference heating energy use reduced for approximately 20% in scenario 1 and approximately 24% in scenario 2 for the lowest supply water temperature of 35.6°C. These findings also indicate that the addition of the insulation layer in scenario 2 reduces the impact of supply water temperature on the heating energy savings.

The results also show an increase in the cooling EUI for the higher supply water temperatures and decrease for the lower supply water temperatures of both scenarios. Furthermore, scenario 1 achieved more substantial cooling energy savings over the wider temperature range (41.6-35.6°C) compared to scenario 2 (39.6-35.6°C). Hence, for the lowest supply water temperature of 35.6°C, the maximum cooling energy savings of scenario 1 were 7.5% and 6.7% of scenario 2. Longer heat retention caused by the addition of insulation layer might be the reason for worse overall cooling energy performance of the second than the first scenario. This negative impact is particularly pronounced for the higher supply water temperatures, and the likely reason is the faster melting of PCM_{28}.

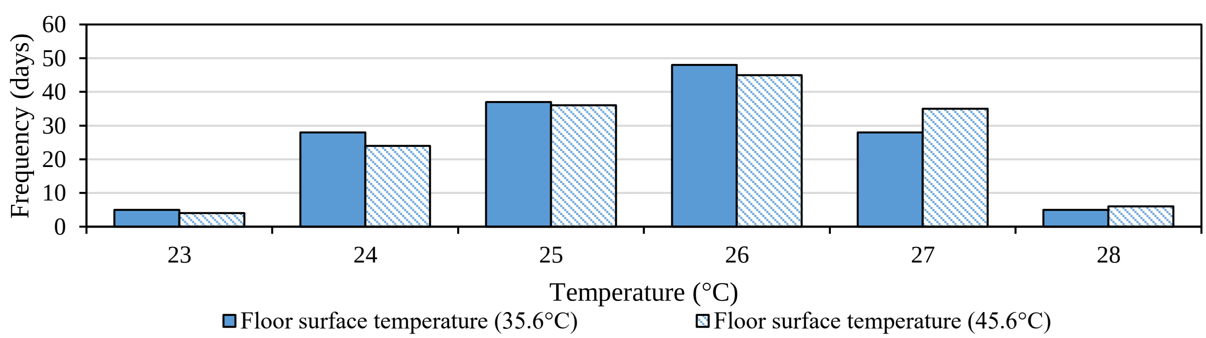

Figure 6.11: Histogram of floor surface temperature distribution, considering the highest and lowest water temperatures.

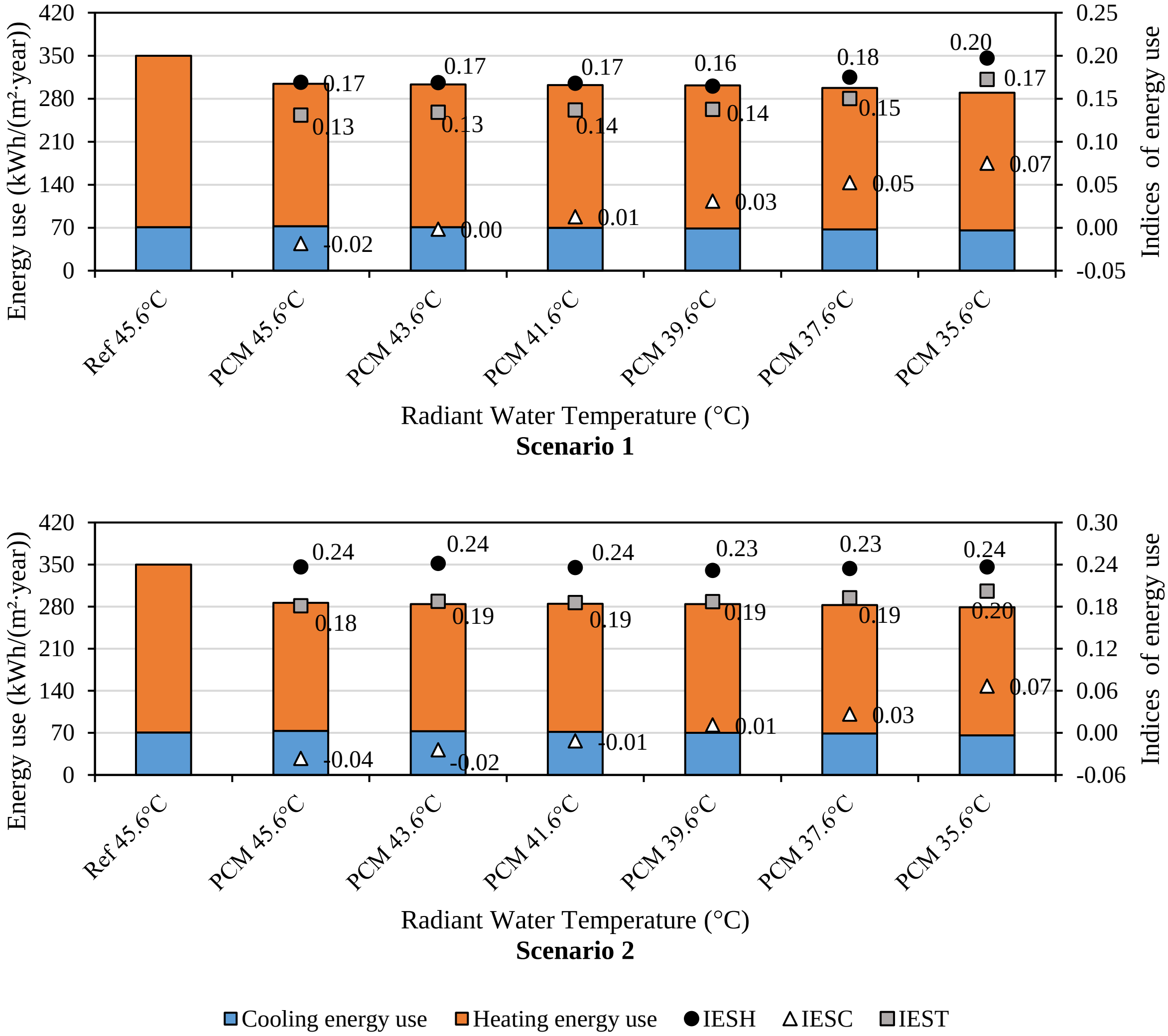

Figure 6.12: Annual heating and cooling demand for both the reference and PCM-incorporated study room. Indices of energy savings for each radiant hot water temperature considering (a) the optimal solution $x_1^* = \{PCM_{mt}, PCM_t\}_{opt}$., and (b) $x_2^* = \{PCM_{mt}, PCM_t, I_t, I_k, F_t, F_k, F_\alpha\}_{opt}$

Table 6.5: Heating and cooling performance for the reference and PCM-incorporated study room for each supply hot water temperature, and energy savings considering the optimal solution $x_1^* = \{PCM_{mt}, PCM_t\}_{opt}$, and $x_2^* = \{PCM_{mt}, PCM_t, I_t, I_k, F_t, F_k, F_\alpha\}_{opt}$.

	Energy demand (kWh/m^2)		R_t (°C)					
			45.6	43.6	41.6	39.6	37.6	35.6
Case 1	Heating	$E_{heat,Ref}$	282.8	282.8	282.8	282.8	282.8	282.8
		$E_{heat,PCM}$	235.0	235.1	235.2	236.2	233.2	227.0
		Savings (%)	16.9	16.9	16.8	16.5	17.5	19.7
	Cooling	$E_{cool,Ref}$	57.9	57.9	57.9	57.9	57.9	57.9
		$E_{cool,PCM}$	59.0	58.0	57.2	56.1	54.9	53.6
		Savings (%)	-1.8	-0.2	1.3	3.1	5.3	7.5
	Total	$E_{total,Ref}$	340.7	340.7	340.7	340.7	340.7	340.7
		$E_{total,PCM}$	294.0	293.1	292.4	292.4	288.1	280.6
		Savings (%)	13.7	14.0	14.2	14.2	15.4	17.7
Case 2	Heating	$E_{heat,Ref}$	282.8	282.8	282.8	282.8	282.8	282.8
		$E_{heat,PCM}$	215.9	214.5	216.1	217.3	216.5	215.8
		Savings (%)	23.7	24.2	23.6	23.2	23.5	23.7
	Cooling	$E_{cool,Ref}$	57.9	57.9	57.9	57.9	57.9	57.9
		$E_{cool,PCM}$	60.1	59.3	58.6	57.2	56.4	54.0
		Savings (%)	-3.6	-2.4	-1.1	1.1	2.7	6.7
	Total	$E_{total,Ref}$	340.7	340.7	340.7	340.7	340.7	340.7
		$E_{total,PCM}$	276.0	273.8	274.7	274.6	272.8	269.8
		Savings (%)	19.0	19.6	19.4	19.4	19.9	20.8

Figure 6.12 shows that in both scenarios, the lowest total energy use (minimum value of cost function) can be expected for the lowest supply-water temperature (i.e., 35.6°C) because less energy is required to meet the specified indoor air temperature within the space. In order to provide a closer view, Figure 6.13 compares the monthly heating and cooling EUI of scenario 1 and scenario 2 against the reference case EUI for the water temperature of 35.6°C. The colored bars denote the heating and cooling load for the reference model for each month. Next, to each colored bars, the dashed-line bars correspond to the heating and cooling energy consumption of the PCM-incorporated models for the same months. Also, the lines on the graph demonstrate the indices of energy savings for each month. Table 6.6 also summarizes the monthly energy performance of the

graduate study room for all of the analyzed hot water temperatures considering the optimized solution $x_1^* = \{PCM_{mt}, PCM_t\}_{opt}$, and $x_2^* = \{PCM_{mt}, PCM_t, I_t, I_k, F_t, F_k, F_\alpha\}_{opt}$.

The results from Figure 6.13 suggest that in both scenarios, the optimized incorporation of PCM into the floor reduce the heating and total energy demand in winter. During this season, the heating energy EUI due to the incorporation of PCM varies slightly between 19% and 21% for case 1 (Figure 6.13.a), and between 19.5% and 22% for case 2 (Figure 6.13.b). The optimal design of PCM also resulted in significant heating energy savings during the shoulder (spring and fall) and summer seasons. For example, from April to June and October to December, the optimized PCM-enhanced floor design achieved monthly heating energy savings ranging from 17% to 25.1% for case 1 and from 24% to 41% for case 2. Additionally, during the summer, the heating energy savings ranged from 24% to 25% for case 1 and from 36% to 44% for case 2. Moreover, Figure 6.14 presents a comparison of monthly energy use between the three models. As illustrated, the optimized solution $x_2^* = \{PCM_{mt}, PCM_t, I_t, I_k, F_t, F_k, F_\alpha\}_{opt}$ resulted in the highest energy savings for heating throughout the year compared to the reference model and case 1.

Although the energy demand in Winnipeg climate is mainly due to the heating during the winter and shoulder seasons, the remaining energy demand is needed for cooling, and in particular during the summer due to higher outdoor air temperatures and excessive solar radiation. During summer, the results suggest that the incorporation of PCM_{28} with the lower supply-water temperature could reduce the cooling energy EUI ranging from 3% in August to 4% in July in both cases. Regarding the winter and shoulder seasons, it can be observed that the cooling energy performance of the PCM-enhanced models is improved compared to the reference model. For instance, from October to June, the cooling energy EUI is reduced ranging from 6% in June to 21% in January for case 1, and from 5% in May to 16% in January for case 2. Additionally, results from Figure 6.14 indicate that compared to case 1, the cooling energy savings in case 2 were insignificantly increased ranging from 5% August to 5.5% in November. A possible reason for this behavior might be that in case 1, PCM was able to partially release the stored heat to the lower floor level, and thereby reduce the cooling energy consumption of the case study. In case 2, the provision of the insulation layer at the lower face of PCM reduced the overall thermal conductivity of the radiant floor, which consequently prevented the heat flow to the lower level and increased space cooling demand.

A comparison of the scenarios' average hourly cooling EUI and interior surface temperatures for the lowest supply water temperature of 35.6°C against the reference case EUI during summer and winter occupied hours allowed further understanding of the discrepancies in cooling energy savings between the two scenarios. As illustrated in Figure 6.15, the addition of the insulation in scenario 2 increased cooling energy demand throughout the average summer and winter days and in particular in the morning and afternoon hours when solar radiation and occupancy were at their peak. Furthermore, Figure 6.15 shows that the surface temperatures of the concrete slab without insulation (i.e., scenario 1) were higher than the surface temperatures of the slab in scenario 2 throughout the average summer and winter days. A possible reason is the ability of PCM to partially dissipate the stored heat, whereas due to the insulation heat dissipation to the lower level was reduced in scenario 2, thus causing an increase in the space cooling demand.

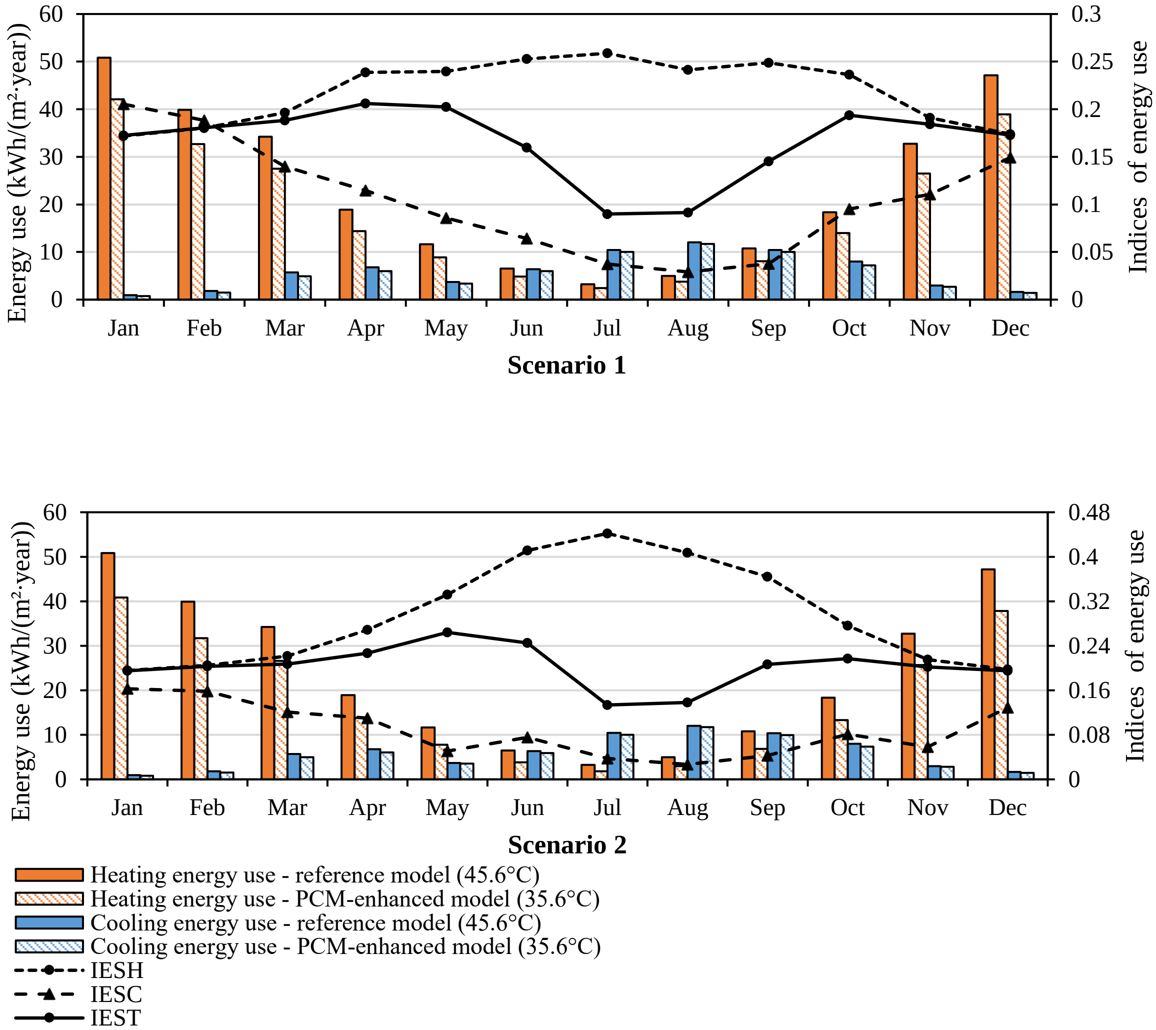

Figure 6.13: Monthly total heating and cooling demand for both the reference and PCM-incorporated study room considering the optimal solution (a) $x_1^* = \{PCM_{mt}, PCM_t\}_{opt}$, and (b) $x_2^* = \{PCM_{mt}, PCM_t, I_t, I_k, F_t, F_k, F_\alpha\}_{opt}$.

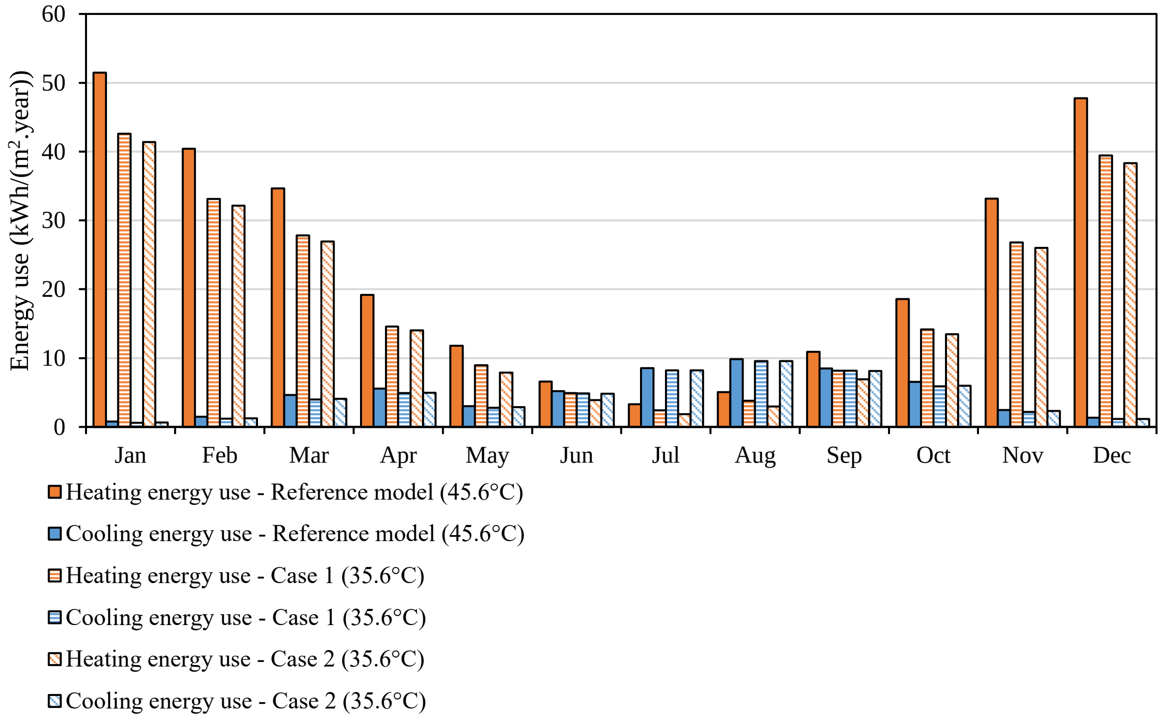

Figure 6.14: Monthly comparison of total heating and cooling energy performance between the reference, case 1, and case 2 models considering the lowest water temperature (best cases).

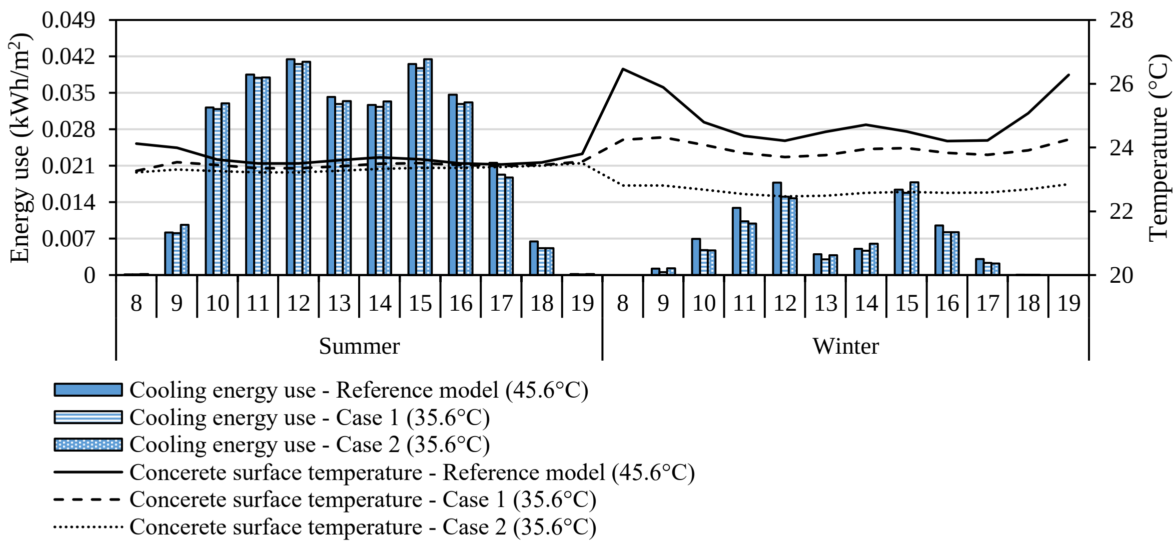

Figure 6.15: Comparison of hourly average cooling energy performance for summer and winter regarding various concrete surface temperatures and the lowest water temperature (best cases).

Table 6.6 : Heating, cooling, and total energy savings for each supply hot water temperature, and energy savings considering the optimal solution $x_1^* = \{PCM_{mt}, PCM_t\}_{opt}$, and $x_2^* = \{PCM_{mt}, PCM_t, I_t, I_k, F_t, F_k, F_\alpha\}_{opt}$.

	Rt (°C)	Energy Savings (kWh/m2)	Jan.	Feb.	Mar.	Apr.	May	Jun.	Jul.	Aug.	Sep.	Oct.	Nov.	Dec.
Case1	45.6	Heating	17.2	15.6	15.6	15.8	21.6	25.1	22.4	21.0	21.5	16.9	15.7	15.9
		Cooling	-17.9	-13.9	-5.3	-3.7	-2.8	0.8	2.2	0.8	0.1	0.2	-7.2	-15.9
		Total	16.6	14.4	13.0	11.4	16.6	14.4	7.8	7.7	12.1	12.5	14.1	15.0
	43.6	Heating	16.3	15.6	15.7	16.3	21.5	24.9	23.1	21.3	21.5	17.2	15.9	15.9
		Cooling	-13.1	-8.4	-1.9	-2.2	-0.1	2.3	2.6	1.3	0.7	1.1	-3.9	-8.9
		Total	15.9	14.8	13.6	12.1	17.1	14.9	8.3	8.1	12.4	13.0	14.6	15.2
	41.6	Heating	15.7	15.6	15.9	17.1	21.6	24.8	23.9	21.6	21.6	17.6	16.0	15.6
		Cooling	-7.4	-4.4	1.2	0.0	1.4	3.3	2.9	1.8	1.3	2.2	-0.7	-4.4
		Total	15.3	14.9	14.2	13.2	17.4	15.3	8.8	8.5	12.7	13.6	14.9	15.0
	39.6	Heating	14.7	14.8	15.6	18.1	21.5	24.5	24.4	22.2	21.5	18.3	15.8	14.9
		Cooling	1.2	1.9	4.8	3.4	3.4	4.5	3.3	2.2	2.1	3.9	2.8	1.0
		Total	14.5	14.3	14.3	14.8	17.8	15.7	9.1	9.0	13.0	14.6	14.9	14.5
	37.6	Heating	15.3	15.9	17.2	20.5	22.0	24.6	25.0	22.9	22.3	20.3	17.0	15.4
		Cooling	10.2	10.3	9.0	7.8	5.6	5.5	3.5	2.6	2.8	6.6	7.2	7.6
		Total	15.2	15.7	16.2	17.7	18.7	16.2	9.5	9.5	13.8	16.7	16.4	15.2
	35.6	Heating	17.2	18.0	19.6	23.9	24.0	25.3	25.9	24.1	24.9	23.6	19.1	17.4
		Cooling	20.5	18.8	14.0	11.5	8.6	6.4	3.7	2.9	3.8	9.5	11.1	14.9
		Total	17.2	18.1	19.0	21.1	20.8	17.0	9.9	10.1	15.6	20.0	18.6	17.3
Case 2	45.6	Heating	22.4	21.1	20.7	25.0	31.8	37.2	35.3	32.9	35.2	26.1	20.9	21.4
		Cooling	-14.8	-10.2	-2.4	0.5	-15.7	-6.4	-0.7	-2.5	-0.7	-0.4	-8.9	-13.9
		Total	21.9	20.0	18.0	19.5	21.5	17.8	9.3	9.4	19.5	19.2	18.8	20.4
	43.6	Heating	22.1	21.6	21.2	25.9	32.8	39.6	38.7	35.8	36.2	27.1	21.4	21.6
		Cooling	-14.3	-10.5	-0.8	1.7	-13.3	-3.9	0.1	-1.8	0.0	0.7	-6.9	-11.8
		Total	21.5	20.4	18.6	20.4	23.0	20.3	10.8	11.0	20.3	20.2	19.4	20.6
	41.6	Heating	20.8	20.7	20.9	25.4	33.0	40.9	41.5	38.7	36.1	26.9	20.9	20.3
		Cooling	-8.4	-7.9	0.6	2.2	-8.8	-1.3	0.5	-0.9	0.8	0.7	-7.5	-7.6
		Total	20.4	19.7	18.5	20.2	24.3	22.3	11.9	12.5	20.6	20.1	18.9	19.6
	39.6	Heating	19.9	20.6	20.9	24.5	32.5	40.9	42.5	39.4	35.6	26.1	20.8	19.9
		Cooling	-2.3	-1.8	3.7	3.3	-4.0	1.5	1.4	0.3	1.8	3.3	-3.3	-2.0
		Total	19.5	19.8	18.9	19.7	25.0	23.5	12.8	13.6	20.8	20.1	19.1	19.3
	37.6	Heating	19.9	20.6	22.0	25.2	32.3	40.3	43.0	39.4	35.3	26.1	21.5	20.2
		Cooling	6.4	4.8	6.0	5.6	-1.7	3.1	1.7	0.8	2.3	4.4	-0.4	3.3
		Total	19.7	20.0	20.1	20.7	25.4	23.9	13.2	13.9	20.8	20.5	20.0	19.7
	35.6	Heating	19.6	20.5	22.2	26.9	33.2	41.1	44.2	40.7	36.4	27.6	21.5	19.7
		Cooling	16.3	15.8	12.1	11.0	5.1	7.5	3.8	2.7	4.3	8.1	5.8	12.9
		Total	19.5	20.3	21.0	23.3	27.4	26.3	15.0	15.6	22.3	22.5	20.5	19.6

A better understanding and comprehensive evaluation of the scenarios' optimal design solutions required investigation of their impact on the energy performance of spaces located beneath the graduate study room. In this regard, Table 6.7 compares the percentage differences of the scenarios' total, heating, and cooling EUI for the lowest and highest supply water temperatures of the three zones below (see Figure 3.6). As presented, the total EUI of the zones below remained almost the same for both water temperatures, and the small increase can be contributed to the increase in the cooling EUI. Thus, under scenario 1, cooling EUI of the zones below the case study increased for approximately 3.9% and 5.5% for the supply water temperatures of 35.6°C and 45.6°C, respectively. Scenario 2 caused approximately 1.4% to 3.5% larger increase in cooling EUI compared to scenario 1. Similar to the case study, both scenarios reduced the heating EUI of the zones below, whereas scenario 2 achieved somewhat larger savings compared to scenario 1. These results support the previous findings and show that the addition of the insulation layer has a positive effect on the heating and a negative on the cooling energy demand of the zones below the graduate study room. Furthermore, similar to the case study, although both supply water temperatures cause an increase in the cooling EUI of the zones below, the more pronounced increase is for, the higher than lower supply water temperature. On the other hand, higher supply water temperature caused somewhat larger (~0.5-1%) heating energy savings compared to the lower supply water temperature.

Table 6.7: Comparison of average percentage differences between total, heating, and cooling EUI of scenarios and reference case for three zones below the graduate study room.

	Scenario 1		Scenario 2	
Percentage difference (%)	Supply water temperature (°C)			
	35.6	*45.6*	*35.6*	*45.6*
Total EUI	0.06	0.06	0.19	0.26
Heating EUI	-0.99	-1.44	-1.21	-2.24
Cooling EUI	3.91	5.51	5.28	8.99

6.3.3 Thermal comfort analysis

Table 6.8 summarizes total comfort, discomfort, overheating, and overcooling hours for all six water temperatures of scenario 1 and scenario 2, along with the reference case. Overall, both scenarios improved the thermal comfort for all supply water temperatures compared to the reference case, and scenario 1 performed slightly better than scenario 2. Thus, scenario 1 increased thermal comfort hours from 36 to 51 hours, whereas scenario 2 increased for 30 to 42 hours. Although a similar trend between the supply water temperatures and comfort hours can be seen for both scenarios, the results also show that scenario 1 reduced overheating and increased overcooling hours compared to scenario 2. These results further explain the lower cooling energy savings of scenario 2 than scenario 1 presented in Section 6.3.2. However, in contrast to the total energy savings, PCM-enhanced hydronic radiant floor system with the lowest supply water temperature of 35.6 °C achieved the lowest reduction of discomfort hours (PMV>0.5 or PMV<-0.5) compared to other supply water temperatures under both scenarios. On the other hand, the supply water temperature of 43.6 °C provided the most significant thermal comfort improvements compared to the reference case by increasing comfort (i.e., 0.5<PMV<0.5) hours for 51 in scenario 1 and 45 in scenario 2.

Table 6.8: Total comfort, discomfort, overcooling, and overheating hours during occupied hours of scenario 1, scenario 2, and reference case.

	Water temperature (°C)	Thermal comfort -0.5< PMV <0.5		Thermal discomfort PMV > 0.5 or PMV < -0.5					
		Total hours	%	Total hours	%	Overcooling hours	%	Overheating hours	%
Base case	45.6	3466	88.53	449	11.46	306	68.15	143	31.84
Scenario 1	45.6	3513	89.73	402	10.26	256	57.01	146	42.98
	43.6	3517	89.83	398	10.16	265	59.02	133	40.97
	41.6	3511	89.68	404	10.31	276	61.46	128	38.53
	39.6	3508	89.60	407	10.39	289	64.36	118	35.63
	37.6	3506	89.55	409	10.44	304	67.70	105	32.29
	35.6	3502	89.45	413	10.54	320	71.26	93	28.73
Scenario 2	45.6	3508	89.60	407	10.39	243	54.12	164	45.87
	43.6	3511	89.68	404	10.31	249	55.45	155	44.54
	41.6	3508	89.60	407	10.39	266	59.24	141	40.75
	39.6	3504	89.50	411	10.49	281	62.58	130	37.41
	37.6	3498	89.34	417	10.65	296	65.92	121	34.07
	35.6	3496	89.29	419	10.70	317	70.60	102	29.39

Furthermore, Figure 6.16 compares the average hourly PMV values of the scenarios' best energy and thermal comfort solutions against the reference case throughout the year. The results indicate that on average, both scenarios and supply water temperatures are effective in improving thermal comfort in warm and cold months, and in particular during the day (10:00 to 17:00) when excessive solar radiation may increase the risk of overheating. For example, on average, PMV improved from 0.4 to 0.03 in fall, from 0.5 to 0.15 in spring, and from 0.35 to 0.025 in winter compared to the reference case. However, both scenarios and supply water temperatures reduced thermal comfort compared to the reference case during the evening and unoccupied hours of fall, spring, and winter. This is particularly pronounced for the lower supply water temperature of 35.6 °C. The vice versa occurred during the evening and unoccupied hours of summer when both scenarios and supply water temperatures improved the thermal comfort.

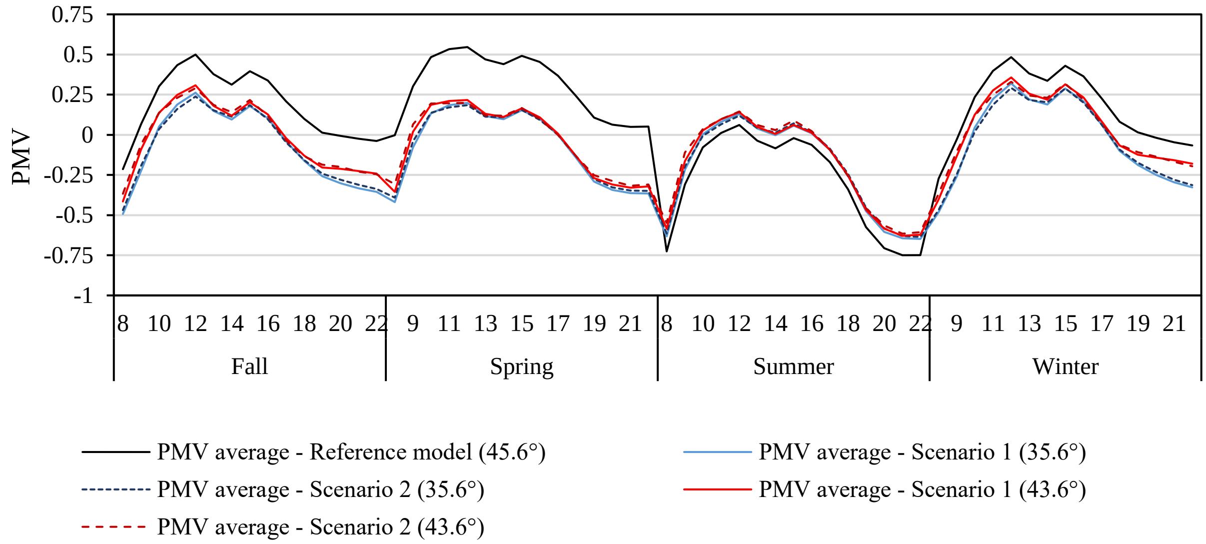

Figure 6.16: Comparison of PMV ratio between three cases over winter, spring, summer, and fall considering the hottest water temperature.

6.3.4 Economic analysis

An economic analysis of the case study with optimal integration of PCM is performed for two analyzed scenarios to evaluate the feasibility of the proposed method. Table 6.9 shows the annual cost for the heating and cooling energy consumption of each model under various radiant water temperatures as well as the capital cost required for the implementation of selected PCM and insulation (Equations 4.15 and 4.16). It can be observed that in both cases, the annual cost of heating energy use was significantly reduced ranged from 16.9% to 23.7% in case 1 and from 23.7% to 24.2% in case 2. However, lowering the supply-water temperature has no significant impact on the annual cost of heating and cooling energy use. For example, comparison of heating energy cost for different water temperature shows that the maximum difference in heating energy cost between different temperatures is equal to CAD $107 in case 1 and CAD $38 in case 2. Also, it is shown that installing an additional layer of insulation to the radiant floor system may bring more considerable annual cost savings for heating (up to CAD $275) compared to the first case.

Table 6.9 also summarizes the anticipated cost of cooling energy use calculated for each of the supply water temperatures. It can be observed that in both cases, the application of PCM might increase the cooling energy cost for higher water temperature (up to 1.8%) and reduce it for lower water temperature (up to 7.5%). In addition, the comparison of PCM cost between two cases shows that installing a thin layer of insulation in case 2 can significantly reduce the initial investment necessary for the integration of PCM into the radiant floor system. For example, compared to case 1, the capital cost of PCM for case 2 can be significantly reduced up to CAD $21,150, which is notably because the PCM thickness is greatly reduced from 15 mm to 5.4mm.

Table 6.9: Annual cost of heating and cooling energy used in each model and capital cost of PCM and insulation.

	Temperature (°C)	Annual cost of heating energy use (CAD)	Annual cost of cooling energy use (CAD)	Cost of PCM (CAD)	Cost of insulation (CAD)
Base case	45.6	3796.9	777.4	0.0	0.0
Case 1	45.6	3154.6	792.0	30146.1	0.0
	43.6	3156.4	778.7	27387.4	0.0
	41.6	3158.2	767.4	25788.1	0.0
	39.6	3171.8	753.3	23389.2	0.0
	37.6	3131.3	736.6	22049.8	0.0
	35.6	3047.5	719.2	21190.2	0.0
Case 2	45.6	2898.4	806.6	8995.9	233.5
	43.6	2879.2	796.4	8196.2	229.7
	41.6	2901.2	786.3	7596.5	216.9
	39.6	2917.5	768.5	6996.8	199.9
	37.6	2906.3	756.6	6417.0	184.8
	35.6	2897.4	725.4	4997.7	174.4

Additionally, to estimate the length of time required to recover the initial investments of PCM and insulation in terms of energy savings, a payback period analysis is also performed for each scenario. The payback period is calculated for the energy savings measures by dividing the total capital cost of PCM and insulation by the total energy savings in CAD. Figure 6.17 demonstrates and Table 6.10 lists the results of payback period calculation for the optimal integration of PCM with a radiant floor system under various supply water temperatures.

Table 6.10: Payback periods of optimal integration of PCM with the radiant floor system under various water temperatures.

	Case1 (°C)						Case 2 (°C)					
	45.6	43.6	41.6	39.6	37.6	35.6	45.6	43.6	41.6	39.6	37.6	35.6
Payback period (year)	48.0	42.8	39.8	36.0	31.2	26.2	10.6	9.4	8.8	8.1	7.2	5.4

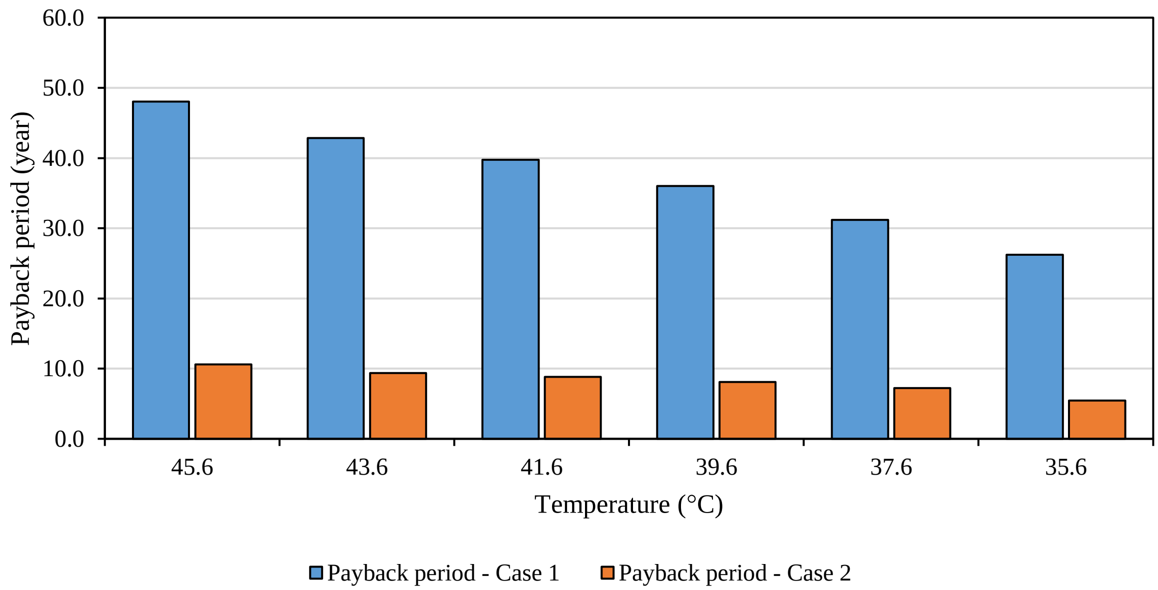

Figure 6.17: Payback periods for the PCM-enhanced radiant floor system under various water temperature

Overall, the payback period presented in Figure 6.17 indicates that including an insulation layer in a PCM-incorporated radiant floor system could result in a significant reduction in the payback period of the initial cost. For example, in the first scenario, application of PCM_{28} yielded a payback period of 48 years for the maximum supply-water temperature of 45.6°C, whereas, in the second scenario, the payback period was significantly reduced to approximately 10 years for the similar water temperature. This great reduction in payback period occurred as the result of a substantial reduction in PCM thickness from 15 mm in case 1 (without insulation) to 4.5 mm in case 2 (with insulation), which eventually decreases the weight of PCM from 5,024Kg in case 1 to 1,500Kg in case 2 due to the reduced volume of PCM. Also, comparison of the payback period for different supply-water temperatures (Table 6.10) shows that in both scenarios, the higher water temperatures result in a more extended payback period, while lower water temperatures cause shorter recovery periods. This result indicates that among the two scenarios, the payback period for case 1 was the longest and ranged from nearly 26 to 48 years while the payback period for case 2 was the shortest and ranged from approximately 5 to 10 years. Assuming the PCM service life of approximately 35 years (Mi et al., 2016), the investment of PCM-enhanced radiant floor with the integration of insulation (i.e., case 2) may not only be recovered within the building service life but also offers a profitable investment in the long term period. Based on the above analysis, it can be concluded that including additional insulation to the PCM-enhanced radiant floor system plays an important role in lowering the payback period and determining the overall cost-effectiveness of the system. Therefore, the energy cost savings resulting from the application of PCM-enhanced radiant floor appear to be more effective and has high economic value when integrated with insulation. At the current price, the investment of PCM in case 1 may require a longer time to be recovered and has no economic benefit, especially for the higher supply-water temperature. However, in the future, with a possible reduction in the price of PCM, and the increase of market demand, the investment incentive in case 1 may be possible.

6.4 Results analysis of optimal design of natural ventilation and solar shading systems

This section further analyzes the impact of developed natural ventilation and solar shading control strategies on the overall energy performance and thermal comfort of the case study. To evaluate each set of the developed control strategies regarding energy use and thermal comfort, this research study analyzed and compared several vital parameters such as the cooling and heating energy demand, the mean air temperature, and the Predicted Mean Vote (PMV). The energy demand is calculated as the heating, and cooling load required to remain the comfort temperature set-points in the room, whereas a commonly used index PMV measured the thermal comfort.

6.4.1 Impact of shading control on annual energy use and thermal comfort

Figure 6.18 and Table 6.11 show the annual heating and cooling energy performance of the reference study room under different shading control strategies. Overall, the results suggest that the applied shading control strategies can result in significant cooling energy reductions ranging from 21.1% (11.8kWh/m^2) for the highest set-points to 32% (18.5kWh/m^2) for the lowest set-points. However, they also indicate that in both modes, the lower set-points caused an increase in the heating demand. A possible reason is that the lower set-points led to more prolonged use of the shading devices, which eventually increased the heating energy consumption due to reduced solar gains.

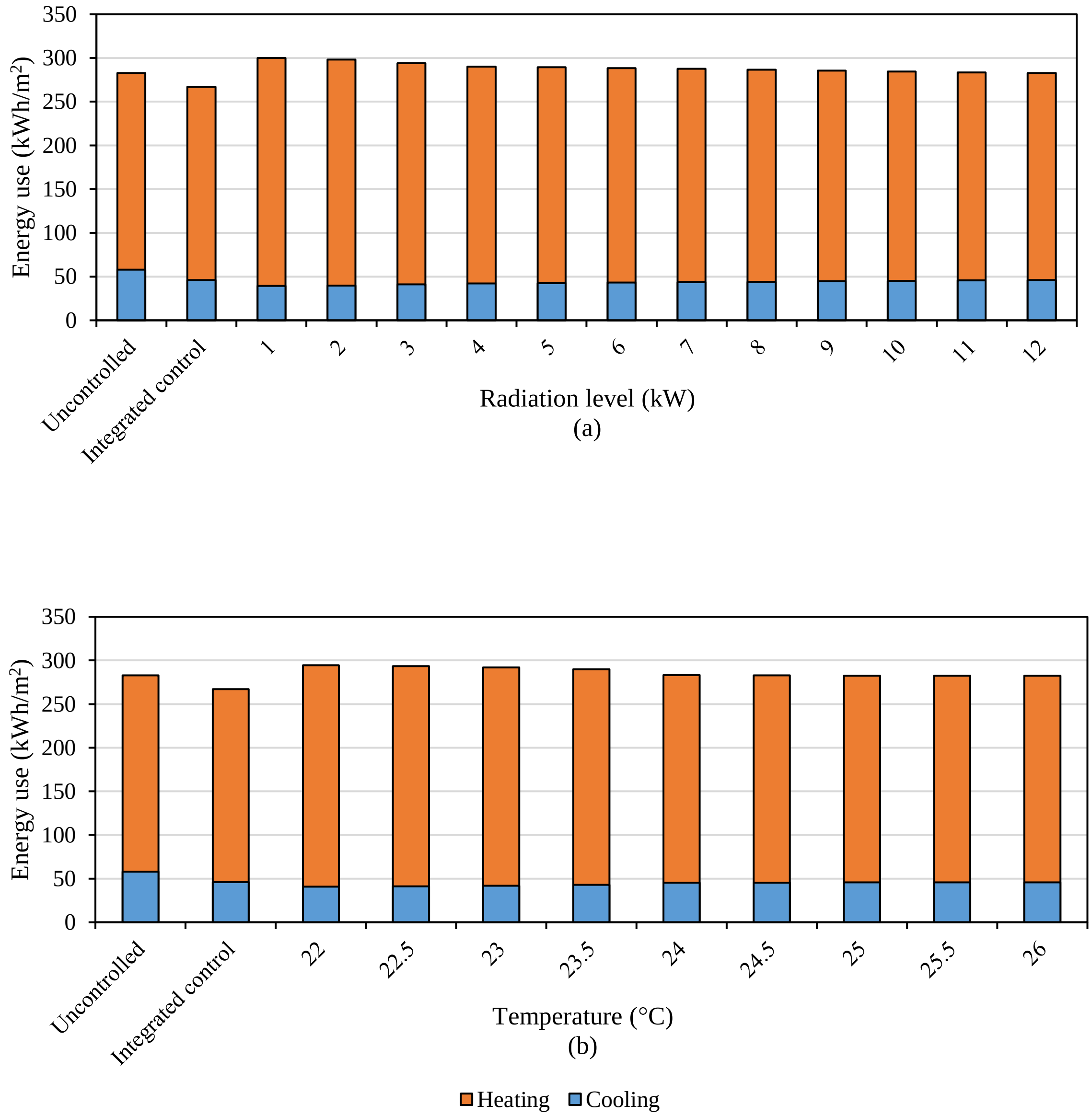

Figure 6.18: A comparison of annual heating and cooling load of the study room for different shading control strategies when (a) radiation level and (b) indoor temperature is used.

Table 6.11: Annual heating and cooling energy demand and savings for the study room under different shading control strategies.

Strategy	set-points	Heating (kWh/m^2 year) (saving %)	Cooling (kWh/m^2 year) (saving %)
No control	-	282.8 (-)	57.9 (-)
Shading			
Case 1	1kW	299.8 (-5.7)	39.3 (32.0)
	3 kW	294.1 (-3.8)	40.9(29.2)
	7 kW	289.3 (-1.7)	42.4 (24.8)
	9 kW	285.5(-0.9)	44.5 (23.1)
	11kW	283.4 (-0.2)	45.5 (21.4)
Case 2	22°C	294.3 (-3.9)	40.7 (29.6)
	23°C	291.9 (-3.1)	42.01 (27.4)
	24°C	283.1 (-0.1)	45.4 (21.6)
	25°C	282.6 (0.1)	45.6 (21.3)
	26°C	282.5 (0.1)	45.7 (21.1)
Case 3	-	266.9 (5.6)	45.8 (20.7)

For example, the energy demand for heating increased by 5% (17kWh/m^2) and 3% (11.5kWh/m^2) when the set-points for radiation level and indoor temperature were fixed at 1kW and 22°C, respectively. On the other hand, the results demonstrate that the use of higher set-points can reduce overheating, without increasing the heating energy use. Therefore, the overall building's energy performance improvement requires analysis of a range of set-points to find those that have a positive impact on both heating and cooling demand. Figure 6.18 also shows that compared to the individual strategies, the integrated control strategy offers more considerable energy savings potentials for both heating and cooling loads. For instance, the heating and cooling energy consumptions were reduced by 5.6% (15.8kWh/m^2) and 20.7% (12kWh/m^2), respectively. Consequently, the integrated shading controls based on both radiation level and indoor temperature have the potential to improve the overall building's energy performance.

As already mentioned, PMV was used to assess the level of thermal performance resulting from the application of different shading control strategies. The hourly PMV values are calculated for the occupied hours (i.e., 8:00 to 17:00). Figure 6.19 shows the comparison of the annual unmet PMV hours (i.e., discomfort hours) and activated hours (i.e., the number of hours that shading is operational) for different shading control strategies under various set-points. It is evident that both radiation and temperature control strategies have a similar impact on room thermal comfort.

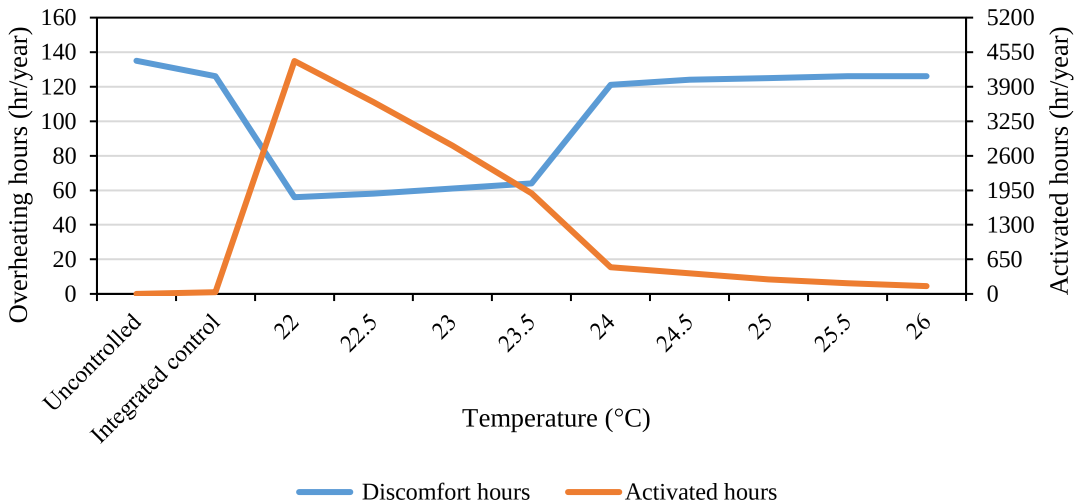

Figure 6.19: Overheating and activated mode hours in a study room for various temperature set-points.

It can be seen that an increase in the radiation level set-point increased the number of discomfort hours. For instance, an increase of the radiation levels above 3kW increased the number of discomfort hours from 25 hours for 4kW to 70 hours for 12kW. Similarly, an increase in the temperature set-point from 22°C to 26°C resulted in a 55% increase of the discomfort hours and a drop of 96% of the activated mode hours.

6.4.2 Impact of natural ventilation control on annual energy use and thermal comfort

Figure 6.20 illustrates whereas Table 6.12 summarizes the impact of the various natural ventilation strategies on the annual heating and cooling energy demands. The bars of cases 1 and 2 correspond to the heating and cooling energy use when natural ventilation is regulated only by indoor air temperature (left bar) and by indoor-outdoor air temperatures (right bar). Cases 3 and 4 relate to the heating and cooling load when natural ventilation is controlled based on cooling load and integrated control design.

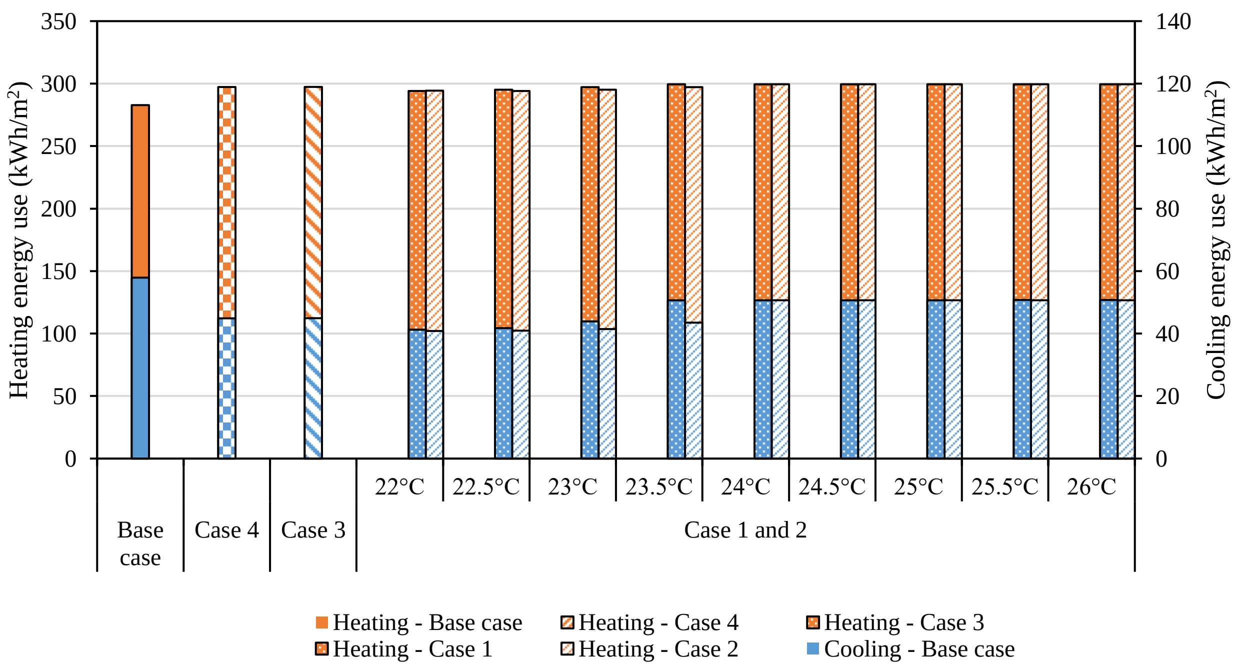

Figure 6.20: A comparison of annual heating and cooling load in a study room for different natural ventilation control strategies.

The overall results indicate that the use of natural ventilation can result in significant cooling energy reductions compared to the uncontrolled mode. Thus, the cooling loads were reduced by around 29% and 30% for the first and second cases, respectively. However, compared to the lower set-points, the modes with higher set-points resulted in lower cooling energy savings. This similarity with the shading control strategies can be explained by the increase in the number of ventilation operation hours with reduced temperature set-points. For example, the cooling savings increased from 12% to 28% when the temperature set-point decreased from 26°C to 22.5°C. Figure 6.20 also shows that incorporation of the outdoor temperature into the first case does not have a significant impact on the cooling or heating energy savings in the cold region.

Table 6.12: Annual heating and cooling energy demand and savings for the study room under different natural ventilation control strategies.

Strategy	set-points	Heating (kWh/m^2 year) (savings %)	Cooling (kWh/m^2 year) (savings %)
No control	-	282.8 (-)	57.9 (-)
Ventilation			
Case 1	22°C	294.1 (-3.9)	41.2 (28.7)
	23°C	297.1 (-4.8)	43.8 (28.7)
	24°C	299.5 (-5.6)	50.7 (24.2)
	25°C	299.5 (-5.6)	50.7 (-5.6)
	26°C	299.5 (-5.6)	50.7 (12.4)
Case 2	22°C	294.4 (-4.0)	40.7 (29.5)
	23°C	295.1 (-4.2)	41.4 (28.5)
	24°C	299.5 (-5.6)	50.6 (12.6)
	25°C	299.5 (-5.6)	50.6 (12.5)
	26°C	299.5 (-5.6)	50.6 (12.5)
Case 3	-	297.3 (-4.9)	44.8 (22.5)
Case 4	-	297.3 (-4.9)	44.9 (22.4)

The results also demonstrate that the incorporation of natural cooling can increase the heating energy load. For example, for the first and second case with the lower set-points, the heating load increased by 3.9% and 3.8%, respectively, whereas for the third and fourth case the heating load increased by 2% and 1.5%, respectively. Berkeley Lab and EnergyPlus development team are currently working on understanding the cause of the increase in the heating load when running a scenario with natural ventilation. For a possible reason, they reported that whenever the fans come on the heating also activates, and although program checks the zone temperature and turns off the heating if not needed, over the entire year, short but frequent heating use adds up in terms of a heating load (U.S. Department of Energy, 2017).

From Figure 6.21 it is also evident that an increase in the temperature set-points resulted in an increase in the overheating hours and a decrease in the number of activated hours. For instance, the temperature set-point increase from 22°C to 26°C led to an increase in the overheating hours from 65 to 120 hours. Moreover, it is shown that the second case (i.e., based on both internal and outside temperature) limiting the flow rate had no major impact on comfort conditions. To enable a closer insight into the thermal comfort of the study room, a more detailed analysis of average indoor temperature and PMV ratio is carried out about the integrated control strategy. Figure 6.22 shows a weekly comparison of average indoor temperature and PMV ratio when integrated natural ventilation control is used. It can be seen that the indoor thermal comfort can be improved and in particular between 10:00 and 15:00 when the solar gains are the largest. Compared to the reference mode, the natural ventilation management resulted in considerable indoor thermal comfort improvements during operational hours.

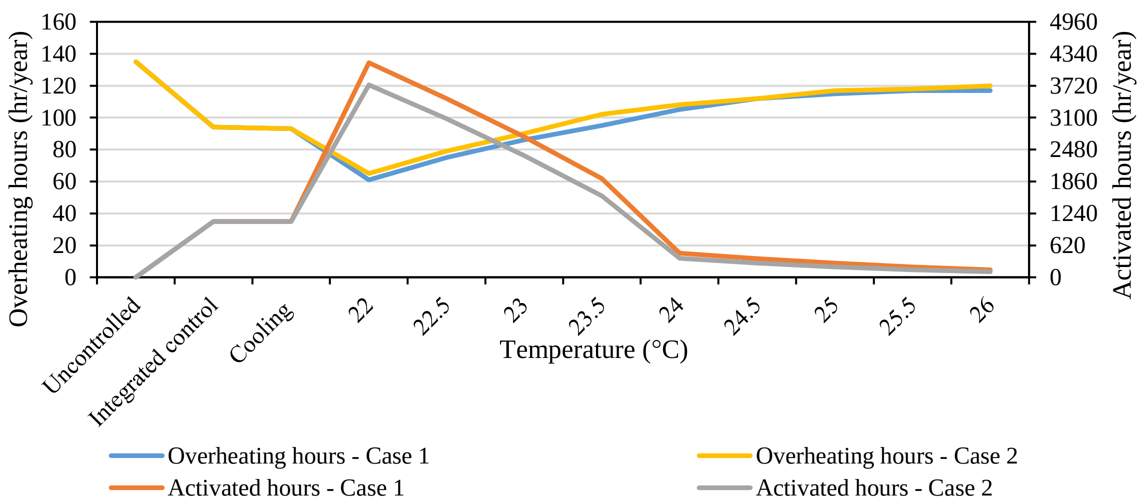

Figure 6.21: Overheating and activated mode hours in a study room for various natural ventilation control strategies.

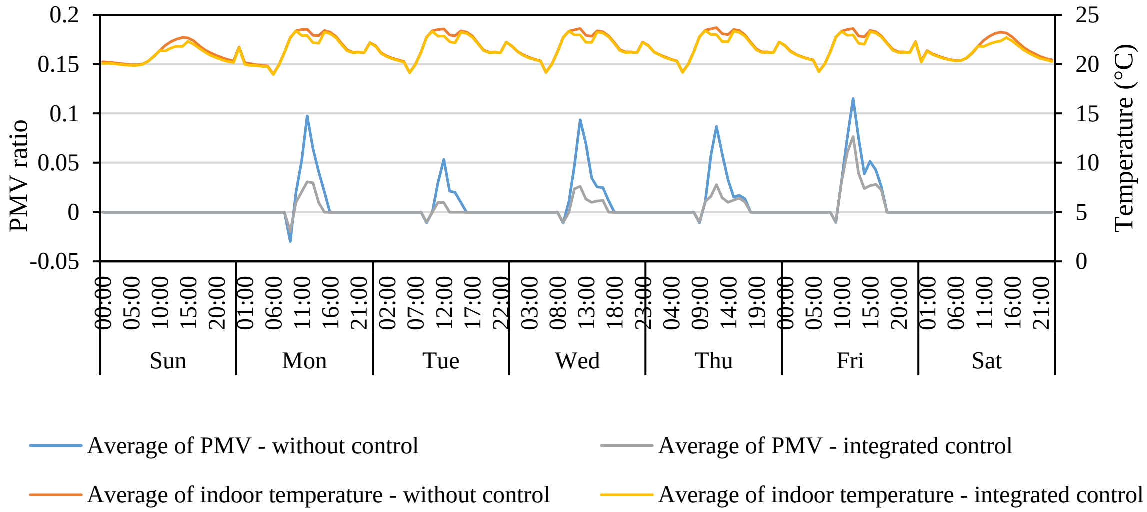

Figure 6.22: A comparison of weekly average indoor temperature and PMV index between integrated ventilation control and uncontrolled models.

6.5 Summary

This chapter provides a detailed performance analysis for each passive energy systems (i.e., PCM, and passive cooling systems) to optimize their design and operation, as well as to quantify their impacts on the thermal performance of a highly glazed study room in Winnipeg. In order to increase confidence in the developed base-case model, its predictions were compared against the predictions of the SPEB model developed in IES. Overall, the results indicate a good agreement between the two models, with discrepancy between the predictions of the total energy consumption and energy use intensity of 2.1% and 1.7%, respectively. Similarly, the difference between the models' predictions of heating energy consumptions was less than 1%, whereas the difference between the predictions of cooling energy consumptions was less than 10%.

Upon verification of the base-case model, the next step involved energy and thermal comfort performance assessment for each passive energy system and measurement of their impacts on energy use (kWh/m^2) and thermal comfort level (PMV ratio) of the case study. The optimization of PCM-enhanced radiant floor system identified PCM_{28} as the optimal melting temperature due to its large potential range for heating energy reduction per square meter. However, optimal thickness of PCM depended on the application of insulation and ranged from 10.6 mm to 15.1 mm for the first scenario (without insulation) and from 2.5 mm to 4.5 mm for the second scenario (with insulation). This analysis also showed that the incorporation of PCM with optimal melting temperature and thickness into a building radiant floor system could effectively improve the overall energy performance of the case study in a cold climate region (i.e., Winnipeg). For example, compared to the base-case model, the optimal solutions in the first and second scenarios achieved approximately 14% and 19% lower total energy use, respectively.

Considering Winnipeg climatic conditions, this vast improvement in total energy savings mainly resulted from the high heating energy savings. Thus, the total heating energy uses in the first and second scenarios are reduced by around 17% and 24%, respectively. Moreover, the economic analysis performed to evaluate the cost-efficiency of each scenario indicates that the use of insulation could effectively reduce the payback periods of PCM to 5-10 years, which is 4 to 6 times lower than the payback periods of PCM in the case without insulation. Analysis of passive cooling systems showed that integrated control of shading system including solar radiation and internal temperature was the most effective form of strategy in reducing heating, and cooling energy uses by 5.6% and 20.7%, respectively. Results also suggest that the integrated control of natural cooling which is based on internal and external environmental factors could offer a considerable cooling energy saving of 22% while reducing overheating hours during the occupied period by 75 hours.

7 Conclusions, limitations, and future work

This research study provides detailed information regarding optimal integration and operation of three passive energy technologies, including phase change materials (PCM), natural ventilation, and shading into a highly glazed building exposed to cold climates. Unlike the majority of previous studies, it focuses on optimal integration of the passive energy technologies with the active building systems such as hydronic radiant floor heating. Therefore, this study provides valuable design recommendations that could considerably improve the energy and thermal comfort performance of the investigated space. Moreover, it suggests novel, integrated operation strategies using different influential environmental factors such as indoor-outdoor air temperature, cooling demand, solar radiation level, and their combination to improve the indoor environmental performance of highly glazed buildings in cold climates. Consequently, the work presented herein provides new and valuable knowledge that can be of value and interest to audiences in both academia and industry.

7.1 Concussions

Overall it can be concluded that improvement of energy and indoor environmental quality of a highly glazed building located in cold climates with high solar radiation intensity such as SPEB requires a combination of different energy-efficient technologies. Furthermore, the successful integration of advanced passive energy technologies in complex buildings such as SPEB depends on various factors. Consequently, a comprehensive numerical optimization analysis combined with a cost analysis is required to determine how best to implement different passive energy technologies and operation strategies.

The main conclusions drawn from this research study can be summarized as follows:

(i) Aggregated predictions of the EnergyPlus and IES models – The results from model verification analysis show that carefully mapping of the input parameters can lead to an excellent agreement between the aggregated energy predictions of the two BPS tools. Possible explanations for better agreement between EnergyPlus and IES compared to the previous studies is the difference in the complexity of the case study along with the use of the newer program versions that are becoming closer in their predictions as a result of the comparative testing methods such as ANSI/ASHRAE Standard 140 (2010). The high consistency between the models' aggregated predictions are particularly pertinent and encouraging for certification programs such as LEED, which take into account aggregated energy consumption data in their assessments.

(ii) Analysis of optimal integration and control of passive energy systems – In general, the findings reveal that incorporating PCM storage into a radiant building floor with optimal melting temperature and thickness can effectively improve the overall energy efficiency of a highly glazed study room in a cold climate region (e.g., Winnipeg). The results of the optimization analysis suggest that PCM_{28} is the optimal melting temperature for all supply water temperatures of the hydronic radiant floor heating system, whereas the ideal thickness of PCM can vary for each scenario depending on the use of insulation. The results also show that including an additional layer of insulation to the lower face of PCM-enhanced radiant floor system can substantially reduce the thickness of PCM.

Additionally, analysis and comparison of annual energy savings indicate that the energy savings potential of PCM with higher melting temperature (i.e., 28°C) is more prominent in reducing heating demand rather than cooling. Moreover, from the economic analysis completed for the energy and capital cost of each scenario, it can be concluded that the incorporation of insulation into the PCM-enhanced radiant floor system can considerably reduce the payback period for more than 75% compared to the model without insulation. Therefore, the application of PCM-enhanced radiant floor system with the incorporation of insulation may offer a better solution in terms of energy savings and cost efficiency.

Because the proposed PCM-enhanced radiant floor method showed limited capability in improving the cooling energy performance of the case study, this study further investigated the optimal operation of passive cooling systems. The overall results suggest that in climates such as Winnipeg where temperatures range from -40°C in winter to + 35°C in summer, the appropriate shading and natural ventilation strategies can have positive impacts on the cooling energy demand but adverse on heating energy demand. The likely reason for the increase in the heating energy demand is the reduction of passive solar heating during the winter months caused by the more extended use of the shading devices.

On the other hand, the integrated solar control strategy, which considers both solar radiation and indoor air temperature, had a positive impact on the overall energy consumption. The results also show that control strategies for the implementation of natural ventilation have great potential to reduce cooling demand while improving indoor thermal comfort in climates such as Winnipeg. Analysis of the high-resolution results (e.g., 15 min) confirms the preliminary findings of the

Berkeley Lab that the use of fans for natural ventilation activates the heating system, resulting in a small increase of the heating energy consumption.

7.2 Limitations

The limitations of the present thesis work can be described as follows:

- *Software limitation* - Many whole-building energy simulation tools such as EnergyPlus use one-dimensional conduction method (Strand and Baumgartner, 2005) for faster calculation of heat balance compared to the three-dimensional method. However, this approach might increase accuracy issues. Furthermore, EnergyPlus's EMS feature has no built-in optimization tool for finding the optimal control strategy that leads to the lowest energy performance in buildings. Also, it is worth mentioning that current capabilities of building energy simulation tools to calculate the daylight level are limited and not as accurate as of the algorithms used in standard daylighting tools. Therefore the co-simulation between energy-based simulation software and daylighting simulation programs is recommended for more precision.

- *Simulation of HVAC systems* - Simulation of building HVAC systems in EnergyPlus software is more complex than the description of building physical components due to the interconnections between different parts of HVAC systems, and the hidden pattern in their operational sequence. Therefore, EnergyPlus uses ZoneHVAC:EquipmentList object to (i) list all HVAC systems serving the zone and (ii) sequence the equipment for heating and cooling. In the sequential method, the primary equipment tries to meet the entire cooling or heating demand using its capacity and then pass the remaining demand to the secondary equipment. However, because of the complex interlink connection between the existing water-based and air-based HVAC systems in the case study, this approach may not entirely represent their real-world relationship.

- *Model validation* - The current model verification approach used in this thesis does not include measured data and is developed based on a detailed comparison of results (i.e., outputs) between EnergyPlus and IES models, as suggested by Sargent (2010). Because the SPEB was under construction at the time of simulation, the experimental verification of SPEB was not possible for this thesis. However, in order to gain confidence in the level of agreement between models prediction and actual outcomes as well as the predictive capability of the model, the developed models in EnergyPlus and IES must be verified against experimental outputs from the real-world building.

- *Generalization* - It should be noted that the results and findings of this investigation exclusively reflect the optimal application of PCM and passive cooling systems in highly glazed buildings in cold climates and the results may differ in different building types located in different climates.

7.3 Future work

The following recommendations for future work can be considered:

- Considering a large number of input variables required for describing the thermal properties of SPEB and its associated operational systems, the deterministic model (physics-based approach) substantially increases the computational effort for optimization purposes. In this regard, future research works can involve gray-box approaches that take advantage of both principle physics and data-driven methods for faster forecasting and prediction of building energy performance.

- The present study emphasizes on the importance of optimizing various variables exist in a model. This is a useful approach in choosing the optimal solution to a given problem by searching intelligently through the entire domain space. The process provides a direction towards the best solution from some set of available alternatives while satisfies objectives and constraints. The general methodology proposed in this paper is mainly focused on a single-objective function in which the total cost function is composed of the combination of heating and cooling. Therefore, further work can be done to extend the present methodology to multi-objective functions by involving more than one objective function (heating and cooling are considered as a single-objective functions separately). In this way a vector of optimal decisions can be obtained based on the presence of trade-offs between more than one conflicting objectives.

- Findings from this study suggest that designers should focus more on the development of the optimal control systems for shadings and natural ventilation systems that can improve the overall energy performance and indoor environmental quality of buildings. For the best results, this type of detailed integrated analysis should be carried out during the early stage of the design when critical decisions have a major impact on the energy performance during the use phase of the building. Future work will include the development of control strategies that integrate shading and natural ventilation.

References

International Energy Agency (IEA). 2019. Energy Conservation through Energy Storage. https://iea-eces.org/annexes/deployment-of-energy-storage-technologies/.

Abdullah, Abul, Ben Cross, and A Aksamija. 2014. Whole building energy analysis: A comparative study of different simulation tools and applications in architectural design , ACEEE Summer Study on Energy Efficiency in Buildings, p. 11.

Actual. 2015. Advanced Climate Technology: Urban Atmospheric Laboratory- Snoozing in the Heat. http://www.actual.ac.uk/2014/07/24/snoozing-in-the-heat/.

Al-janabi, Ali, Miroslava Kavgic, Ali Mohammadzadeh, and Afaf Azzouz. 2019. Comparison of EnergyPlus and IES to model a complex university building using three scenarios: Free-floating, ideal air load system, and detailed . Journal of Building Engineering 22, 262–80.

Al-Obaidi, Karam M, Mazran Ismail, and Abdul Malek Abdul Rahman. 2014. Passive cooling techniques through reflective and radiative roofs in tropical houses in Southeast Asia: A literature review . Frontiers of Architectural Research 3(3), 283–97.

American Society of Heating, Refrigerating and Air-conditioning, and Engineers (ASHRAE). 2017. Thermal environmental Conditions for Human Occupancy, ASHRAE Standard 55–2017. Vol. 55. Atlanta, Georgia: American Society of Heating, Refrigerating and Air-Conditioning Engineers.

Anisur, MR, MH Mahfuz, MA Kibria, R Saidur, IHSC Metselaar, and TMI Mahlia. 2013. Curbing global warming with phase change materials for energy storage. Renewable and Sustainable Energy Reviews 18, 23–30.

Anselm, Akubue Jideofor. 2008. Passive annual heat storage principles in earth sheltered housing, a supplementary energy saving system in residential housing. Energy and Buildings 40(7), 1214–19.

Asfour, O. 2015. Natural ventilation in buildings: An overview . Natural Ventilation: Strategies, Health Implications and Impacts on the Environment, 1–26.

ASHRAE. 2010. Energy standard for buildings except low-rise residential buildings . ASHRAE Standard 90.1-2010.

ASHREA. 1995. “Handbook: Fundamentals, Chapter 30-Energy Estimating and Modeling Methods.”

ANSI/ASHRAE Standard 140. 2010. Standard Method of Test for the Evaluation of Building Energy Analysis Computer Programs, American Society of Heating, Refrigerating and Air-Conditioning Engineers.

Baniassadi, Amir, Behrang Sajadi, Majid Amidpour, and Navid Noori. 2016. Economic optimization of PCM and insulation layer thickness in residential buildings. Sustainable Energy Technologies and Assessments 14, 92–99.

Barzin, Reza, John JJ Chen, Brent R Young, and Mohammed M Farid. 2015. Application of PCM energy storage in combination with night ventilation for space cooling. Applied energy 158, 412–21.

Bellia, Laura, Concetta Marino, Francesco Minichiello, and Alessia Pedace. 2014. An overview on solar shading systems for buildings. Energy Procedia 62, 309–17.

Ben-David, Tom, and Michael S Waring. 2016. Impact of natural versus mechanical ventilation on simulated indoor air quality and energy consumption in offices in fourteen US cities. Building and Environment 104, 320–36.

Berkeley, Lawrence, OAK Ridge, Managed BY Ut-battelle, Alliance For, Sustainable Energy, Duced Or, Transmitted In, ANY Form, OR By, ANY Means, and Without The. 2017. Application Guide for EMS.

Boyce, Peter, Claudia Hunter, and Owen Howlett. 2003. The benefits of daylight through windows. Troy, New York: Rensselaer Polytechnic Institute.

Breitenbach, J, S Lart, I Längle, and JLJ Rosenfeld. 2001. Optical and thermal performance of glazing with integral venetian blinds. Energy and Buildings 33(5), 433–42.

Brittle, John P. 2017. Passive system integration for office buildings in hot climates.

Cabeza, LF, and A de Gracia. 2015. Thermal energy storage (TES) systems for cooling in residential buildings, Advances in Thermal Energy Storage Systems. Elsevier, pp. 549–72.

Caldas, Luisa Gama, and Leslie K Norford. 2002. A design optimization tool based on a genetic algorithm. Automation in construction 11(2), 173–84.

Canada, Natural resources. 2014. Natural resources Canada.

Carson, II, and S John. 2002. Verification validation: model verification and validation, Proceedings of the 34th conference on Winter simulation: exploring new frontiers. Winter Simulation Conference, pp. 52–58.

Castell, Albert, Ingrid Martorell, M Medrano, G Pérez, and Luisa F Cabeza. 2010. Experimental study of using PCM in brick constructive solutions for passive cooling . Energy and Buildings 42(4), 534–40.

Chen, Shuqin, Weiwei Yang, Hiroshi Yoshino, Mark D Levine, Katy Newhouse, and Adam Hinge. 2015. Definition of occupant behavior in residential buildings and its application to behavior analysis in case studies. Energy and Buildings 104, 1–13.

Clarke, JA, J Cockroft, S Conner, JW Hand, NJ Kelly, R Moore, T O'Brien, and P Strachan. 2002. Simulation-assisted control in building energy management systems. Energy and buildings 34(9), 933–40.

Claros, Santiago-Tomás, and Alfonso Soler. 2001. Indoor daylight climate-comparison between light shelves and overhang performances in Madrid for hours with unit sunshine fraction and realistic values of model reflectance. Solar energy 71(4), 233–39.

Canadian Green Building Council (CaGBC). 2018. LEED-Canada NC version 1.0, Reference Guide: https://www.cagbc.org/

Crawley, D. B., Hand, J. W., Kummert, M., & Griffith, BT. 2006. Contrasting the capabilities of building energy performance simulation programs Drury. Building and environment 10, 264–73.

CWEC. 2017. Canadian Climate Normals 1981-2010 Station Data.

Datta, Gouri. 2001. Effect of fixed horizontal louver shading devices on thermal perfomance of building by TRNSYS simulation. Renewable energy 23(3–4), 497–507.

Djuric, Natasa, Vojislav Novakovic, Johnny Holst, and Zoran Mitrovic. 2007. Optimization of energy consumption in buildings with hydronic heating systems considering thermal comfort by use of computer-based tools 39, 471–77.

Doukas, Haris, Konstantinos D Patlitzianas, Konstantinos Iatropoulos, and John Psarras. 2007. Intelligent building energy management system using rule sets. Building and Environment 42(10), 3562–69.

Dounis, AI, M Bruant, G Guarracino, P Michel, and M Santamouris. 1996. Indoor air-quality control by a fuzzy-reasoning machine in naturally ventilated buildings. Applied Energy 54(1), 11–28.

Dounis, AI, MJ Santamouris, CC Lefas, and A Argiriou. 1995. Design of a fuzzy set environment comfort system. Energy and Buildings 22(1), 81–87.

Dutton, Spencer, Hui Zhang, Yongchao Zhai, Ed Arens, Youness Bennani Smires, Sam Brunswick, Kyle Konis, and Phil Haves. 2012. Application of a stochastic window use model in EnergyPlus. Proceedings of SimBuild 5(1), 63–70.

Edwards, L, and P Torcellini. 2002. Literature review of the effects of natural light on building occupants. National Renewable Energy Lab., Golden, CO.(US).

Ellis, Peter G, Paul A Torcellini, and D Crawley. 2008. Simulation of energy management systems in EnergyPlus. National Renewable Energy Lab.(NREL), Golden, CO (United States).

Elsevier. 2019. Elsevier Copyright Policy. https://www.elsevier.com/about/policies/copyright.

EnergyPlus. 2018. EnergyPlus Application Guide for EMS. US Department of Energy. https://energyplus.net/sites/all/modules/custom/nrel_custom/pdfs/pdfs_v8.5.0/EMS_Application_Guide.pdf.

EnergyPlus. 2018. Engineering References. The Reference to EnergyPlus Calculations. US Department of Energy https://energyplus.net/sites/all/modules/custom/nrel_custom/pdfs/pdfs_v8.9.0/EngineeringReference.pdf.

EnergyPlus. 2018. Getting Started with EnergyPlus. Basic Concepts Manual - Essential Information You Need about Running EnergyPlus. US Department of Energy. https://energyplus.net/sites/default/files/pdfs_v8.3.0/GettingStarted.pdf.

EnergyPlus. 2018. Input Output Reference. The Encyclopedic Reference to EnergyPlus Input and Output. . US Department of Energy. https://energyplus.net/sites/default/files/pdfs/pdfs_v8.3.0/InputOutputReference.pdf.

Esen, Mehmet. 2000. Thermal performance of a solar-aided latent heat store used for space heating by heat pump. Solar energy 69(1), 15–25.

Evola, G, L Marletta, and F Sicurella. 2013. A methodology for investigating the effectiveness of PCM wallboards for summer thermal comfort in buildings. Building and Environment 59, 517–27.

Fanger, PO. 1984. Moderate Thermal Environments Determination of the PMV and PPD Indices and Specification of the Conditions for Thermal Comfort. ISO 7730.

Fanger, Poul O, and others. 1970. Thermal comfort. Analysis and applications in environmental engineering Thermal comfort Analysis and applications in environmental engineering.

Farid, M, and WJ Kong. 2001. Underfloor heating with latent heat storage . Proceedings of the Institution of Mechanical Engineers, Part A: Journal of Power and Energy 215(5), 601–9.

Farid, MM, and XD Chen. 1999. Domestic electrical space heating with heat storage . Proceedings of the Institution of Mechanical Engineers, Part A: Journal of Power and Energy 213(2), 83–92.

Favoino, Fabio, Ylenia Cascone, Lorenza Bianco, Francesco Goia, Michele Zinzi, Mauro Overend, Valentina Serra, and Marco Perino. 2015. Simulating switchable glazing with energyplus: an empirical validation and calibration of a thermotropic glazing model, Proceedings of building simulation.

Feustel, Helmut E. 1995. Simplified numerical description of latent storage characteristics for phase change wallboard. Lawrence Berkeley Lab., CA (United States).

Feustel, Helmut E, and Corina Stetiu. 1997. Thermal performance of phase change wallboard for residential cooling application. Lawrence Berkeley National Lab., CA (United States).

Firth, SK, KJ Lomas, and AJ Wright. 2010. Targeting household energy efficiency measures using sensitivity analysis. Building Research & Information 38(1), 25–41.

Fox, Michael A, and Bryant P Yeh. 2000. Intelligent kinetic systems in architecture, Managing interactions in smart environments. Springer, pp. 91–103.

Givoni, Baruch. 1994. Passive low energy cooling of buildings. John Wiley & Sons.

Gómez-Muñoz, Victor M, Miguel Ángel Porta-Gándara, and Christopher Heard. 2003. Solar performance of hemispherical vault roofs. Building and Environment 38(12), 1431–38.

Guide, Lighting. 1999. Daylighting and window design. CIBSE.

Gunay, H Burak, William O'Brien, and Ian Beausoleil-Morrison. 2016. Implementation and comparison of existing occupant behaviour models in EnergyPlus. Journal of Building Performance Simulation 9(6), 567–88.

Gupta, Neha, and Gopal N Tiwari. 2016. Review of passive heating/cooling systems of buildings. Energy Science & Engineering 4(5), 305–33.

Hammad, Fawwaz, and Bassam Abu-Hijleh. 2010. The energy savings potential of using dynamic external louvers in an office building. Energy and Buildings 42(10), 1888–95.

Hammou, Zouhair Ait, and Marcel Lacroix. 2006. A hybrid thermal energy storage system for managing simultaneously solar and electric energy. Energy Conversion and Management 47(3), 273–88.

Hasanain, SM. 1998. Review on Sustainable thermal energy storage technologies, part I: heat storage materials and techniques. Energy Conservation and managment 39(39), 1127–38.

Haves, Philip, Leslie K Norford, and Mark DeSimone. 1998. A standard simulation test bed for the evaluation of control algorithms and strategies. ASHRAE transactions 104, 460.

Heim, Dariusz, and Joe A Clarke. 2004. Numerical modelling and thermal simulation of PCM–gypsum composites with ESP-r. Energy and buildings 36(8), 795–805.

Hoes, P, M Trcka, JLM Hensen, and B Hoekstra Bonnema. 2011. Investigating the potential of a novel low-energy house concept with hybrid adaptable thermal storage. Energy Conversion and Management 52(6), 2442–47.

Huang, W, and HN Lam. 1997. Using genetic algorithms to optimize controller parameters for HVAC systems. Energy and Buildings 26(3), 277–82.

Hydro, Manitoba. 2019. Manitoba Hydro Energy Cost Rate. https://www.hydro.mb.ca/accounts_and_services/rates/commercial_rates/#ng-hvf.

IES VE. 2015. Integrated environmental solutions virtual environment: https://www.iesve.com/.

Iqbal, Imran, and Mohammad S Al-Homoud. 2007. Parametric analysis of alternative energy conservation measures in an office building in hot and humid climate. Building and environment 42(5), 2166–77.

Kanarachos, A, and K Geramanis. 1998. Multivariable control of single zone hydronic heating systems with neural networks. Energy Conversion and Management 39(13), 1317–36.

Kauranen, P, K Peippo, and PD Lund. 1991. An organic PCM storage system with adjustable melting temperature. Solar Energy 46(5), 275–78.

Kaygusuz, (Kamil.). 2003. Phase change energy storage for solar heating systems. Energy sources 25(8), 791–807.

Kaygusuz, (Kamil). 1999a. Investigation of a combined solar–heat pump system for residential heating. Part 1: experimental results. International journal of energy research 23(14), 1213–23.

Kaygusuz, K, and T Ayhan. 1999. Experimental and theoretical investigation of combined solar heat pump system for residential heating. Energy Conversion and Management 40(13), 1377–96.

Kaygusuz, Kamil. 1995. Performance of solar-assisted heat-pump systems. Applied Energy 51(2), 93–109.

Kaygusuz, Kamil. 1999b. Investigation of a combined solar–heat pump system for residential heating. Part 2: simulation results. International journal of energy research 23(14), 1225–37.

Keeney, Kevin, and James Braun. 1996. A simplified method for determining optimal cooling control strategies for thermal storage in building mass. HVAC&R Research 2(1), 59–78.

Kelly, GE, WB May, JY Kao, and C Park. 1994. Using emulators to evaluate the performance of building energy management systems. ASHRAE Transactions 100(1), 1482–93.

Kendrick, Christopher, and Nicholas Walliman. 2007. Removing unwanted heat in lightweight buildings using phase change materials in building components: simulation modelling for PCM plasterboard. Architectural Science Review 50(3), 265–73.

Khatami, Narguess, Malcolm J Cook, Steven K Firth, and N Hudleston. 2013. Control of carbon dioxide concentration in educational spaces using natural ventilation. International Journal of Ventilation 11(4), 339–52.

Kolokotsa, D, K Kalaitzakis, E Antonidakis, and GS Stavrakakis. 2002. Interconnecting smart card system with PLC controller in a local operating network to form a distributed energy management and control system for buildings. Energy conversion and Management 43(1), 119–34.

Koo, So Young, Myoung Souk Yeo, and Kwang Woo Kim. 2010. Automated blind control to maximize the benefits of daylight in buildings. Building and Environment 45(6), 1508–20.

Kośny, Jan. 2015. PCM-enhanced building components: an application of phase change materials in building envelopes and internal structures. Springer.

Kosny, Jan, Nitin Shukla, and Ali Fallahi. 2013. Cost analysis of simple phase change material-enhanced building envelopes in southern US climates. Fraunhofer CSE, Cambridge, MA (United States).

Kua, HW, and SE Lee. 2002. Demonstration intelligent building—a methodology for the promotion of total sustainability in the built environment. Building and Environment 37(3), 231–40.

Kumar, Rakesh, Shweta Sachdeva, and SC Kaushik. 2007. Dynamic earth-contact building: A sustainable low-energy technology. Building and Environment 42(6), 2450–60.

Kunping, Lin, Zhang Yinping, and D Hongfa. 2005. Experimental study of underfloor electric heating system with latent thermal storage a air supply. Acta Energiae solaris sinica 26(6), 820.

Kuznik, Frédéric, Joseph Virgone, and Kevyn Johannes. 2011. In-situ study of thermal comfort enhancement in a renovated building equipped with phase change material wallboard. Renewable Energy 36(5), 1458–62.

Kuznik, Frédéric, Joseph Virgone, and Jean Noel. 2008. Optimization of a phase change material wallboard for building use. Applied Thermal Engineering 28(11–12), 1291–98.

Lane, George A. 1983. Solar heat storage: latent heat materials.

Leather, Phil, Mike Pyrgas, Di Beale, and Claire Lawrence. 1998. Windows in the workplace: Sunlight, view, and occupational stress. Environment and behavior 30(6), 739–62.

Lebrun, J. 1992. IEA Annex 17 final report. University of Li* ge, Belgium.

Lee, ES, DL DiBartolomeo, and SE Selkowitz. 1998. Thermal and daylighting performance of an automated venetian blind and lighting system in a full-scale private office. Energy and buildings 29(1), 47–63.

Lee, Kyoung Ok, Mario A Medina, Erik Raith, and Xiaoqin Sun. 2015. Assessing the integration of a thin phase change material (PCM) layer in a residential building wall for heat transfer reduction and management. Applied Energy 137, 699–706.

Lei, Jiawei, Jinglei Yang, and En-Hua Yang. 2016. Energy performance of building envelopes integrated with phase change materials for cooling load reduction in tropical Singapore.

Applied energy 162, 207–17.

Lin, Kunping, Yinping Zhang, Hongfa Di, and Rui Yang. 2007. Study of an electrical heating system with ductless air supply and shape-stabilized PCM for thermal storage. Energy Conversion and Management 48(7), 2016–24.

Lin, Kunping, Yinping Zhang, Xu Xu, Hongfa Di, Rui Yang, and Penghua Qin. 2004. Modeling and simulation of under-floor electric heating system with shape-stabilized PCM plates. Building and Environment 39(12), 1427–34.

Linden, Paul F. 1999. The fluid mechanics of natural ventilation. Annual review of fluid mechanics 31(1), 201–38.

Littlefair, PJ. 1999. Solar shading of buildings. CRC.

LLC., PureTemp. 2019. No Title. http://www.puretemp.com/stories/contact-us.

Lollini, R, L Danza, and I Meroni. 2010. Energy efficiency of a dynamic glazing system. Solar Energy 84(4), 526–37.

Lomas, Kevin J, and Stephen M Porritt. 2017. Overheating in buildings: lessons from research. Taylor & Francis.

Loonen, Roel CGM, Fabio Favoino, Jan LM Hensen, and Mauro Overend. 2017. Review of current status, requirements and opportunities for building performance simulation of adaptive facades. Journal of Building Performance Simulation 10(2), 205–23.

Loonen, Roel CGM, Marija Trčka, Daniel Cóstola, and Jan LM Hensen. 2013. Climate adaptive building shells: State-of-the-art and future challenges. Renewable and sustainable energy reviews 25, 483–93.

Manitoba, Government of. 2017. Manitoba Sustainable Development. https://www.gov.mb.ca/sd/.

Marco, I. 2005. Seminar on phase change materials and innovation products—Brianza Plastica. Beijing, China, October 20.

Marjanovic, Ljiljana, and Mahroo Eftekhari. 2004. Design and simulation of a fuzzy controller for naturally ventilated buildings. Building services engineering research and technology 25(1), 33–53.

Maryam Saaly, Pooneh Maghoul, Miroslava Kavgic, and Dimos Polyzois. 2019. Performance analysis of a proposed geothermal pile system for heating and cooling energy demand for a building in cold regions. Sustainable cities and society 45, 669–82.

Maryam Saaly, Pooneh Maghoul, Hartmut Holländer. 2019. Thermo-mechanical performance of a geothermal energy pile system for re-harvesting the energy loss through the basement of a building in cold regions,. 72th Canadian Geotechnical Conference (Geo St John’s 2019), St.John’s, Canada.

Mateus, Ricardo, Sara Neiva, Luís Bragança, Paulo Mendonça, and Mónica Macieira. 2013. Sustainability assessment of an innovative lightweight building technology for partition walls–comparison with conventional technologies . Building and Environment 67, 147–59.

Manitoba Energy Code for Buildings (MECB). 2011. Manitoba Energy Code for Buildings.

MECB. 2015. Manitoba Energy Code for Buildings. home page: http://www.firecomm.gov.mb.ca/codes_energy. National Research Council of Canada (NRC).

Meng, Qinglin, and Lei Zhang. 2006. The rooftop shading system of the Humanities Building at SCUT. Energy and buildings 38(11), 1356–59.

Mi, Xuming, Ran Liu, Hongzhi Cui, Shazim Ali Memon, Feng Xing, and Yiu Lo. 2016. Energy and economic analysis of building integrated with PCM in different cities of China. Applied energy 175, 324–36.

Van Moeseke, Geoffrey, Isabelle Bruyère, and André De Herde. 2007. Impact of control rules on the efficiency of shading devices and free cooling for office buildings 42, 784–93.

Myles Allen, Heleen de Coninck, Opha Pauline, and et al Dube, Ove Hoegh-Guldberg, Daniela Jacob, Kejun Jiang. 2018. Technichal summary in: Global warming of 1.5°C. An IPCC Special Report on the Impacts of global warming of 1.5°C above pre-industrial levels and related global greenhouse gass emission pathway, in the context of strengthening the global response.

National climate data and information archive. https://web.archive.org/web/20130120050347/.

Navarro, Lidia, Alvaro de Gracia, Dervilla Niall, Albert Castell, Maria Browne, Sarah J McCormack, Philip Griffiths, and Luisa F Cabeza. 2016. Thermal energy storage in building integrated thermal systems: A review. Part 2. Integration as passive system. Renewable Energy 85, 1334–56.

Nielsen, Martin Vraa, Svend Svendsen, and Lotte Bjerregaard Jensen. 2011. Quantifying the potential of automated dynamic solar shading in office buildings through integrated simulations of energy and daylight. Solar Energy 85(5), 757–68.

National Research Council Canada (NRC). 1978. National Research Council Canada.

NRC. 2015. National Energy Code of Canada for Building: https://nrc.canada.ca/en/certifications-evaluations-standards/codes-canada/codes-canada-publications/national-energy-code-canada-buildings-2015.

NRC. 2017. National Energy Code of Canada for Buildings:

https://nrc.canada.ca/en/certifications-evaluations-standards/codes-canada/codes-canada-publications/national-energy-code-canada-buildings-2017.

Ochoa, Carlos Ernesto, and Isaac Guedi Capeluto. 2006. Evaluating visual comfort and performance of three natural lighting systems for deep office buildings in highly luminous climates. Building and Environment 41(8), 1128–35.

Osterman, Eneja, Vincenc Butala, and Uroš Stritih. 2015. PCM thermal storage system for “free”heating and cooling of buildings. Energy and buildings 106, 125–33.

Pacheco, Rosalia, Javier Ordóñez, and Germán Martínez. 2012. Energy efficient design of building: A review. Renewable and Sustainable Energy Reviews 16(6), 3559–73.

Page, Jessen, Darren Robinson, and Jean-Louis Scartezzini. 2007. Stochastic simulation of occupant presence and behaviour in buildings , Proc. Tenth Int. IBPSA Conf: Building Simulation, pp. 757–64.

Pasupathy, A_, R Velraj, and R V Seeniraj. 2008. Phase change material-based building architecture for thermal management in residential and commercial establishments. Renewable and Sustainable Energy Reviews 12(1), 39–64.

Rammelberg, Holger U, Thomas Osterland, Boris Priehs, Oliver Opel, and Wolfgang KL Ruck. 2016. Thermochemical heat storage materials – Performance of mixed salt hydrates. Solar Energy 136, 571–89.

Roetzel, Astrid, Aris Tsangrassoulis, Udo Dietrich, and Sabine Busching. 2010. A review of occupant control on natural ventilation. Renewable and Sustainable Energy Reviews 14(3), 1001–13.

Rossi, Monica. 2011. Innovative façades lightweight and thin systems with high inertia for the thermal comfort application in office buildings in Southern Europe. Journal of Green Building 6(2), 107–21.

Sadineni, Suresh B, Srikanth Madala, and Robert F Boehm. 2011. Passive building energy savings: A review of building envelope components. Renewable and sustainable energy reviews 15(8), 3617–31.

Saffari, Mohammad, Alvaro de Gracia, Cèsar Fernández, and Luisa F Cabeza. 2017. Simulation-based optimization of PCM melting temperature to improve the energy performance in buildings. Applied Energy 202, 420–34.

Saltelli, A. 2000. Sensitivity Analysis; Saltelli A, Chan K, Scott M, editors. New York, NY: Wiley.

Saman, Wasim, Frank Bruno, and Edward Halawa. 2005. Thermal performance of PCM thermal storage unit for a roof integrated solar heating system. Solar energy 78(2), 341–49.

Samuel, DG Leo, SM Shiva Nagendra, and MP Maiya. 2013. Passive alternatives to mechanical air conditioning of building: A review. Building and Environment 66, 54–64.

Santamouris, Matheos, and Dimosthénis Asimakopoulos. 1996. Passive cooling of buildings. Earthscan.

Sargent, Robert G. 2010. Verification and validation of simulation models, Proceedings of the 2010 Winter Simulation Conference. IEEE, pp. 166–83.

Sari, Ahmet, and Kamil Kaygusuz. 2006. Thermal energy storage characteristics of myristic and stearic acids eutectic mixture for low temperature heating applications. Chinese Journal of Chemical Engineering 14(2), 270–75.

Sarı, Ahmet. 2003. Thermal characteristics of a eutectic mixture of myristic and palmitic acids as phase change material for heating applications. Applied Thermal Engineering 23(8), 1005–17.

Schossig, P, HM Henning, S Gschwander, and T Haussmann. 2005. Micro-encapsulated phase-change materials integrated into construction materials. Solar Energy Materials and Solar Cells 89(2–3), 297–306.

Schulze, Tobias, and Ursula Eicker. 2013. Controlled natural ventilation for energy efficient buildings. Energy and Buildings 56, 221–32.

Schwartz, Yair, and Rokia Raslan. 2013. Variations in results of building energy simulation tools, and their impact on BREEAM and LEED ratings: A case study . Energy and Buildings 62, 350–59.

Sekhar, SC, and SE Goh. 2011. Thermal comfort and IAQ characteristics of naturally/mechanically ventilated and air-conditioned bedrooms in a hot and humid climate . Building and Environment 46(10), 1905–16.

Seppanen, Olli, William J Fisk, and QH Lei. 2006. Effect of temperature on task performance in officeenvironment. Ernest Orlando Lawrence Berkeley NationalLaboratory, Berkeley, CA (US).

Sharan, Girja, and Ratan Jadhav. 2003. Performance of single pass earth tube heat exchanger: An experimental study.

Sharma, Atul, V Veer Tyagi, CR Chen, and Dharam Buddhi. 2009. Review on thermal energy storage with phase change materials and applications. Renewable and Sustainable energy reviews 13(2), 318–45.

Shilei, L V, Feng Guohui, Zhu Neng, and Dongyan Li. 2007. Experimental study and evaluation of latent heat storage in phase change materials wallboards. Energy and buildings 39(10), 1088–91.

Simões, N, J Prata, and A Tadeu. 2014. Contribution of linear thermal bridges to the overall thermal performance of the building envelope: dynamic analysis. Eco-Architecture V: Harmonisation between Architecture and Nature 142, 321.

Soares, N, AR Gaspar, P Santos, and JJ Costa. 2014. Multi-dimensional optimization of the incorporation of PCM-drywalls in lightweight steel-framed residential buildings in different climates. Energy and Buildings 70, 411–21.

Soares, Nelson, José J Costa, Adélio Rodrigues Gaspar, and Paulo Santos. 2013. Review of passive PCM latent heat thermal energy storage systems towards buildings' energy efficiency. Energy and buildings 59, 82–103.

Solé, Aran, Ingrid Martorell, and Luisa F Cabeza. 2015. State of the art on gas-solid thermochemical energy storage systems and reactors for building applications. Renewable and Sustainable Energy Reviews 47, 386–98.

Stefanopoulou, AG, and Y Kim. 2015. System-level management of rechargeable lithium-ion batteries, Rechargeable Lithium Batteries. Elsevier, pp. 281–302.

Stevanović, Sanja. 2013. Optimization of passive solar design strategies: A review. Renewable and Sustainable Energy Reviews 25, 177–96.

Strand, Richard Karl, and KT Baumgartner. 2005. Modeling radiant heating and cooling systems: integration with a whole-building simulation program . Energy and Buildings 37(4), 389–97.

Sun, Biao, Peter B Luh, Qing-shan Jia, Ziyan Jiang, and Fulin Wang. 2010. An Integrated Control of Shading Blinds, Natural Ventilation, and HVAC Systems for Energy Saving and Human Comfort, 7–14.

Swami, Muthusamy V, and Subrato Chandra. 1987. Procedures for calculating natural ventilation airflow rates in buildings. ASHRAE Final Report FSEC-CR-163-86, ASHRAE Research Project.

Tabares-Velasco, Paulo Cesar, Craig Christensen, and Marcus Bianchi. 2012. Verification and validation of EnergyPlus phase change material model for opaque wall assemblies. Building and Environment 54, 186–96.

Teuffel, P. 2004. Entwerfen Adaptiver Strukturen, University of Stuttgart: Institute for Lightweight Structures and Conceptual Design. PhD-thesis), Stuttgart.

Turányi, Tamás. 1990. Sensitivity analysis of complex kinetic systems. Tools and applications. Journal of mathematical chemistry 5(3), 203–48.

Tzempelikos, Athanassios, and Andreas K Athienitis. 2007. The impact of shading design and control on building cooling and lighting demand. Solar energy 81(3), 369–82.

United Nations (2014) Kyoto Protacol: Status of the Doha Amendment: https://unfccc.int/process/the-kyoto-protocol/the-doha-amendment

United Nations (2016) “The Paris Agreement.”: https://unfccc.int/process-and-meetings/the-paris-agreement/the-paris-agreement

U.S. Department of Energy. (2017). Natural Ventilation — Heating load increases. September. https://windows.lbl.gov/tools/knowledge-base/articles/natural-ventilation.

Versteeg, HK, and W Malalasekera. 1996. An introduction to computation fluid dynamites. Berlin: Springer.

Ward, Rebecca, Ruchi Choudhary, Yeonsook Heo, and Adam Rysanek. 2016. Exploring the impact of different parameterisations of occupant-related internal loads in building energy simulation. Energy and Buildings 123, 92–105.

Wong, Johnny KW, Heng Li, and SW Wang. 2005. Intelligent building research: a review. Automation in construction 14(1), 143–59.

Wong, Nyuk Hien, and Agustinus Djoko Istiadji. 2004. Effect of external shading devices on daylighting penetration in residential buildings. Lighting Research & Technology 36(4), 317–30.

Wyon, David P, and Pawel Wargocki. 2013. How indoor environment affects performance . thought 3(5), 6.

Xu, Xiaoyan, Qingshan Jia, Xi Chen, Xiaohong Guan, and Ziyan Jiang. 2011. Analysis of energy saving potential using shadings and natural ventilation in four major cities in China , Control Conference (CCC), 2011 30th Chinese. IEEE, pp. 417–23.

Yi, Yun Kyu, and Ali M Malkawi. 2009. Optimizing building form for energy performance based on hierarchical geometry relation. Automation in Construction 18(6), 825–33.

Zaheer-Uddin, M. 1993. Optimal, sub-optimal and adaptive control methods for the design of temperature controllers for intelligent buildings. Building and Environment 28(3), 311–22.

Zaheer Uddin, M. 1994. Intelligent control strategies for HVAC processes in buildings. Energy 19(1), 67–79.

Zeng, JL, Z Cao, DW Yang, LX Sun, and L Zhang. 2010. Thermal conductivity enhancement of Ag nanowires on an organic phase change material. Journal of Thermal Analysis and Calorimetry 101(1), 385–89.

Zhang, Yinping, Guobing Zhou, Kunping Lin, Qunli Zhang, and Hongfa Di. 2007. Application of latent heat thermal energy storage in buildings: State-of-the-art and outlook. Building and environment 42(6), 2197–2209.

Zhou, Xin, Tianzhen Hong, and Da Yan. 2014. Comparison of HVAC system modeling in EnergyPlus, DeST and DOE-2.1E. Building Simulation 7(1), 21–33.

Zhu, Na, Zhenjun Ma, and Shengwei Wang. 2009. Dynamic characteristics and energy performance of buildings using phase change materials: a review. Energy Conversion and Management 50(12), 3169–81.

Appendix A: Source Code of the implemented optimization problem

```
%% Read idf file and move it into cell A
fid = fopen('PCM89.idf','r');
i = 1;
tline = fgetl(fid);
A{i} = tline;
while ischar(tline)
i = i+1;
tline = fgetl(fid);
A{i} = tline;
end

fclose(fid);
```

Figure A.1: Code snippet that shows how MATLAB reads an IDF text file.

```
%% Change design variables in cell A
A{4247} = sprintf('%s, !- Layer 2','PCM 28');% PCM melting temp
A{3497} = sprintf('%d, !- Thickness {m}',x(1));%PCM thickness
A{3552} = sprintf('%d, !- Thickness {m}',x(2));% Insulation thickness
A{3553} = sprintf('%d, !- Conductivity {W/m·K}',x(3));%Insulation Conductivity
A{3431} = sprintf('%d, !- Thickness{m}',x(4));% Floor radiant thickness
A{3432} = sprintf('%d, !- Conductivity {W/m·K}',x(5));% Floor radiant conductivity
A{3436} = sprintf('%d, !- SolarAbsorptance',x(6));% Floor radiant solar Absorptance
```

Figure A.2: Code snippet that illustrates how MATLAB changes design variables.

```
%% Write cell A into txt
fid = fopen('PCM89.idf', 'w');
for i = 1:numel(A)
if A{i+1} == -1
fprintf(fid,'%s', A{i});
break
else
fprintf(fid,'%s\n', A{i});
end
end

fclose(fid);
```

Figure A.3: Code snippet that illustrates how MATLAB writes a new IDF text file.

```
%% Run Model
system('C:\EnergyPlusV8-9-0\RunEPlus.bat PCM89 CAN_MB_Winnipeg.718520_CWEC');
```

Figure A.4: Code snippet that shows how MATLAB runs EnergyPlus

```
%% Problem Definition
global NFE;% Number of Evaluation (NFE)
NFE=0;
CostFunction=@(x,y) ObjectiveFunction(x,y);% Cost Function
nVar=6;% Number of Decision Variable
VarSize=[1 nVar];% Decision Variables Matrix Size
DisDesIn = {'PCM23', 'PCM25','PCM27','PCM28', 'PCM29'};% Discrete Design variables
VarMax= [2.5, 2.5, 1, 2.5, 2, 1];% Upper Bound of continuous Variables
VarMin= [ 0.01, 0.01, 0.02,0.01, 0.02, 0];% Lower Bound of continuous Variables
```

Figure A.5: Code source for problem definition in MATLAB.

```
%% GA Parameters
MaxIt=40;% Maximum Number of Iterations
nPop= 30;% Population Size
pc=0.85;% Crossover Percentage
nc=2*round(pc*nPop/2);% Number of Offsprings (Parnets)
pm=0.5;% Mutation Percentage
nm=round(pm*nPop);% Number of Mutants
gamma=0.08;% Crossover rate
mu=0.15;% Mutation Rate
```

Figure A.6: Code source for the definition of GA parameters in MATLAB.

```
%% Initialization of population
empty_individual.Position=[];
empty_individual.Cost=[];
empty_individual.RadiantEn=[];% Store Energy results
empty_individual.FanCoilEn=[];% Store Energy results
empty_individual.PMV=[];% Store PMV results
pop=repmat(empty_individual,nPop,1);
A = zeros(nPop, nVar);
B = zeros(1,nVar);
for i = 1:nPop
    for j = 1:nVar
    A(i,j) = unifrnd(VarMin(j),VarMax(j),1);
    end
end
for i=1:nPop% Initialize Position
pop(i).Position = A(i,:);
RAND = randi(5);
    if RAND == 1
    pop(i).PCM = 'PCM23';
       elseif RAND == 2
       pop(i).PCM = 'PCM25';
       elseif RAND == 3
       pop(i).PCM = 'PCM27';
       elseif RAND == 4
       pop(i).PCM = 'PCM28';
       elseif RAND == 5
       pop(i).PCM = 'PCM29';
    end
end
```

Figure A.7: Code source for problem initialization in MATLAB

```
%% Main Loop
for it=1:MaxIt
   % Crossover
    popc=repmat(empty_individual,nc/2,2);
    for k=1:nc/2
        i1=TournamentSelection(pop,TournamentSize);
        i2=TournamentSelection(pop,TournamentSize);
       % Select Parents
        p1=pop(i1);
        p2=pop(i2);
       % Apply Crossover
        [popc(k,1).Position, popc(k,2).Position,popc(k,1).PCM,
popc(k,2).PCM]=...
        Crossover(p1.Position, p2.Position, p1.PCM, p2.PCM, gamma, VarMin,
VarMax);
```

```
        % Evaluate Offsprings
         [popc(k,1).Heating, popc(k,1).RadiantEn, popc(k,1).FanCoilEn, ...
          popc(k,1).PMV]=CostFunction(popc(k,1).Position, ...
          popc(k,1).PCM);
         [popc(k,2).Heating, popc(k,2).RadiantEn, popc(k,2).FanCoilEn, ...
          popc(k,2).PMV]=CostFunction(popc(k,2).Position, popc(k,2).PCM);
          popc=popc(:);
    end
    % Mutation
    popm=repmat(empty_individual,nm,1);
    for k=1:nm
        % Select Parent
        i=randi([1 nPop]);
        p=pop(i);
        % Apply Mutation
        [popm(k).Position, popm(k).PCM] = Mutate(p.Position, mu, VarMin, VarMax);
        % Evaluate Mutant
         [popm(k).Heating, popm(k).RadiantEn, popm(k).FanCoilEn, ...
          popm(k).PMV]=CostFunction(popm(k).Position, popm(k).PCM);
    end
    % Create Merged Population
    pop=[pop
    popc
    popm];
    for l = 1:size(pop,1)
        pop(l).Cost = pop(l).Heating - Heating_Reference;
    end
    % Penalty for PMV
    for i = 1:nPop
        if pop(i).PMV >0.5 || pop(i).PMV<-0.5
           pop(i).Cost = pop(i).Cost * 1000;
        end
    end
    % Penalty for Cooling
    for i = 1:nPop
        if pop(i).Cooling > 0.1 * TotalCooling
           pop(i).Cost = pop(i).Cost * 1000;
        end
    end
    % Sort Population
    Costs=[pop.Cost];
    [Costs, SortOrder]=sort(Costs);
    pop = pop(SortOrder);
    % Update Worst Cost
    WorstCost=max(WorstCost,pop(end).Cost);
    % Truncation
    pop=pop(1:nPop);
    Costs=Costs(1:nPop);
    % Store Best Solution Ever Found
    BestSol=pop(1);
    % Store Best Cost Ever Found
    BestCost(it)=BestSol.Cost;
    % Store NFE
    nfe(it)=NFE;
```

```
% Show Iteration Information
 disp(['Iteration ' num2str(it) ': NFE = ' num2str(nfe(it)) ', Best
Cost = '
 num2str(BestCost(it))]);
 disp(['Fan Coil Energy Use = ' num2str(pop(1).FanCoilEn) ': ...
 Radiant Energy Use = ' num2str(pop(1).RadiantEn) ', PMV = ' ...
 num2str((pop(1).PMV))]);
end
```

Figure A.8: Code source for main Genetic Algorithm loop in MATLAB